

CIBERES COMMUNICATIONS

16.ª Jornada de Formación CIBERES-CIBERINFEC del Centro de Investigación Biomédica en Red (CIBERES)

Madrid, 15 y 16 de junio de 2023

2. RELEVANCE OF THE SYSTEMATIC SLEEP STUDY ON IDIOPATHIC PULMONARY FIBROSIS (IPF)

Jaume Bordas-Martínez¹, Neus Salord², Vanesa Vicens-Zygmunt¹, Sandra Pérez², Eliseo Prado², Maria Calvo², Guadalupe Bermudo¹, Ana Montes-Worboys¹, Salud Santos³, Carmen Monasterio^{*2}, Maria Molina-Molina^{*1}

¹Interstitial Lung Disease Unit, Respiratory Department, Bellvitge University Hospital, IDIBELL, CIBERES, University of Barcelona, Hospitalet de Llobregat, Spain. ²Sleep Unit, Respiratory Department, Bellvitge University Hospital, IDIBELL, University of Barcelona, Hospitalet de Llobregat, Spain. ³Respiratory Department, Bellvitge University Hospital, IDIBELL, University of Barcelona, Hospitalet de Llobregat, Spain. *Equal contribution

Introduction: Sleep breathing disorders (SBD) are a relevant comorbidity in IPF. Differences in SBD prevalence, features and impact may depend on the methodology used.

Objectives: This study aims to evaluate the SBD features and the treatment effect depending on the type of methodology: systematic sleep study (SSS) versus conventional study due to clinical SBD suspicion.

Methods: SBD study in two IPF cohorts; a retrospective cohort (RC) and a prospective cohort (PC) with SSS in consecutive patients that initiated anti-fibrotic treatment. Polysomnography, biomarkers and quality of life were performed at inclusion and after 1-year in PC. Mortality, IPF progression and exacerbations were compared. SBDs were classified into obstructive sleep apnea (OSA), central sleep apnea (CSA), and sleep-related hypoxemia (SRH). SBD were treated with CPAP and/or nocturnal oxygen therapy (NOT) as appropriate.

Results: 181 IPF patients (131 RC and 50 PC) were included. RC identified 12% OSA, while PC found 70% SDB, 36% OSA, 22% CSA and 12% SRH. CPAP was used in 11% of RC and 54% of PC. NOT was used in 16% of PC. No differences in IPF progression or mortality were found between cohorts at one year. PC showed fewer mild-moderate exacerbations ($p = 0.002$). PSG under SBD treatment found improved SBD, but 6/35 patients had to add NOT or CPAP. 5/15 patients without SBD at baseline presented SBD at one year and initiated appropriate treatment. MMP-1 was higher in IPF patients with OSA and CSA that decreased after 1-year of SBD treatment ($p = 0.029$ and $p = 0.027$).

Conclusions: The systematic study of SBD identifies subclinical sleep disorders, including OSA, that may require specific treatment. SBD and its treatment may influence some profibrotic pathways.

Funding: This study has been funded by: Instituto de Salud Carlos III through the grants CM20/00093 (Co-funded by European Social Fund. ESF investing in your future) and PI18/00367 (Co-funded by European Regional Development Fund, ERDF, a way to build Europe); Spanish Society of Pneumology and Thoracic Surgery (SEPAR) grants 631/2018 and 685/2018; Emerging ILD Group of SEPAR grant 005 (Boehringer-Roche); Pneumology Foundation of Catalonia (FUCAP) grant 2019; Spanish Sleep Society (SES) grant 2019. Investigation support BRN-Fundació Ramon Pla Armengol. We thank CERCA Programme/Generalitat de Catalunya for institutional support.

5. HOSPITALIZATION BURDEN AND COMORBIDITIES RELATED TO PNEUMOCOCCAL DISEASE IN SPAIN (2019-2021)

David García-Reyes¹, **Enrique Gea-Izquierdo**^{1,2}, Ángel Gil-de-Miguel^{1,3}

¹Rey Juan Carlos University, Preventive Medicine and Public Health, Alcorcón, Spain. ²María Zambrano Program, European Union-Spain, Alcorcón, Spain. ³Centro de Investigación Biomédica en Red de Enfermedades Respiratorias (CIBERES), Madrid, Spain.

Introduction: Pneumococcal disease (PD) showed a substantial morbidity and mortality in Spain, with great care and economic impact on the Spanish health system.

Objectives: The objective is to describe the hospital burden of PD and associated comorbidities.

Methods: Cross-sectional descriptive study based on the minimum basic data set and 2019-2021 series. The Charlson Comorbidity Index (CCI) was used in the analysis of comorbidities potentially associated with PD.

Results: The mean age was 67 years with a total hospitalization rate of 10.65 x 10,000 inhabitants and a fatality rate of 14.37 x 10,000 inhabitants, with higher values in males. A decrease in hospitalizations and an increase in lethality were identified. 58.34% of the patients were admitted due to pneumonia. The most prevalent diseases related to admissions for PD were: chronic obstructive pulmonary disease,

congestive heart failure, cancer, and diabetes. The average stay was 13 days and the total average cost 8,533 euros per episode. The annual cost was 370, 455 and 462 million euros in 2019, 2020 and 2021, respectively.

Conclusions: Due to the great burden that it continues to pose for the Spanish health system, PD and the most frequent comorbidities associated with it must be approached from a preventive point of view, considering essential measures such as vaccination and correct sentinel surveillance of the disease.

6. LEVELS OF INFLAMMATORY AND CARDIAC BIOMARKERS AS A PREDICTOR FACTOR FOR COMPLICATIONS AND OUTCOMES IN HOSPITALIZED COVID-19 PATIENTS

Nona Rovira Ribalta¹, **Catja Cillóniz**^{1,2}, **Rubén López Aladid**¹, **Ana Motos Galera**^{1,2,3}, **Josep Lluís Bedini**⁴, **Alba Soler Comas**¹, **Roberto Cabrera Ortega**^{1,2}, **Kasra Kiarostami**^{1,3}, **Blanca Llönch**^{1,3}, **Laia Fernández Barat**^{1,2,3}, **Antoni Torres Martí**^{1,2,3,5}

¹IDIBAPS, Fundació Clínica, Barcelona, Spain. ²Centro de Investigación Biomédica en Red de Enfermedades Respiratorias (CIBERES), Madrid, Spain. ³Universitat de Barcelona, Barcelona, Spain. ⁴Core Lab, Hospital Clinic, Barcelona, Spain. ⁵Hospital Clínic de Barcelona, Barcelona, Spain.

Introduction: SARS-CoV-2 physiopathology is linked to an uncontrolled response of the immune system as well as a hypercoagulopathy status.

Objectives: We aimed to characterize phenotypes according to inflammatory and cardiac biomarkers.

Methods: Patients admitted to the Hospital Clinic of Barcelona due to COVID-19 infection between 28th January and 14th June 2021 were prospectively included. A blood sample during the first 48h from hospital admission was collected for each patient to measure interleukin (IL)-6 and NT-proBNP. Biomarkers concentrations were quantified by bead-based multiplex assays (Millipore Iberica, S.A., Spain). For the

Table 1. Baseline characteristics and outcomes according to study groups.

	No abnormalities ^a n=65	Inflammatory phenotype ^b n=35	Cardiac phenotype ^c n=41	Inflammatory and cardiac phenotype ^d n=28	p-value
Baseline characteristics					
Sex, male	37 (57)	25 (71)	24(59)	19 (68)	0.45
Age, years	60 [40 – 60]	71 [63 – 73]	66 [61 – 72]	74 [57 – 79]	<0.001
Comorbidities, n (%)					
Cardiopathy	4 (6)	1 (3)	14 (34)	7 (25)	<0.001
Liver disease	1 (1)	5 (3)	1 (1)	2 (1)	0.041
Kidney disease	5 (8)	3 (9)	5 (12)	3 (11)	0.88
Chronic respiratory disease	7 (11)	4 (11)	7 (17)	8 (29)	0.15
Active malignant neoplasia	1 (2)	1 (3)	3 (7)	4 (14)	0.070
Immunodeficiency	4 (6)	4 (11)	1 (2)	1 (4)	0.38
Arterial hypertension	13 (20)	12 (34)	24 (59)	14 (50)	<0.001
Diabetes mellitus	5 (8)	9 (26)	8 (20)	7 (25)	0.064
Obesity (BMI >25 kg/m ²)	26 (65)	13 (69)	20 (67)	17 (81)	0.619
Alcoholism	9 (14)	4 (11)	5 (12)	3 (11)	0.973
Smoker	18 (28)	16 (46)	13 (32)	14 (50)	0.108
Biomarkers concentrations at hospital admission					
IL-6, pg/mL	43 [33-50]	152 [101-280]	31 [20-52]	152 [111-270]	<0.001
NT-proBNP, pg/mL	<34.3	<34.3	36 [35-117]	53 [35-131]	<0.001
Complications and treatment during hospital admission, n (%)					
Corticosteroids treatment	54 (83)	31 (89)	33 (81)	27 (96)	0.24
Acute cardiac injury	2 (3)	2 (6)	5 (12)	4 (14)	0.17
Coagulation disorder	3 (5)	8 (23)	9 (22)	9 (32)	0.004
PTE	0 (0)	5 (14)	6 (14)	4 (14)	0.016
Acute liver injury	2 (3)	4 (11)	3 (7)	2 (7)	0.44
Acute kidney injury	3 (5)	3 (9)	6 (15)	7 (25)	0.031
ARDS	16 (25)	22 (63)	15 (37)	17 (61)	<0.001
Outcomes n (%)					
Length of hospital stay, days	6 [4-9]	11 [5-32]	8 [6-16]	12 [8-24]	<0.001
ICU admission	13 (20)	19 (54)	11(27)	13 (46)	0.002
Length of ICU stay, days	5 [3-9]	15 [6-33]	12 [3-24]	7 [5-25]	0.11
Requirement of IMV	2 (3)	10 (29)	4 (10)	5 (18)	0.002
IMV length, days	30 [7-52]	32 [21-36]	18 [9-26]	24 [20-32]	0.57
In-hospital mortality	0 (0)	3 (9)	4 (10)	6 (21)	0.004
90-days mortality ^e	0 (0)	4 (12)	5 (13)	7 (25)	0.002

Results were expressed as median and IQR (25-75th percentiles) or number (percentage). ^a No abnormalities group was defined as IL-6 <80pg/mL and NT-proBNP <34.3 pg/mL. ^b Inflammatory phenotype was defined as IL-6 ≥ 80pg/mL and NT-proBNP <34.3 pg/mL. ^c Cardiac phenotype was defined as IL-6 < 80pg/mL and NT-proBNP ≥ 34.3 pg/mL. ^d Inflammatory and cardiac phenotype was defined as IL-6 ≥ 80pg/mL and NT-proBNP ≥ 34.3 pg/mL. ^e Calculated only for patients with 90 days follow-up (4 patients with missing data). **Abbreviations:** ARDS, Acute Respiratory Distress Syndrome; BMI, Body Mass Index; ICU, Intensive Care Unit; IL, Interleukin; IMV, Invasive Mechanical Ventilation; NT-proBNP, N-terminal pro B-type Natriuretic Peptide; PTE, Pulmonary Thromboembolism.

analysis, patients were categorized into four groups depending on inflammation (IL-6 < or ≥ 80 pg/mL) and cardiac phenotypes (NT-proBNP < or ≥ 34.3 pg/mL). Clinical information was collected.

Results: One hundred sixty-nine patients were included in the study (Table). Cardiovascular comorbidities were more frequently observed in patients with the cardiac phenotype. Coagulation disorders were more prevalent in patients with both altered markers. Patients with the inflammatory phenotype had a longer length of stay, higher rates of ICU admission and IMV requirements. In addition, a higher mortality rate was observed when both phenotypes were present.

Conclusions: High levels of inflammatory and cardiac biomarkers were associated with poor outcomes in hospitalized COVID-19 patients.

Funding: This work was supported by an award from Institut de Salut Carlos III, proyecto de investigación en salud PI19/00207.

7. SARCOPENIA IS ASSOCIATED WITH MILD-TO-MODERATE BRONCHIECTASIS: HINTS FROM FUNCTIONAL, HISTOLOGICAL, AND IMAGING ASSESSMENT

Mariela Alvarado-Miranda^{1,2,3}, **Adriana Núñez-Robainas**^{1,3,4}, **Salvatore Marsico**⁵, **Alberto Solano-López**⁵, **Esther Barreiro**^{1,3,4}

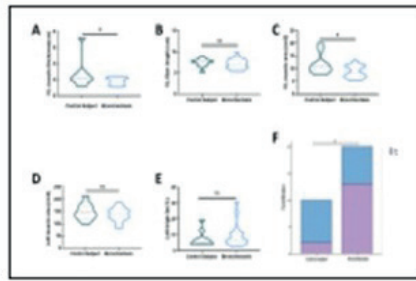
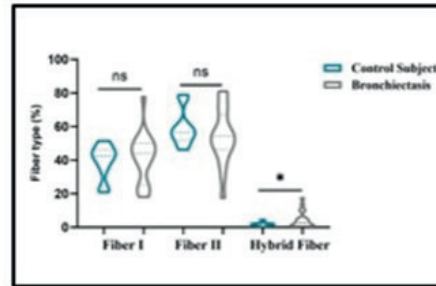
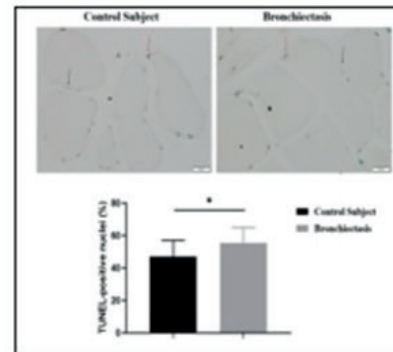
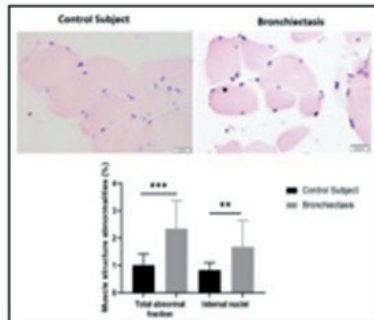
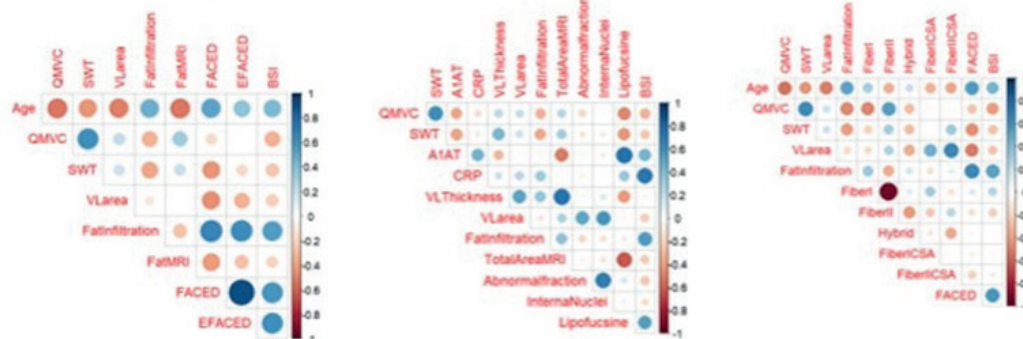
¹Department of Medicine and Life Sciences (MELIS), Universitat Pompeu Fabra (UPF), Barcelona, Spain. ²Hospital Universitario Salut Sant Joan, Reus, Spain. ³Grupo CB06/06/0043 del Centro de Investigación Biomédica en Red de Enfermedades Respiratorias (CIBERES), Instituto de Salud Carlos III (ISCIII), Madrid, Spain. ⁴Pulmonology Department-Muscle Wasting and Cachexia in Chronic Respiratory Diseases and Lung Cancer Research Group, IMIM-Hospital del Mar, Parc de Salut Mar, Barcelona, Spain. ⁵Radiology Department, Imatge Mèdica Intercentres-Parc de Salut Mar, Hospital del Mar, Barcelona, Spain.

Introduction: Bronchiectasis is a heterogeneous and multidimensional disease, whose systemic manifestations are not completely studied.

Objectives: Our aim, to evaluate the severity of BQ and its relationship with muscle phenotype, muscle alterations and functional parameters by imaging and morphometric study in samples of the vastus lateralis (VL) of the quadriceps in patients in stable phase of disease.

Methods: Twenty patients with stable bronchiectasis and sarcopenia and ten healthy subjects were recruited. General clinical and severity indices (FACED, EFACED, BSI), nutritional, and functional features were evaluated in all the participants. Ultrasound and magnetic resonance were used to evaluate the muscle architecture of the quadriceps muscle (vastus lateralis, VL). In muscle specimens (open biopsy technique), muscle fiber type and morphometry including hybrid fiber analysis, apoptotic nuclei and structural abnormalities were assessed using immunohistochemical procedures.

	Control Subject (N = 10)	Bronchiectasis (N = 20)
FACED score (SD)		
Mild, N	NA	2.15 (1.1)
Moderate, N	NA	10
Severe, N	NA	10
EFACED score (SD)		
Mild, N	NA	2.6 (1.1)
Moderate, N	NA	17
Severe, N	NA	3
BSI score (SD)		
Mild, N	NA	5.0 (3.2)
Moderate, N	NA	11
Severe, N	NA	17
	NA	2

Graphic 1. Imaging study (ultrasound and MRI)**Graphic 2. Fiber type****Graphic 3. Muscle structural****Graphic 4. Correlations**

Results: Compared to control subjects, in bronchiectasis patients (mild-to-moderate disease scores), nutritional and muscle functional assessment were significantly worse along with an increase in systemic inflammatory parameters, the thickness and area of VL was smaller together with increased fat infiltration within the muscle fibers (imaging evaluation), muscle abnormalities including the number of both internal and TUNEL-positive nuclei and hybrid fiber proportions were greater. Significant positive correlations were found between disease severity scores and age, fat infiltration, and inflammatory parameters, whereas those scores negatively correlated with muscle strength, exercise capacity, and VL area.

Conclusions: In patients with mild-to-moderate bronchiectasis, the presence of sarcopenia was confirmed using functional and imaging approaches. From a structural standpoint, sarcopenia was also confirmed by the presence of several features that conform a specific phenotype characterized by a disruption of the architecture of the VL along with regenerative events. The status of the bronchiectasis as measured by several disease severity scores inversely correlated with muscle structural abnormalities, suggesting that the impact of sarcopenia is greater in patients with a more advanced disease even in stable conditions. These observations prompt the need of assessing nutritional and muscle function in patients with bronchiectasis, even at early stages of their respiratory disease.

Funding: FIS 21/00215 (FEDER, ISC-III), BA21/00003, Intensificación INT19/00002, CIBERES (ISC-III), SEPAR-2020.

9. MICRORNA 146A-5P AND 155-3P MODULATE INFLAMMATORY RESPONSES IN HUMAN ALVEOLAR EPITHELIAL CELLS *IN VITRO*

Gema Sánchez-Helguera¹, Raquel Herrero^{1,2,3}, Antonio Ferruelo², Raquel Murillo⁴, Marta de Paula¹, José Ángel Lorente^{1,2,4,3}

¹Hospital Universitario de Getafe, Getafe, Spain. ²Centro de Investigación Biomédica en Red de Enfermedades Respiratorias (CIBERES), Madrid, Spain. ³Universidad Carlos III, Madrid, Spain. ⁴Universidad Europea, Madrid, Spain.

Introduction: In Acute Respiratory Distress Syndrome (ARDS), alveolar epithelial cells release cytokines and chemokines that contribute to inflammation in the alveoli by activating resident alveolar macrophages and promoting leukocyte migration into the lung. MicroRNAs regulate gene expression and could modulate inflammatory responses. **Objectives:** Our objectives were: 1) to identify microRNAs expressed by human alveolar epithelial cells, and 2) to determine the role of those microRNAs in the expression of cytokines/chemokines by these cells under a proinflammatory stimulus *in vitro*.

Methods: Monolayers of human primary alveolar epithelial cells (HAEPiCs) were treated with IL-1 β (1 ng/mL) for 15 hours. In these cells, we measured the expression of several miRNA candidates (RT-qPCR), caspase 3 activity (enzymatic assay) and cell viability (resazurin method). The expression of cytokines and chemokines were measured in the supernatant (ELISA). Then, the expression of two miRNAs identified, miR 146a-5p and miR 155-3p, were modulated by cell transfection with a miR 146a-5p inhibitor (5 nM) or a miR 155-3p mimic (0.1 nM), respectively. The expression of these miRNAs, the activity of caspase-3, cell viability and cytokine expression were also measured. Statistical analysis: one-way ANOVA, p value < 0.05 was considered statically significant. Each experiment was performed in triplicate.

Results: Compared with control, incubation with IL-1 β increased miR 146a-5p and reduced miR-155-3p expressions in HAEPiCs *in vitro*. Also, it increased the expression of IL-6, IL-8, and MCP-1 and decreased TGF- β 1 concentration, with no changes in caspase 3 activity or viability. Transfection of IL-1 β -treated HAEPiC with miR 146a-5p inhibitor attenuated the elevated expression of IL-8 induced by IL-1 β , without causing changes in the other cytokines, and reduced caspase-3 activity. Transfection of IL-1 β -treated HPAEPiC with miR 155-3p mimic attenuated the increased expression of IL-6 and IL-8 and enhanced the elevated expression of MCP-1 induced by IL-1 β but did not change the activity of caspase-3. No changes in cell viability were observed in any condition compared with their corresponding controls.

Conclusions: Under IL-1 β stimulus, miR 146a-5p and miR 155-3p modulate the cytokine/chemokine expression of human alveolar epithelial cells *in vitro*. These miRNAs could be used as biomarkers and constitute potential therapeutic targets in the pathogenesis of ARDS, as well as in other pulmonary inflammatory diseases.

Funding: IISCIIII (PI19/01091 and PI22/01611), Comunidad de Madrid-Fondos FEDER (S2017/BMD-3727-EXOHEP-CM), María Rosa Concustell 2021 (Fundación José Luis Castaño-SEQC).

11. OXIDIZED LOW DENSITY LIPOPROTEIN MEDIATES NLRP3 ACTIVATION IN PATIENTS WITH SLEEP APNEA AND EARLY SUBCLINICAL ATHEROSCLEROSIS

Elena Díaz García¹, David Sanz-Rubio², Sara García Tovar¹, Enrique Alfaro¹, Pablo Cubero², Ana V. Gil², José M Marin², Carolina Cubillos Zapata¹, Francisco García Río¹

¹IdiPAZ, Madrid, Spain. ²IISAragon, Zaragoza, Spain.

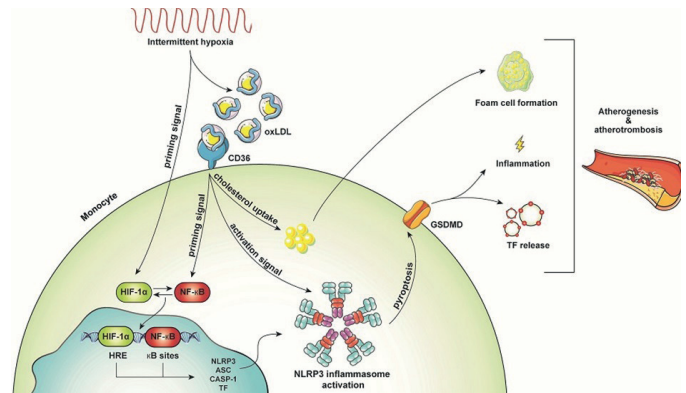
Introduction: Atherosclerosis is a frequent comorbidity of obstructive sleep apnea (OSA) patients, caused by the interaction of dyslipidemia and systemic inflammation. Our group recently published OSA pro-inflammatory response is mediated by NLRP3 inflammasome activation.

Objectives: Given that the recognition of oxidized low-density lipoproteins (oxLDL) seems to play a regulatory role in the NLRP3 inflammasome, this work proposes to study the expression of oxLDL in OSA patients with or without early subclinical atherosclerosis (eSA) and its contribution to NLRP3 activation.

Methods: We analyzed oxLDL, key components of the NLRP3 inflammasome cascade, and TF levels in plasma and leukocytes from OSA patients and non-apneic subjects, with or without eSA (determined by increased carotid intima-media thickness without the appearance of atherosclerotic plaques). Furthermore, the oxLDL contribution to NLRP3 inflammasome activation was assessed using *in vitro* models.

Results: High levels of oxLDL were identified in plasma from OSA patients, particularly in those with eSA, as well as an overexpression of NLRP3 cascade components and TF. Furthermore, *in vitro* models showed that oxLDL present in plasma from OSA patients with eSA, through its receptor CD36, act synergistically with intermittent hy-

poxia as a priming and activation signal of NLRP3 inflammasome, enhancing the inflammatory response and triggering pyroptosis. Finally, our results suggest a role of NLRP3-pyroptosis axis in the release of TF into plasma, which levels were higher in patients with eSA.



Summary of inflammasome activation mediated by oxidised low-density lipoprotein (oxLDL) in obstructive sleep apnoea (OSA) patients with sleep apnoea and early sub-clinical atherosclerosis. In patients with OSA, the priming signal of NLRP3 is triggered by intermittent hypoxia (IH), inducing hypoxia inducible factor (HIF)-1 α activation and in combination with the presence of oxLDL in OSA plasma. The NLRP3 activation by IH and soluble factors from plasma in OSA patients was previously demonstrated by DIAZ-GARCIA [21]. oxLDL, through CD36 recognition, may play a role in both NLRP3 priming and activation pathways. This NLRP3 activation drives the formation of a multiprotein complex, triggering caspase-1 (CASP1), which cleaves gasdermin D (GSDMD), leading to pyroptosis and interleukin (IL)-1 β and tissue factor (TF) release. TF levels are related to early atherosclerosis and the development of subclinical atherothrombosis. HRE: hypoxia responsive element.

Conclusions: OSA patients with eSA exhibit NLRP3 activation mediated by intermittent hypoxia and the presence of high plasma oxLDL levels, constituting a pathway for the interaction between dyslipidemia and systemic inflammation in the development of atherosclerotic lesions. In addition, NLRP3 activation may underlie elevated plasma TF levels found in patients with OSA and eSA, potentially contributing to the increased cardiovascular risk of these patients.

Funding: This study was supported by grants from Fondo de Investigación Sanitaria (FIS) and European Regional Development Funds PI13/01512, PI16/00201, and PI19/01612 to F. García-Río; PI12/02175, PI15/01949 and PI18/01524 to Jose M. Marin and CP18/00028 and PI19-01363 to C. Cubillos-Zapata. Funding information for this article has been deposited with the Crossref Funder Registry.

12. IMPAIRED KALLIKREIN-KININ SYSTEM IN COVID-19 PATIENTS' SEVERITY

Enrique Alfaro^{1,2,3}, Elena Díaz-García^{1,2}, Sara García-Tovar¹, Ester Zamarrón^{1,2}, Alberto Mangas^{1,2}, Raúl Galera^{1,2}, Kapil Nanwani-Nanwani⁴, Rebeca Pérez-de-Diego^{5,6}, Eduardo López-Collazo⁷, Francisco García-Río^{1,2,3}, Carolina Cubillos-Zapata^{1,2}

¹Grupo de Enfermedades Respiratorias, Servicio de Neumología, Hospital Universitario de La Paz, IdiPAZ, Madrid, Spain. ²Centro de Investigación Biomédica en Red de Enfermedades Respiratorias (CIBERES), Madrid, Spain. ³Facultad de Medicina Universidad Autónoma de Madrid, Madrid, Spain. ⁴Departamento de Medicina Intensiva Hospital Universitario La Paz, Madrid, Spain. ⁵Laboratorio de Inmunogenética de Enfermedades Humanas Hospital Universitario La Paz, Madrid, Spain. ⁶Grupo Interdepartamental de Inmunodeficiencias, IdiPAZ, Madrid, Spain. ⁷Grupo de Respuesta Inmune Innata, IdiPAZ, Madrid, Spain.

Introduction: COVID-19 has emerged as a devastating disease in the last 3 years. Many authors appointed to the importance of

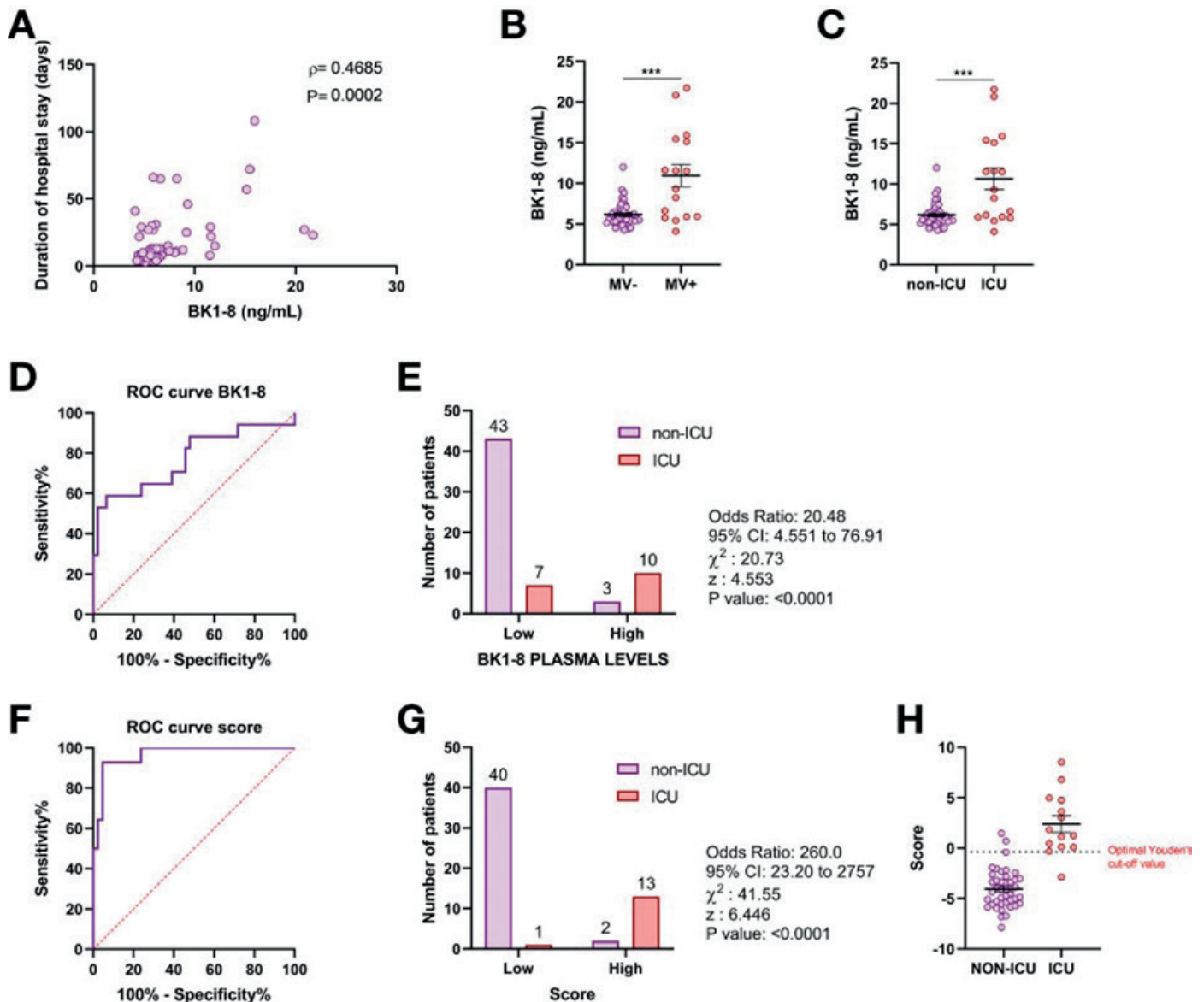
kallikrein-kinin system (KKS) in COVID-19 pathophysiology as it is involved in inflammation, vascular homeostasis, and coagulation. The KKS is a complex regulatory system of vascular homeostasis which include multiple peptides and enzymes including angiotensin converting enzyme 2 (ACE2) which is the main target for SARS-CoV-2 internalization in host cells.

Objectives: We aim to study the bradykinin cascade and its involvement in severity of patients with COVID-19.

Methods: This is an observational cohort study involving 63 consecutive patients with severe COVID-19 pneumonia and 27 healthy subjects as control group. Clinical laboratory findings and plasma protein concentration of KKS peptides [bradykinin (BK) and BK1-8], KKS proteins [high molecular weight kininogen (HK)], and KKS enzymes [carboxypeptidase N subunit 1 (CPN1), kallikrein B1 (KLKB1), angiotensin converting enzyme 2 (ACE2), and C1 esterase inhibitor (C1INH)] were analyzed.

Results: We detected dysregulated KKS in patients with COVID-19, characterized by an accumulation of BK1-8 in combination with decreased levels of BK. Accumulated BK1-8 was related to severity of patients with COVID-19. A multivariate logistic regression model retained BK1-8, BK, and D-dimer as independent predictor factors to intensive care unit (ICU) admission. A Youden's optimal cutoff value of -0.352 was found for the multivariate model score with an accuracy of 92.9%. Multivariate model score-high group presented an odds ratio for ICU admission of 260.0. BK1-8 was related to inflammation, coagulation, and lymphopenia markers.

Conclusions: Our data suggest that BK1-8/BK plasma concentration in combination with D-dimer levels might be retained as independent predictors for ICU admission in patients with COVID-19. Moreover, we reported KKS dysregulation in patients with COVID-19, which was related to disease severity by means of inflammation, hypercoagulation, and lymphopenia.



BK1-8 association with COVID-19 severity. (A) Correlation of BK1-8 plasma concentration and duration of hospital stay (n = 60). Spearman's correlation coefficient and P-value are shown. (B) Comparison of BK1-8 plasma concentration in patients not requiring mechanical ventilation (MV-, n = 47) and those requiring it (MV+, n = 16). (C) Comparison of BK1-8 plasma concentration in patients not derived to ICU (non-ICU, n = 46) and patients derived to ICU (ICU, n = 17). Mean differences were analyzed by Mann-Whitney U-test. Error bars: mean \pm SEM. ***P < 0.001. (D) Receiver operating characteristic (ROC) curve for predictive performance value for ICU admission of BK1-8 (n = 63). (E) Contingency table comparing ICU admission for patients with high and low BK1-8 plasma levels. (F) ROC curve for predictive performance value for ICU admission of multivariate model score (n = 56). (G) Contingency table comparing ICU admission for patients with high and low multivariate model score. ROC curves were analyzed by Wilson/Brown test. Contingency tables were analyzed by chi-squared test. (H) Multivariate model score in patients with COVID-19 not derived to ICU (non-ICU, n = 42) and derived to ICU (ICU, n = 14).

Funding: This research was funded by Health Research Fund (Fondo de Investigación Sanitario [FIS])-European Regional Development Fund (FEDER), Spain, through PI19/01612 (FG-R) and COV20/00207 and PI19-01363 (CC-Z) and ISCIII (CP18/00028), co-funded by ESF, "Investing in your future".

14. SYSTEMATIC ANALYSIS OF SARS-COV-2 CO-INFECTIONS THROUGHOUT THE PANDEMIC AND SEGREGATION OF THE STRAINS INVOLVED

Daniel Peñas-Utrilla¹, Laura Pérez-Lago¹, Andrea Molero-Salinas¹, Agustín Estévez¹, Amadeo Sanz-Pérez¹, Marta Herranz¹, Carolina Martínez-Laperche¹, Cristina Andrés-Zayas¹, Cristina Veintimilla¹, Pilar Catalán¹, Roberto Alonso¹, Patricia Muñoz^{1,2}, Darío García de Viedma^{1,2}

¹Instituto de Investigación Sanitaria Gregorio Marañón (IiSGM), Madrid, Spain. ²Centro de Investigación Biomédica en Red de Enfermedades Respiratorias (CIBERES), Madrid, Spain.

Introduction: Recombination events between SARS-CoV-2 strains of the Delta and Omicron lineages have been described. The recombination requires the coexistence of two SARS-CoV-2 strains in the same individual. However, only a limited number of studies have focused on the identification of co-infections, restricted to co-infections involving Delta/Omicron lineages.

Objectives: This study aims to systematically identify SARS-CoV-2 co-infections throughout the pandemic and segregate the strains involved to allow their analysis.

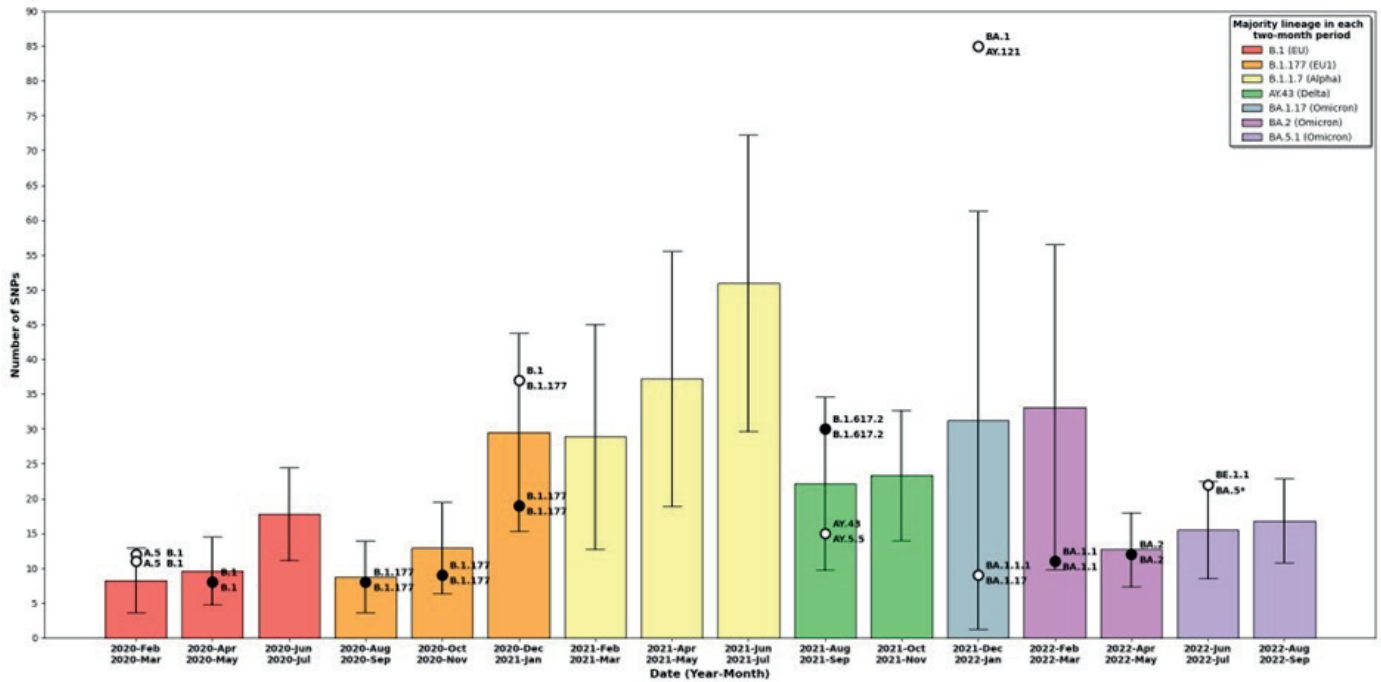
Methods: Whole genome sequencing of SARS-CoV-2 positive samples was performed using ARTIC nCoV-2019 primers; libraries were se-

quenced on a MiSeq instrument. An in-house bioinformatics pipeline allowed us to identify potential co-infections based on the distribution of heterozygous SNPs and to segregate strains implicated in co-infection.

Results: Sequences from the 7,609 COVID-19 patients (March 2020 to September 2022) in our population in Madrid, Spain were analysed. Fourteen co-infections were identified (0.18% of the total), based on the presence of at least 8 robust heterozygous SNP calls (Figure). These coinfections were confirmed through a comprehensive set of validations including: phylogenetic validation, resequencing of the same sample or detection of the coinfection in a separate sample, and Short Tandem Repeats (STR) analysis. Co-infections were identified throughout the pandemic, covering all but one of the pandemic waves. These co-infections not only involved Delta/omicron lineages but half of the cases involved precedent lineages. Coinfections involved either strains from different lineages/sublineages (including pre-Alpha variants, Delta and Omicron) or strains from the same lineage, in equal proportions (see Table). Analysis of additional samples from five co-infected cases revealed four persistent co-infections and one case where one strain outcompeted the other. The co-infected cases were mainly unvaccinated, with a mild or asymptomatic clinical presentation and most were at risk of overexposure associated with the healthcare setting (57.1%). In addition, strain segregation enabled the integration of sequences to clarify their involvement in nosocomial outbreaks where analysis had been impaired due to co-infection.

Conclusions: Co-infection cases were identified throughout the pandemic and were not restricted to Delta/Omicron lineages. Co-infections involving strains from different lineages or strains from the same lineage were occurring in the same proportion. Most cases were mild, did not require medical care, were unvaccinated and a large proportion were associated with the hospital environment. Segrega-

Patient	Sample	Ct_N2	COV >30X	Total_HTZ	Mean_htz_proportion	Std_htz_proportion	%_SNPs_between_std	Min_pangolin	Max_pangolin	Date
1	64404512	n.a	99,69	12	0,66	0,04	0,83	A.5	B.1	2020-03-09
	64404512-BIS	n.a	99,58	12	0,67	0,02	0,83	A.5	B.1	2020-03-09
2	64404505	n.a	99,08	11	0,64	0,03	0,91	A.5	B.1	2020-03-09
	64404505-BIS	n.a	99,58	12	0,63	0,07	0,92	A.5	B.1	2020-03-09
3	64431418	n.a	99,02	8	0,73	0,03	0,88	B.1	B.1	2020-04-08
	64431418-BIS	n.a	99,1	8	0,66	0,05	0,88	B.1	B.1	2020-04-08
4	64601021	20	99,66	8	0,66	0,04	0,75	B.1.177	B.1.177	2020-08-11
	64601021-BIS	20	99,58	8	0,67	0,03	0,88	B.1.177	B.1.177	2020-08-11
5	64875518	25	98,71	9	0,54	0,03	1	B.1.177	B.1.177	2020-11-01
	64875518-BIS	25	99,02	9	0,55	0,04	0,89	B.1.177	B.1.177	2020-11-01
6	65468636	31	99,02	37	0,6	0,05	0,76	B.1.177	B.1	2021-01-18
	65486708	14	98,97	37	0,76	0,06	0,89	B.1	B.1.177	2021-01-27
	65496510	22	99,58	1	0,52	0	1	B.1.177	B.1.177	2021-02-01
7	65474622	16	99,58	19	0,78	0,03	0,95	B.1.177	B.1.177	2021-01-21
	65474716	18	99,67	19	0,61	0,04	0,84	B.1.177	B.1.177	2021-01-21
8	65785846	25	98,79	30	0,55	0,06	0,9	B.1.617.2	B.1.617.2	2021-08-08
	65785846-BIS	25	99,56	32	0,57	0,04	0,91	B.1.617.2	B.1.617.2	2021-08-08
9	65792349	26	99,67	15	0,58	0,03	0,93	AY.5.5	AY.43	2021-08-25
	65792349-BIS	26	99,66	15	0,64	0,03	0,73	AY.5.5	AY.43	2021-08-25
10	65955285	12	98,44	9	0,71	0,03	0,89	BA.1.17	BA.1.1.1	2021-12-14
	65955285-BIS	12	98,41	9	0,74	0,05	0,89	BA.1.17	BA.1.1.1	2021-12-14
11	65951829	16	99,62	85	0,71	0,07	0,74	AY.121	BA.1	2021-12-17
	65951829-BIS	16	99,58	89	0,76	0,04	0,79	AY.121	BA.1	2021-12-17
	65978408	29	99,58	1	0,81	0	1	AY.121	AY.121	2021-12-23
12	66400368	18	98,73	9	0,7	0,07	0,67	BA.1.1	BA.1.1	2022-02-09
	66415447	31	98,91	11	0,73	0,04	0,73	BA.1.1	BA.1.1	2022-02-11
13	66516800	14	99,3	12	0,57	0,07	0,92	BA.2	BA.2	2022-05-12
	66511040	23	98,69	11	0,53	0,02	0,91	BA.2	BA.2	2022-05-17
14	66663744	18	98,61	22	0,7	0,05	0,82	BA.5*	BE.1.1	2022-06-27
	66671149	28	95	14	0,79	0,05	0,86	BA.5	BE.1.1	2022-07-08



Epidemiological validation of the co-infections. Each bar corresponds to the mean pairwise SNP distance and standard deviation between any two circulating strains in our population in each two-month period during the pandemic. Each black dot or open circle corresponds to a co-infected case and is plotted by taking into account the number of SNPs between co-infecting strains. Co-infections involving strains from the same or different lineage/sublineages are shown as black dots or open circles, respectively. The majority and minority lineages involved in each co-infection are shown top and bottom, respectively (except for the first 2-month period where they are shown as left and right). The colour of the bar indicates the majority lineage in each period (see legend).

tion of the strains involved in co-infection allowed longitudinal intra-patient analysis of the strains and their integration into population-based surveillance.

Funding: This work was supported by the Instituto de Salud Carlos III (PI21/01823) together with the FEDER fund “A way of making Europe”, and the ECDC (2021/PHF/23776). Miguel Servet Contract (CPII20/00001) to LPL. 2022-II-PREDOC-IA-01 intramural contract from IISGM to DPU. Patient sequence/specimen characteristics of validated SARS-CoV-2 co-infections. *Lineage assigned after discarding segregated positions with lower confidence.

16. FREQUENT EMERGENCE OF RESISTANCE MUTATIONS FOLLOWING COMPLEX INTRA-HOST GENOMIC DYNAMICS IN SARS-COV-2 PATIENTS RECEIVING SOTROVIMAB

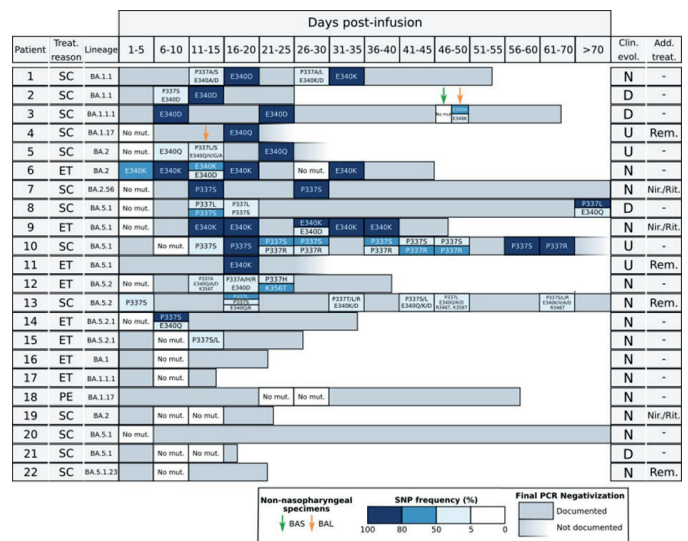
Rosalía Palomino-Cabrera¹, Francisco Tejerina^{1,2}, Andrea Molero-Salinas¹, María Ferris¹, Cristina Veintimilla¹, Pilar Catalán¹, Gabriela Rodríguez Macías¹, Roberto Alonso¹, Patricia Muñoz^{1,3}, Darío García de Viedma^{1,3}, Laura Pérez-Lago¹

¹Servicio de Microbiología Clínica y Enfermedades infecciosas; Instituto de Investigación Sanitaria Gregorio Marañón, Madrid, Spain. ²Centro de Investigación Biomédica en Red de Enfermedades infecciosas (CIBERINFEC), Madrid, Spain. ³Centro de Investigación Biomédica en Red de Enfermedades respiratorias (CIBERES), Madrid, Spain.

Introduction: The emergence of the SARS-CoV-2 Omicron variant has had a major impact on the treatment of COVID-19 due to its intrinsic resistance to most monoclonal antibodies (mAbs). However, Sotrovimab, which targets an epitope in the receptor-binding domain (RBD) of the spike protein, maintains partial *in vitro* activity against different Omicron sublineages. In Spain, Sotrovimab has been authorized since December 2021 for high-risk patients or as compassionate use in hospitalized immunocompromised seronegative patients with severe COVID-19.

Objectives: The aim of this study is to trace the acquisition of resistance mutations to Sotrovimab in patients who have been receiving this treatment at our institution since its approval and determine their intra-host dynamics.

Methods: We conducted a retrospective study of 28 COVID-19 immunocompromised patients who had received a Sotrovimab infusion



Sotrovimab resistance mutations identified in the patients in study. Each horizontal bar corresponds to the RT-PCR positivity period for each patient. For the specimens which were sequenced we indicated if we detected or not mutations and the colour gradient indicates the allele frequencies for the SNPs identified. The reasons for Sotrovimab treatment: SC (severe COVID), ET (early treatment) or PE (SARS-CoV-2 persistence) and the clinical evolution: D (died), N (negativization documented by RT-PCR), U (undefined negativization due to lack of a negative PCR) are indicated. Those patients with additional anti-viral treatment (Add. Treat) other than Sotrovimab are specified: Rem (remdesivir), Nir./Rit. (nirmatrelvir/ritonavir, paxlovid). BAL/BAS specimens are highlighted by arrows.

Patient	Days	GenN2_Ct	Resistance mutations (frequency)	Sample	Lineage	STRs	ENA		GISAID	
							R1 fastq	R2 fastq	EPI_SET ID	Virus name
1	-2	25.0	-	NP	BA.1.1		6476398_R1.fastq.gz	6476398_R2.fastq.gz	EPI_ISL_16980979	hCoV-19/Spain/MD-HGUGM-6476398/2022
	11	22.3	P337S (35%), P337A (6%), E340A (13%), E340D (13%)	NP	BA.1.1		6499076_R1.fastq.gz	6499076_R2.fastq.gz	EPI_ISL_16980980	hCoV-19/Spain/MD-HGUGM-6499076/2022
	20	30.0	E340D (94%)	NP	BA.1.1		6401941_R1.fastq.gz	6401941_R2.fastq.gz	EPI_ISL_16980981	hCoV-19/Spain/MD-HGUGM-6401941/2022
	26	32.0	P3337A (7%), P337L (25%), E340K (15%), E340D (44%)	NP	BA.1.1	Same host	6410096_R1.fastq.gz	6410096_R2.fastq.gz	EPI_ISL_16980982	hCoV-19/Spain/MD-HGUGM-6410096/2022
	35	18.0	E340K (100%)	NP	BA.1.1	Same host	6429316_R1.fastq.gz	6429316_R2.fastq.gz	EPI_ISL_16980983	hCoV-19/Spain/MD-HGUGM-6429316/2022
2	-1	25.0	-	NP	BA.1.1		6429993_R1.fastq.gz	6429993_R2.fastq.gz	EPI_ISL_10680589	hCoV-19/Spain/MD-HGUGM-6429993/2022
	6	19.0	P337S (8%), E340D (23%)	NP	BA.1.1		6439980_R1.fastq.gz	6439980_R2.fastq.gz	EPI_ISL_16980992	hCoV-19/Spain/MD-HGUGM-6439980/2022
	13	16.0	E340D (95%)	NP	BA.1.1		6548194_R1.fastq.gz	6548194_R2.fastq.gz	EPI_ISL_16980993	hCoV-19/Spain/MD-HGUGM-6548194/2022
3	-3	24.0	-	NP	BA.1.1.1		6492151_R1.fastq.gz	6492151_R2.fastq.gz	EPI_ISL_16981066	hCoV-19/Spain/MD-HGUGM-6492151/2022
	8	16.0	E340D (96%)	NP	BA.1.1.1		6410608_R1.fastq.gz	6410608_R2.fastq.gz	EPI_ISL_16981067	hCoV-19/Spain/MD-HGUGM-6410608/2022
	22	26.0	E340D (100%)	NP	BA.1.1.1	Same host	6435900_R1.fastq.gz	6435900_R2.fastq.gz	EPI_ISL_16981068	hCoV-19/Spain/MD-HGUGM-6435900/2022
	47	22.0	-	BAS	BA.1.1.1	Same host	6562623_R1.fastq.gz	6562623_R2.fastq.gz	EPI_ISL_16981069	hCoV-19/Spain/MD-HGUGM-6562623/2022
	49	24.0	E340K (29%), E340A (67%)	BAL	BA.1.1.1	Same host	6574618_R1.fastq.gz	6574618_R2.fastq.gz	EPI_ISL_16981070	hCoV-19/Spain/MD-HGUGM-6574618/2022
4	-6	26.0	-	NP	BA.1.17		6454099_R1.fastq.gz	6454099_R2.fastq.gz	EPI_ISL_16981035	hCoV-19/Spain/MD-HGUGM-6454099/2022
	5	28.0	-	NP	BA.1.17		6475538_R1.fastq.gz	6475538_R2.fastq.gz	EPI_ISL_16981036	hCoV-19/Spain/MD-HGUGM-6475538/2022
	16	28.0	E340Q (100%)	NP	BA.1.17		6482093_R1.fastq.gz	6482093_R2.fastq.gz	EPI_ISL_16981037	hCoV-19/Spain/MD-HGUGM-6482093/2022
5	3	23.0	-	NP	BA.2		6671573_R1.fastq.gz	6671573_R2.fastq.gz	EPI_ISL_16980987	hCoV-19/Spain/MD-HGUGM-6671573/2022
	7	31.0	E340Q (9%)	NP	BA.2		6672844_R1.fastq.gz	6672844_R2.fastq.gz	EPI_ISL_16980988	hCoV-19/Spain/MD-HGUGM-6672844/2022
	10	24.0	E340Q (7%)	NP	BA.2	Same host	6694664_R1.fastq.gz	6694664_R2.fastq.gz	EPI_ISL_16980989	hCoV-19/Spain/MD-HGUGM-6694664/2022
	11	27.0	P337L (8%), P337S (18%), E340Q (7%), E340V (7%), E340G (7%), E340A (39%)	BAL	BA.2	Same host	6697660_R1.fastq.gz	6697660_R2.fastq.gz	EPI_ISL_16980990	hCoV-19/Spain/MD-HGUGM-6697660/2022
	22	26.0	E340Q (89%)	NP	BA.2		6680820_R1.fastq.gz	6680820_R2.fastq.gz	EPI_ISL_16980991	hCoV-19/Spain/MD-HGUGM-6680820/2022
6	-2	19.2	-	NP	BA.2		6515896_R1.fastq.gz	6515896_R2.fastq.gz	EPI_ISL_16980998	hCoV-19/Spain/MD-HGUGM-6515896/2022
	5	14.7	E340K (58%)	NP	BA.2		6511722_R1.fastq.gz	6511722_R2.fastq.gz	EPI_ISL_16980999	hCoV-19/Spain/MD-HGUGM-6511722/2022
	6	16.0	E340K (24%)	NP	BA.2		6511919_R1.fastq.gz	6511919_R2.fastq.gz	EPI_ISL_16981000	hCoV-19/Spain/MD-HGUGM-6511919/2022
	9	20.0	E340K (95%)	NP	BA.2		6525312_R1.fastq.gz	6525312_R2.fastq.gz	EPI_ISL_16981001	hCoV-19/Spain/MD-HGUGM-6525312/2022
	13	23.4	E340K (77%), E340D (18%)	NP	BA.2		6526289_R1.fastq.gz	6526289_R2.fastq.gz	EPI_ISL_16981002	hCoV-19/Spain/MD-HGUGM-6526289/2022
	19	22.8	E340K (100%)	NP	BA.2		6522946_R1.fastq.gz	6522946_R2.fastq.gz	EPI_ISL_16981003	hCoV-19/Spain/MD-HGUGM-6522946/2022
	26	28.0	-	NP	BA.2		6539039_R1.fastq.gz	6539039_R2.fastq.gz	EPI_ISL_16981004	hCoV-19/Spain/MD-HGUGM-6539039/2022
	33	28.0	E340K (98%)	NP	BA.2		6643220_R1.fastq.gz	6643220_R2.fastq.gz	EPI_ISL_16981005	hCoV-19/Spain/MD-HGUGM-6643220/2022

(Cont)

Patient	Days	GenN2_Ct	Resistance mutations (frequency)	Sample	Lineage	STRs	ENA		GISAID	
							R1 fastq	R2 fastq	EPI_SET ID	Virus name
7	-1	21.0	-	NP	BA.2.56		6606849_R1.fastq.gz	6606849_R2.fastq.gz	EPI_ISL_16981023	hCoV-19/Spain/MD-HGUGM-6606849/2022
	5	20.0	-	NP	BA.2.56		6600931_R1.fastq.gz	6600931_R2.fastq.gz	EPI_ISL_16981024	hCoV-19/Spain/MD-HGUGM-6600931/2022
	14	24.0	P337S (96%)	NP	BA.2.56		6619433_R1.fastq.gz	6619433_R2.fastq.gz	EPI_ISL_16981025	hCoV-19/Spain/MD-HGUGM-6619433/2022
	26	30.0	P337S (84%)	NP	BA.2.56		6612465_R1.fastq.gz	6612465_R2.fastq.gz	EPI_ISL_16981026	hCoV-19/Spain/MD-HGUGM-6612465/2022
8	-7	18.3	-	NP	BA.5.1		6643810_R1.fastq.gz	6643810_R2.fastq.gz	EPI_ISL_13343191	hCoV-19/Spain/MD-HGUGM-6643810/2022
	4	16.0	-	NP	BA.5.1		6659538_R1.fastq.gz	6659538_R2.fastq.gz	EPI_ISL_16980976	hCoV-19/Spain/MD-HGUGM-6659538/2022
	11	14.0	P337S (66%), P337L (28%)	NP	BA.5.1		6663630_R1.fastq.gz	6663630_R2.fastq.gz	EPI_ISL_16980977	hCoV-19/Spain/MD-HGUGM-6663630/2022
	19	18.0	P337S (34%), P337L (46%)	NP	BA.5.1		6675169_R1.fastq.gz	6675169_R2.fastq.gz	EPI_ISL_16980978	hCoV-19/Spain/MD-HGUGM-6675169/2022
	107	16.1	P337L (85%), E340Q (14%)	NP	BA.5.1		6757020_R1.fastq.gz	6757020_R2.fastq.gz	EPI_ISL_15284361	hCoV-19/Spain/MD-HGUGM-6757020/2022
9	4	24.0	-	NP	BA.5.1		6680194_R1.fastq.gz	6680194_R2.fastq.gz	EPI_ISL_16981009	hCoV-19/Spain/MD-HGUGM-6680194/2022
	12	26.0	E340K (35%)	NP	BA.5.1		6606993_R1.fastq.gz	6606993_R2.fastq.gz	EPI_ISL_16981010	hCoV-19/Spain/MD-HGUGM-6606993/2022
	14	18.3	E340K (96%)	NP	BA.5.1		6606293_R1.fastq.gz	6606293_R2.fastq.gz	EPI_ISL_16981011	hCoV-19/Spain/MD-HGUGM-6606293/2022
	18	16.0	E340K (99%)	NP	BA.5.1		6600129_R1.fastq.gz	6600129_R2.fastq.gz	EPI_ISL_16981012	hCoV-19/Spain/MD-HGUGM-6600129/2022
	26	22.0	E340K (85%), E340D (15%)	NP	BA.5.1		6619487_R1.fastq.gz	6619487_R2.fastq.gz	EPI_ISL_16981013	hCoV-19/Spain/MD-HGUGM-6619487/2022
	32	23.0	E340K (100%)	NP	BA.5.1		6619315_R1.fastq.gz	6619315_R2.fastq.gz	EPI_ISL_16981014	hCoV-19/Spain/MD-HGUGM-6619315/2022
	38	24.0	E340K (100%)	NP	BA.5.1		6612466_R1.fastq.gz	6612466_R2.fastq.gz	EPI_ISL_16981015	hCoV-19/Spain/MD-HGUGM-6612466/2022
10	-1	19.1	-	NP	BA.5.1		6689576_R1.fastq.gz	6689576_R2.fastq.gz	EPI_ISL_16981038	hCoV-19/Spain/MD-HGUGM-6689576/2022
	6	28.0	-	NP	BA.5.1		6680824_R1.fastq.gz	6680824_R2.fastq.gz	EPI_ISL_16981039	hCoV-19/Spain/MD-HGUGM-6680824/2022
	14	26.0	P337S (17%)	NP	BA.5.1		6606779_R1.fastq.gz	6606779_R2.fastq.gz	EPI_ISL_16981040	hCoV-19/Spain/MD-HGUGM-6606779/2022
	18	26.0	P337S (99%)	NP	BA.5.1		6600468_R1.fastq.gz	6600468_R2.fastq.gz	EPI_ISL_14921010	hCoV-19/Spain/MD-HGUGM-6600468/2022
	21	23.0	P337S (58%), P337R (24%)	NP	BA.5.1		6600138_R1.fastq.gz	6600138_R2.fastq.gz	EPI_ISL_16981041	hCoV-19/Spain/MD-HGUGM-6600138/2022
	29	18.9	P337S (59%), P337R (24%)	NP	BA.5.1		6619456_R1.fastq.gz	6619456_R2.fastq.gz	EPI_ISL_16981042	hCoV-19/Spain/MD-HGUGM-6619456/2022
	37	25.0	P337S (64%), P337R (19%)	NP	BA.5.1		6611774_R1.fastq.gz	6611774_R2.fastq.gz	EPI_ISL_16981043	hCoV-19/Spain/MD-HGUGM-6611774/2022
	44	26.0	P337S (30%), P337R (69%)	NP	BA.5.1		6612967_R1.fastq.gz	6612967_R2.fastq.gz	EPI_ISL_16981044	hCoV-19/Spain/MD-HGUGM-6612967/2022
	49	22.0	P337S (43%), P337R (50%)	NP	BA.5.1		6638731_R1.fastq.gz	6638731_R2.fastq.gz	EPI_ISL_16981045	hCoV-19/Spain/MD-HGUGM-6638731/2022
	56	24.0	P337S (98%)	NP	BA.5.1	Same host	6639006_R1.fastq.gz	6639006_R2.fastq.gz	EPI_ISL_16981046	hCoV-19/Spain/MD-HGUGM-6639006/2022
11	-1	17.4	-	NP	BA.5.1	Same host	6748850_R1.fastq.gz	6748850_R2.fastq.gz	EPI_ISL_16981047	hCoV-19/Spain/MD-HGUGM-6748850/2022
	68	18.0	P337R (100%)	NP	BA.5.1		6741028_R1.fastq.gz	6741028_R2.fastq.gz	EPI_ISL_16981048	hCoV-19/Spain/MD-HGUGM-6741028/2022
	18	27.0	E340K (95%)	NP	BA.5.1		6605646_R1.fastq.gz	6605646_R2.fastq.gz	EPI_ISL_16981059	hCoV-19/Spain/MD-HGUGM-6605646/2022
										hCoV-19/Spain/MD-HGUGM-6614076/2022

(Cont)

(500 mg) between December 2021 and August 2022. We performed genomic analyses on positive samples (Ct ≤ 32) ≥ 3 days after Sotrovimab infusion, focusing on the mutations conferring resistance to Sotrovimab reported in assays on cellular cultures and clinical studies.

Results: We obtained genomic data from 95 samples from 22 patients (1-12 samples/patient; 3-107 days post-infusion). 14 different substitutions involved in Sotrovimab resistance were identified in 15 cases (68%) since day 5 post-treatment. They were located in P337, E340,

Patient	Days	GenN2_Ct	Resistance mutations (frequency)	Sample	Lineage	STRs	ENA		GISAID	
							R1 fastq	R2 fastq	EPI_SET ID	Virus name
12	-1	12.7	-	NP	BA.5.2		6659324_R1.fastq.gz	6659324_R2.fastq.gz	EPI_ISL_13577617	hCoV-19/Spain/MD-HGUGM-6659324/2022
	5	19.0	-	NP	BA.5.2		6663154_R1.fastq.gz	6663154_R2.fastq.gz	EPI_ISL_16981019	hCoV-19/Spain/MD-HGUGM-6663154/2022
	11	24.0	P337A (5%), E340Q (14%), E340A (8%), E340D (16%), E340D (20%), K356T (33%)	NP	BA.5.2		6675795_R1.fastq.gz	6675795_R2.fastq.gz	EPI_ISL_16981020	hCoV-19/Spain/MD-HGUGM-6675795/2022
	19	26.0	P337A (26%), P337H (35%), P337R (6%), E340D (20%)	NP	BA.5.2	Same host	6672924_R1.fastq.gz	6672924_R2.fastq.gz	EPI_ISL_16981021	hCoV-19/Spain/MD-HGUGM-6672924/2022
	25	29.0	P337H (7%), K356T (65%)	NP	BA.5.2	Same host	6694215_R1.fastq.gz	6694215_R2.fastq.gz	EPI_ISL_16981022	hCoV-19/Spain/MD-HGUGM-6694215/2022
13	-7	13.4	-	NP	BA.5.2		6694819_R1.fastq.gz	6694819_R2.fastq.gz	EPI_ISL_16981050	hCoV-19/Spain/MD-HGUGM-6694819/2022
	5	14.2	P337S (5%)	NP	BA.5.2		6680142_R1.fastq.gz	6680142_R2.fastq.gz	EPI_ISL_16981051	hCoV-19/Spain/MD-HGUGM-6680142/2022
	20	15.0	P337S (22%), P337L (59%), E340Q (6%), E340K (6%)	NP	BA.5.2		6614473_R1.fastq.gz	6614473_R2.fastq.gz	EPI_ISL_16981052	hCoV-19/Spain/MD-HGUGM-6614473/2022
	34	15.0	P337T (6%), P337L (38%), P337R (13%), E340K (15%), E340D (17%)	NP	BA.5.2		6611513_R1.fastq.gz	6611513_R2.fastq.gz	EPI_ISL_16981053	hCoV-19/Spain/MD-HGUGM-6611513/2022
	41	18.0	P337S (5%), P337L (24%), E340Q (11%), E340K (33%), E340D (19%)	NP	BA.5.2		6612856_R1.fastq.gz	6612856_R2.fastq.gz	EPI_ISL_16981054	hCoV-19/Spain/MD-HGUGM-6612856/2022
	48	18.0	P337L (23%), E340Q (9%), E340K (29%), E340D (12%), R346T (8%), K356T (14%)	NP	BA.5.2		6638060_R1.fastq.gz	6638060_R2.fastq.gz	EPI_ISL_16981055	hCoV-19/Spain/MD-HGUGM-6638060/2022
	67	18.0	P337S (19%), P337L (14%), P337R (6%), E340K (27%), E340V (6%), E340A (10%), E340D (9%), R346T (20%)	NP	BA.5.2		6741358_R1.fastq.gz	6741358_R2.fastq.gz	EPI_ISL_16981056	hCoV-19/Spain/MD-HGUGM-6741358/2022
14	-1	15.5	-	NP	BA.5.2.1		6694207_R1.fastq.gz	6694207_R2.fastq.gz	EPI_ISL_16980984	hCoV-19/Spain/MD-HGUGM-6694207/2022
	4	14.0	-	NP	BA.5.2.1		6680547_R1.fastq.gz	6680547_R2.fastq.gz	EPI_ISL_16980985	hCoV-19/Spain/MD-HGUGM-6680547/2022
	10	21.0	P337S (82%), E340Q (7%)	NP	BA.5.2.1		6605622_R1.fastq.gz	6605622_R2.fastq.gz	EPI_ISL_16980986	hCoV-19/Spain/MD-HGUGM-6605622/2022
15	-1	25.0	-	NP	BA.5.2.1		6675119_R1.fastq.gz	6675119_R2.fastq.gz	EPI_ISL_16980994	hCoV-19/Spain/MD-HGUGM-6675119/2022
	6	15.0	-	NP	BA.5.2.1		6672923_R1.fastq.gz	6672923_R2.fastq.gz	EPI_ISL_16980995	hCoV-19/Spain/MD-HGUGM-6672923/2022
	11	17.0	-	NP	BA.5.2.1		6694098_R1.fastq.gz	6694098_R2.fastq.gz	EPI_ISL_16980996	hCoV-19/Spain/MD-HGUGM-6694098/2022
	14	21.0	P337S (5%), P337L (6%)	NP	BA.5.2.1		6689899_R1.fastq.gz	6689899_R2.fastq.gz	EPI_ISL_16980997	hCoV-19/Spain/MD-HGUGM-6689899/2022
16	7	25.0	-	NP	BA.1		5984788_R1.fastq.gz	5984788_R2.fastq.gz	EPI_ISL_16981057	hCoV-19/Spain/MD-HGUGM-5984788/2021
	10	26.0	-	NP	BA.1		5981371_R1.fastq.gz	5981371_R2.fastq.gz	EPI_ISL_16981058	hCoV-19/Spain/MD-HGUGM-5981371/2021
17	7	22.0	-	NP	BA.1.1.1		5981621_R1.fastq.gz	5981621_R2.fastq.gz	EPI_ISL_16981049	hCoV-19/Spain/MD-HGUGM-5981621/2021

(Cont)

Patient	Days	GenN2_Ct	Resistance mutations (frequency)	Sample	Lineage	STRs	ENA		GISAID	
							R1 fastq	R2 fastq	EPI_SET ID	Virus name
18	-1	30.0	-	NP	BA.1.17		6550115_R1.fastq.gz	6550115_R2.fastq.gz	EPI_ISL_16981006	hCoV-19/Spain/MD-HGUGM-6550115/2022
	21	22.6	-	NP	BA.1.17		6585286_R1.fastq.gz	6585286_R2.fastq.gz	EPI_ISL_16981007	hCoV-19/Spain/MD-HGUGM-6585286/2022
	27	29.0	-	NP	BA.1.17		6588282_R1.fastq.gz	6588282_R2.fastq.gz	EPI_ISL_16981008	hCoV-19/Spain/MD-HGUGM-6588282/2022
19	-3	23.6	-	NP	BA.2		6694058_R1.fastq.gz	6694058_R2.fastq.gz	EPI_ISL_16981016	hCoV-19/Spain/MD-HGUGM-6694058/2022
	6	28.0	-	NP	BA.2		6680882_R1.fastq.gz	6680882_R2.fastq.gz	EPI_ISL_16981017	hCoV-19/Spain/MD-HGUGM-6680882/2022
	13	32.0	-	NP	BA.2		6606584_R1.fastq.gz	6606584_R2.fastq.gz	EPI_ISL_16981018	hCoV-19/Spain/MD-HGUGM-6606584/2022
20	-3	17.7	-	NP	BA.5.1		6694191_R1.fastq.gz	6694191_R2.fastq.gz	EPI_ISL_14258147	hCoV-19/Spain/MD-HGUGM-6694191/2022
	1	22.0	-	BAL	BA.5.1		6692733_R1.fastq.gz	6692733_R2.fastq.gz	EPI_ISL_16981061	hCoV-19/Spain/MD-HGUGM-6692733/2022
	5	24.0	-	NP	BA.5.1		6680802_R1.fastq.gz	6680802_R2.fastq.gz	EPI_ISL_16981062	hCoV-19/Spain/MD-HGUGM-6680802/2022
21	-8	18.0	-	NP	BA.5.1		6680711_R1.fastq.gz	6680711_R2.fastq.gz	EPI_ISL_14258126	hCoV-19/Spain/MD-HGUGM-6680711/2022
	8	25.7	-	NP	BA.5.1		6600361_R1.fastq.gz	6600361_R2.fastq.gz	EPI_ISL_16981063	hCoV-19/Spain/MD-HGUGM-6600361/2022
	14	24.0	-	NP	BA.5.1		6614159_R1.fastq.gz	6614159_R2.fastq.gz	EPI_ISL_16981064	hCoV-19/Spain/MD-HGUGM-6614159/2022
22	7	19.0	-	NP	BA.5.1.23		6539175_R1.fastq.gz	6539175_R2.fastq.gz	EPI_ISL_16981034	hCoV-19/Spain/MD-HGUGM-6539175/2022

R346 and K356 codons (most commonly in P337 and E340). Twelve of the cases eventually fixed at least one of those changes along the course of the infection. The dynamics of resistance acquisition were highly complex, with up to 11 distinct amino acid changes in specimens from the same individual. Also, two individuals showed a different distribution of mutations in respiratory specimens from different compartments. Patients acquiring resistance mutations showed a significant increase in the average days needed for viral clearance (40.67 vs 19.5 days; $p = 0.003$). Three out of the four patients who died due to COVID-19 had fixed mutations. Our study adds BA.5 to the lineages showing acquisition to resistance mutations, without finding genomic or clinical differences between BA.5 and BA.1/BA.2 sublineages.

Conclusions: Genomic analysis of SARS-CoV-2 patients treated with Sotrovimab has shown that i) resistance mutations were acquired (since day 5 post-treatment) in 68% of cases, ii) the distribution of resistance mutations may differ in different respiratory compartments and iii) the appearance of resistance mutations increases the time needed for viral clearance, regardless of the Omicron variants involved.

Funding: ISCIII (PI21/01823, CPII20/00001), IISGM (2021-II-PI-01) and European Regional Development Funds (FEDER) from the European Commission, "A way of making Europe".

19. THE S.P.I.R.E.S. SCORE AND MORTALITY TRENDS IN ACUTE RESPIRATORY DISTRESS SYNDROME

Jesús María González¹, Estrella Gómez¹, Cristina Fernández¹, Rosa Fernández¹, José Manuel Añón², Jesús Villar¹

¹Centro de Investigación Biomédica en Red de Enfermedades Respiratorias (CIBERES), Madrid, Spain, Research Unit, Hospital Universitario Dr. Negrín, Las Palmas de Gran Canaria, Spain. ²Intensive Unit Care, Hospital Universitario La Paz, IdiPaz, Madrid, Spain.

Introduction: Acute respiratory distress syndrome (ARDS) is a severe form of acute hypoxemic respiratory failure developed in patients after inciting injuries. The use of scoring models for stratifying ARDS patients in relation to mortality has not been well characterized.

Objectives: We describe trends in annual ICU mortality in patients with moderate/severe ARDS in relation to the SPIRES (Stratification for identification of Prognostic categories In the acute RESpiratory distress syndrome) score, developed by our group (CCM 2021;49:e920).

Methods: This is an ancillary study of patients enrolled by the SIESTA network. Calendar years with < 100 patients were excluded from analysis. The SPIRES score was based on patient's age (< 50, 50-70, > 70 years), number of extrapulmonary organ failures (< 2, 2, > 2 organs), plateau pressure (< 29, 29-30, > 30 cmH₂O), and PaO₂/FiO₂ ratio (> 200, 101-200, ≤ 100 mmHg) assessed at 24h of ARDS diagnosis. Minimum total score is 4 points and maximum score is 12 points. Primary outcome was ICU mortality.

Results: We analyzed 986 ARDS patients over a 5-year period (2014-2018). Overall ICU mortality of 36.5%. The SPIRES score stratified patients in 3 distinct prognostic classes that followed a relatively uniform pattern through the years, independent of the underlying disease and cause of death. Mean ICU mortality was 14.5 ± 4.9% in Class 1 (SPIRES < 8 points, n = 594), 56.3 ± 11% in Class 2 (SPIRES 8 points, n = 179), and 86 ± 5.3% in Class 3 (SPIRES > 8 points, n = 213) ($p < 0.001$).

Conclusions: The SPIRES score represents a novel strategy for assessing early prognostic categories of patients with ARDS.

Funding: Supported in part by Instituto de Salud Carlos III (CB06/06/1088, PI19/00141) and Fundación Canaria Instituto de Investigación Sanitaria de Canarias (PIFIISC20-51, PIFIISC21-36).

20. MORTALITY TRENDS OF ACUTE RESPIRATORY DISTRESS SYNDROME FROM THE SIESTA NETWORK

Estrella Gómez¹, Cristina Fernández¹, Jesús María González¹, Rosa Fernández¹, José Manuel Añón², Jesús Villar¹

¹Centro de Investigación Biomédica en Red de Enfermedades Respiratorias (CIBERES), Madrid, Spain, Research Unit, Hospital Universitario Dr. Negrín, Las Palmas de Gran Canaria, Spain.

²Intensive Unit Care, Hospital Universitario La Paz, IdiPaz, Madrid, Spain.

Introduction: Acute respiratory distress syndrome (ARDS) is a severe form of acute hypoxemic respiratory failure developed in patients after inciting injuries. The burden of ARDS mortality in the intensive care unit (ICU) has not been well characterized in Spain.

Objectives: We aimed to describe trends in the annual ICU mortality in mechanically ventilated patients with moderate-to-severe ARDS enrolled in several observational studies by the Spanish Initiative for the Epidemiology, Stratification, and Therapy in ARDS (SIESTA) network.

Methods: This is an ancillary study of patients from the SIESTA cohorts. Calendar years with < 100 patients were excluded from analysis. We also described demographic characteristics, categories of severity after assessment under standardized ventilatory settings, and causes of death. Due to sample size, we did not examine annual seasonal variations.

Results: We analyzed a relatively large representative sample of 986 ARDS patients over a 5-year period (2014-2018). Overall ICU mortality of 36.5%. The annual crude ICU mortality did not follow a uniform pattern (ranging from 26.9% to 40.6%). Pneumonia and sepsis were the most common causes of ARDS, and trauma-associated ARDS had the lowest ICU fatality rate. Mortality increased by age [22.4% (< 50 years), 37.3% (50-70 years), 53.5% (> 70 years old)]. Although there were more males than females, both sexes had similar annual mortality (36.3% in women vs. 36.6% in men). Patients with PaO₂/FiO₂ ≤ 100 mmHg at 24h of diagnosis had the highest mortality rate.

Conclusions: Annual ICU mortality rates did not follow a uniform pattern (ranging from 27% to 41%).

Funding: Supported in part by Instituto de Salud Carlos III (CB06/06/1088, PI19/00141) and Fundación Canaria Instituto de Investigación Sanitaria de Canarias (PIFIISC20-51, PIFIISC21-36).

21. CUTIBACTERIUM SPECIES INFECTIVE ENDOCARDITIS IN SPAIN. DATA FROM THE GAMES COHORT (2008-2022)

David Alonso-Menchén¹, Mercedes Marín^{1,2}, Miguel Villamarín³, Nuria Fernández-Hidalgo^{3,4}, Antonio Ramos⁵, Eloy Gómez⁶, Carmen Hidalgo⁷, Aristides de Alarcón⁸, Miguel Ángel Goenaga⁹, M^a Ángeles Rodríguez¹⁰, Elisa García¹¹, Patricia Muñoz^{1,2,12}

¹Servicio de Microbiología Clínica y Enfermedades Infecciosas, Fundación de Investigación Biomédica Gregorio Marañón, Hospital General Universitario Gregorio Marañón, Madrid, Spain. ²Centro de Investigación Biomédica en Red de Enfermedades Respiratorias (CIBERES, CB06/06/0058), Madrid, Spain. ³Servei de Malalties Infeccioses, Hospital Universitari Vall d'Hebron, Barcelona, Universitat Autònoma de Barcelona, Barcelona, Vall d'Hebron Institut de Recerca (VHIR), Barcelona, Spain. ⁴Centro de Investigación Biomédica en Red de Enfermedades Infecciosas (CIBERINFEC), Madrid, Spain. ⁵Hospital Universitario Puerta de Hierro, Madrid, Spain. ⁶Hospital Dr. Negrín, Las Palmas de Gran Canaria, Spain. ⁷Hospital Virgen de las Nieves, Granada, Spain. ⁸Hospital Virgen del Rocío, Sevilla, Spain. ⁹Hospital Donosti, San Sebastián, Spain. ¹⁰Hospital Central de Asturias, Oviedo, Spain. ¹¹Hospital Virgen de la Arrixaca, Murcia, Spain. ¹²Universidad Complutense de Madrid, Madrid, Spain.

Introduction: The genus *Cutibacterium* is composed of slow-growing anaerobic Gram-positive bacilli that are part of the normal skin flora. This genus has been associated with endovascular infections, especially when prosthetic material is involved.

Objectives: The objectives of our study were: to determine the incidence and clinical characteristics of infective endocarditis (IE) due to *Cutibacterium* spp. in Spain and to analyse the results of the microbiological tests used to reach the diagnosis, their positivity rate and the concordance between them.

Methods: This is an observational, prospective and multicentre study of the GAMES (Spanish Collaboration on Endocarditis study group) series and Vall d'Hebron University Hospital, including data from 46 Spanish hospitals from 2008 to 2022. The microbiological tests analysed were blood cultures, conventional cultures and 16SrARN gene PCR and sequencing (16SPCR).

Results: Of the 6,689 episodes of IE, 64 cases (0.9%) were caused by *Cutibacterium* species, and most of them were due to *C. acnes* (92%). The majority of cases were male (86%) with a high number of comorbidities. Most cases occurred on prosthetic valves (66%) or cardiac devices (25%), although 8 cases (13%) occurred on natural valves. In cases of prosthetic IE, the mean time from prosthesis implantation to hospital admission was 45 months (Table 1). The median time from hospital admission to echocardiogram was 3 days. Fifty-two cases received a beta-lactam-based treatment. Intracardiac complications were observed in 22 episodes. Surgery was performed in 51 out of 64 patients (80%). Overall mortality was 14%. Overall, 31/59 blood cultures (52.5%), 34/47 valve or device cultures (72%) and 22/27 16SPCR tests (81%) were positive. Table 2 shows the positivity rate of diagnostic tests in cases of valvular IE and cardiac implantable electronic device-related IE (CIED-IE). 16SPCR was positive in 19/22 (86%) of prosthetic IE cases. Blood cultures were positive in just 20% of CIED-IE (Table 2).

Table 1. Clinical characteristics of 64 cases of IE caused by *Cutibacterium* spp.

Variable	Cutibacterium spp. IE (64)
Age. Median (IQR)	66 (55-75)
Sex (Men)	55 (85.9)
Location	
Aortic	37 (57.8)
Mitral	11 (17.2)
Native valve IE	8 (12.5)
Prosthetic valve IE	42 (65.6)
CIED IE	16 (25.0)
Months from prosthesis implantation to admission	45 (22-90)
Comorbidities	
Pulmonary disease	9 (14.1)
Coronary artery disease	21 (32.8)
Heart failure	24 (37.5)
Diabetes	15 (23.4)
Previous renal insufficiency	13 (20.4)
Cerebrovascular disease	14 (21.9)
Natural valve disease	34 (53.1)
Charlson comorbidity index. Median (IQR)	2 (1-3)
Place of acquisition	
Community	47 (73.4)
Nosocomial	11 (17.2)
Healthcare related	6 (9.4)

CIED: cardiac implantable electronic device.

Conclusions: IE due to *Cutibacterium* spp. is a rare entity that usually affects almost entirely males with comorbidities, with prosthetic valves or cardiac devices, and usually requires surgical treatment. Mortality in our series was 14%. In cases in which molecular diagnostic tests were performed, 16SrRNA PCR was the diagnostic test with the highest sensitivity.

Table 2. Positivity rate of diagnostic tests used in 64 cases of *Cutibacterium* spp. infective endocarditis involving cardiac valves or cardiac devices

Test	Valvular IE (n=48)	CIED IE (n=16)	Total
BC positive/performed (%)	28/44 (63.6%)	3/15 (20.0%)	31/59 (52.5%)
Only BC	17/28	1/3	18/31
BC and cultures	4/28	1/3	5/31
BC and 16SPCR	5/28	0/3	5/31
BC, cultures and 16SPCR	2/28	1/3	3/31
Cultures positive/performed (%)	19/31 (61.3%)	15/16 (93.7%)	34/47 (72.3%)
Only cultures	8/19	11/15	19/34
Cultures and BC	4/19	1/15	5/34
Cultures and 16SPCR	5/19	2/15	7/34
Cultures, BC and 16SPCR	2/19	1/15	3/34
16SPCR positive/performed (%)	19/22 (86.3%)	3/5 (60.0%)	22/27 (81.4%)
Only 16SPCR	7/19	0/3	7/22
16SPCR and BC	5/19	0/3	5/22
16SPCR and cultures	5/19	2/3	7/22
16SPCR, BC and cultures	2/19	1/3	3/22

Funding: DA (CM21/00274) is recipient of a Río Hortega contract supported by FIS. This research was supported by grants PI20/00575 from Fondo de Investigación Sanitaria (FIS; Instituto de Salud Carlos III. Plan Nacional de I+D+I 2017 to 2020). The study was cofounded by the European Regional Development Fund (FEDER) "A way of making Europe".

22. THE NEW ERS/ATS 2022 RECOMMENDATION OF RESPONSE TO BRONCHODILATOR: COMPARISON WITH THE PREVIOUS VERSION IN AN ASTHMA COHORT

Diana Betancor¹, Carlos Villalobos-Vilda¹, José María Olaguibel², Jose Manuel Rodrigo-Muñoz³, María José Alvarez-Puebla², Ebymar Arismendi⁴, Pilar Barranco⁵, Blanca Barroso⁶, Irina Bobolea⁷, Blanca Cárdena⁸, María Jesús Cruz⁹, Elena Curto¹⁰, Victoria del Pozo¹¹, Javier Dominguez-Ortega⁵, Francisco Javier Gonzalez-Barcala¹², Juan Alberto Luna-Porta¹³, Carlos Martinez-Rivera¹⁴, Joaquim Mullol¹⁵, Xavier Muñoz¹⁶, Cesar Picado⁷, Vicente Plaza¹⁷, Santiago Quirce¹³, Manuel Jorge Rial¹⁸, Lorena Soto-Retes¹⁹, Antonio Valero²⁰, Marcela Valverde-Monge²¹, **Joaquín Sastre**²¹

¹Allergy Department, Hospital Universitario Fundación Jiménez Díaz, Madrid, Spain. ²Servicio de Alergología, Hospital Universitario de Navarra, Pamplona, Spain. ³Servicio de Inmunología, IIS Hospital Universitario Fundación Jiménez Díaz, Madrid, Spain. ⁴Allergy Unit & Severe Asthma Unit, Pneumology and Allergy Department, Hospital Clínic; IDIBAPS; Universitat de Barcelona, Barcelona, Spain. ⁵Servicio de Alergia, Hospital Universitario La Paz, IdiPAZ, Madrid, Madrid, Spain. ⁶Servicio de Alergología, Hospital Universitario Fundación Jiménez Díaz, Madrid, Madrid, Spain. ⁷Allergy Unit & Severe Asthma Unit, Pneumology and Allergy Department, Hospital Clínic; IDIBAPS; Universitat de Barcelona, Barcelona, Spain. ⁸Servicio de Inmunología,

IIS Hospital Universitario Fundación Jiménez Díaz, Madrid, Madrid, Spain. ⁹Departamento de Biología Celular, Fisiología e Inmunología, Universitat Autònoma de Barcelona, Barcelona, Barcelona, Spain. ¹⁰Servicio de Neumología y Alergia, Hospital de la Santa Creu i Sant Pau, Instituto de Investigación Biomédica Sant Pau (IIB Sant Pau), Universidad Autónoma de Barcelona; Departamento de Medicina, Barcelona, Barcelona, Spain. ¹¹Servicio de Inmunología, Instituto de Investigación Sanitaria Hospital Universitario Fundación Jiménez Díaz, Madrid, Madrid, Spain. ¹²Servicio de Neumología, Complejo Hospitalario Universitario de Santiago, Santiago de Compostela, Santiago de Compostela, Spain. ¹³Servicio de Alergia, Hospital Universitario La Paz, IdiPAZ, Madrid, Spain. ¹⁴Servicio de Neumología, Hospital Germans Trias i Pujol, Institut d'Investigació Germans Trias i Pujol, Badalona, Spain. ¹⁵Rhinology Unit & Smell Clinic, ENT Department; Clinical and Experimental Respiratory Immunoallergy (IDIBAPS); Universitat de Barcelona, Barcelona, Spain. ¹⁶Servicio de Neumología, Hospital Vall d'Hebron, Barcelona, Spain. ¹⁷Servicio de Neumología y Alergia, Hospital de la Santa Creu i Sant Pau, Instituto de Investigación Biomédica Sant Pau (IIB Sant Pau), Universidad Autónoma de Barcelona; Departamento de Medicina, Barcelona, Spain. ¹⁸Servicio de Alergología, Complejo Hospitalario Universitario A Coruña, A Coruña, Spain. ¹⁹Servicio de Neumología y Alergia, Hospital de la Santa Creu i Sant Pau, Instituto de Investigación Biomédica Sant Pau (IIB Sant Pau), Universidad Autónoma de Barcelona, Barcelona, Spain. ²⁰Allergy Unit & Severe Asthma Unit, Pneumology and Allergy Department, Hospital Clínic; IDIBAPS, Barcelona, Spain. ²¹Servicio de Alergología, Hospital Universitario Fundación Jiménez Díaz, Madrid, Spain.

Introduction: Bronchodilator response (BDR) in asthmatic patients may have a significant impact on clinical course, management, and symptoms and has been suggested as a potentially modifiable risk factor for exacerbations. Nevertheless, BRD is widely influenced by anti-inflammatory asthma treatment.

Objectives: This study aimed to describe the frequency of positive and negative BDR using two different criteria in a large real-life cohort of asthmatic patients and to analyze patient clinical characteristics.

Methods: This prospective observational study reviewed the MEGA cohort electronic database, a well-characterized real-life cohort of asthmatic patients of several severities. Positive BDR was defined as recommended by ERS/ATS 2022 [(post-bronchodilator value(L)-pre-bronchodilator value (L)) × 100/predicted value(L), a change of > 10%]] and also using the former criteria (≥ 12% and ≥ 200 ml increase in FEV1 after administration of 200 µg salbutamol). The Ethics Committees of each participating hospital approved this study. All subjects provided signed informed consent.

Results: Data from 368 subjects with complete study data were used. Mean age was 47.8 ± 12.5 years, and 67% were female. Most of the patients were receiving antiasthma treatment. Ninety-six (26.5%) and 122 (33.2%) patients had positive BDR, according to ERS/ATS-2022 and

Demographic and clinical characteristics of the studied asthma patients cohort

Demographic characteristics	former criteria			ERS/ATS 2022 criteria ^a		
	BD positive (N = 122)	BD negative (N = 246)	p value	BDR positive (N = 96)	BDR Negative (N = 266)	p value
Age (years)	47.7 (12.2)	47.8 (12.9)	NS	48.7 (12.2)	47.5 (12.7)	NS
Sex (female)	84 (68.8%)	164 (66.6%)	NS	68 (70.8)	173 (65.0)	NS
Atopy	95 (77.9%)	183 (74.4%)	NS	51 (50.1)	202 (75.9)	< 0.001
Allergic rhinitis	64 (52.5%)	139 (56.5%)	NS	40 (41.7)	139 (52.2)	NS
CRSsNP	5 (4.1%)	29 (11.8%)	< 0.05	3 (3.1)	25 (9.4)	NS (0.07)
			OR 0.32 (95%CI, 0.13-0.82)			
CRSwNP	39 (31.9%)	75 (30.5%)	NS	3 (3.1)	83 (31.2)	< 0.001
Current place of residence (urban)	81 (66.4%)	181 (73.6%)	NS	45 (50.0)	193 (72.5)	< 0.001
Smoking habit						
Current smoker	7 (5.7%)	19 (7.7%)	NS	2 (2.1)	19 (7.1)	NS (0.07)
Never smoker	87 (71.3)	148 (50.2%)	NS	51 (53.1)	167 (62.7)	NS

(Cont)

Demographic and clinical characteristics of the studied asthma patients cohort (cont.)

Comorbidities	former criteria			ERS/ATS 2022 criteria ⁸		
	BD positive (N = 122)	BD negative (N = 246)	p value	BDR positive (N = 96)	BDR Negative (N = 266)	p value
Ex-smoker	30 (24%)	74 (30.1%)	NS	14 (14.6)	76 (28.6)	0.006
Bronchiectasis	8 (6.5%)	21 (8.5%)	NS	3 (3.1)	21 (7.9)	NS
Diabetes	7 (5.7%)	12 (4.8%)	NS	5 (5.2)	12 (4.5)	NS
Heart disease	5 (4.1%)	8 (3.2%)	NS	3 (3.1)	10 (3.7)	NS
Hyperlipidemia	17 (13.9%)	39 (15.8%)	NS	12 (12.5)	37 (13.9)	NS
Hypertension	17 (13.9%)	32 (13.0%)	NS	12 (12.5)	28 (10.5)	NS
Education level (secondary or higher)	88 (72.1%)	173 (70.3%)	NS			
Clinical characteristics						
Symptoms at diagnosis of asthma	114 (93.4%)	235 (95.5%)	NS			
Exacerbations						
Exacerbations, previous year	2.86 (2.5)	2.69 (2.4)	NS	34 (35.4)	122 (45.8)	NS
Emergency department visits, previous year	0.81 (1.9)	0.65 (1.3)	NS	21 (21.9)	68 (25.6)	NS
Hospital admissions, previous year (no ICU)	0.22 (0.6)	0.09 (0.4)	< 0.05	11 (11.4)	20 (7.5)	NS
			AUC = 0.54 (95%CI, 0.47-0.59)			
ICU admissions	0.07 (0.3)	0.11 (0.4)	NS	6 (6.2)	20 (7.5)	NS
Severity at Diagnosis (GINA)						
Intermittent	12 (9.8%)	16 (6.0%)	NS	2 (2.1)	16 (6.0)	NS
Mild persistent	31 (25.4%)	49 (19.9%)	NS	10 (10.4)	49 (18.4)	NS (0.07)
Moderate persistent	45 (44.2%)	86 (34.9%)	NS	39 (40.6)	95 (35.7)	NS
Severe persistent	34 (27.8%)	92 (37.3%)	NS	43 (44.8)	104 (39.1)	NS
Treatment						
Inhaled corticosteroids and LABA	106 (86.8%)	197 (80.1%)	NS	82 (85.4)	216 (81.2)	NS
Long-term OCS	8 (6.5%)	27 (10.9%)	NS	6 (6.2)	26 (9.7)	NS
Short-acting bronchodilators	69 (56.6%)	132 (53.7%)	NS	57 (59.3)	142 (53.4)	NS
Treatment with biologics	20 (16.4%)	42 (17.07%)	NS	16 (16.6)	58 (21.8)	NS
Asthma control						
ACT ≤ 20 (uncontrolled)	50 (40.9%)	71 (28.8%)	< 0.05	37 (38.5)	79 (29.7)	NS
			OR 1.7 (95%CI, 1.0-2.7)			
ACT ≥ 20 (controlled)	72 (59%)	175 (71.1%)	< 0.05	59 (61.4)	179 (67.3)	NS
			OR 0.5 (95%CI, 0.4-0.9)			
Lung function test						
FEV ₁ (%) at diagnosis	75.9%	89.9%	< 0.01	77.2 (18.2)	87.4 (21.4)	< 0.0001
			AUC = 0.7 (95%CI, 0.6-0.7), p = 0.001			
FVC (%) at diagnosis	93.9%	101.6%	< 0.01	95.2 (18.9)	99.9 (20.9)	0.02
			AUC = 0.6 (95%CI, 0.5-0.6) p = 0.006			
FEV1/FVC	66.2 (11.2)	72.2 (12.9)	< 0.01	71.1 (16.1)	78.6 (16.5)	0.009
			AUC = 0.6 (95%, CI 0.5-0.6), p = 0.004			
RV/TCL	113.0 (32)	97.9 (62)	NS	115.7 (24.9)	124.0 (63.0)	NS
Methacholine challenge, PC20 mean (SD)	2.3 (7.0)	2.7 (3.7)	< 0.01	3.1 (8.6)	3.1 (5.6)	0.02
			AUC = 0.6 (95%CI, 0.5-0.7) p = 0.003			
FeNO, ppb (mean, SD)	45.63 (29.6)	43.8 (40.9)	NS	45.5 (28.5)	44.2 (40.4)	NS
Spirometric pattern						
Normal	42 (43.4%)	131 (58.5%)	< 0.01	43 (44.8)	142 (53.0)	NS
			OR 0.4 (95%CI, 0.3-0.7)			
Obstructive	33 (34%)	50 (22.3%)	< 0.05	29 (30.2)	55 (20.7)	NS
			OR 1.4 (95%CI, 0.8-2.3)			
Air trapping	22 (22.7%)	43 (19.2%)	NS	24 (25.0)	69 (25.9)	NS
Inflammatory biomarker						
Total IgE, IU/mL (mean,SD)	426.1 (893.3)	410.7 (685.1)	NS	459.4 (979.9)	391.0 (667.4)	NS
Blood eosinophils, cells/μL (mean, SD)	414 (460.2)	312 (215.80)	< 0.05	374.2 (249.8)	349.6 (362.2)	NS
			AUC = 0.5 (95% 0.5-0.6)			
Sputum eosinophils (%) at diagnosis	13.4 (21.2)	8.9 (16.7)	NS	10.1 (18.5)	10.4 (18.2)	NS
> 3% eosinophils in sputum, N (%)	21 (61.7%)	35 (44.9%)	NS	12 (12.5)	43 (16.2)	NS
< 3% eosinophils in sputum, N (%)	13 (38.2%)	43 (55.1%)	NS	12 (12.5)	39 (14.6)	NS

ACT: asthma control test; AUC: area under the curve; BD: bronchodilator; CRSwNP: Chronic rhinosinusitis without polyposis, CRSsNP: Chronic rhinosinusitis with polyposis; FEV₁: forced expiratory volume in one second; FeNO: fractional exhaled nitric oxide; FVC: forced vital capacity; IC: interval of confidence; ICU: intensive care unit; IgE: immunoglobulin E; LABA: Long-acting β₂-receptor agonists; NS: non-significant; OCS: oral corticosteroids; OR: odds ratio; ROC: receiver operating characteristic; PC20: provocative concentration of methacholine causing a 20% fall in FEV₁; RV: residual volume; TLC: total lung capacity.

the former recommendation, respectively. Overall, 88 patients coincided with positive bronchodilation according to both criteria and 226 with negative results. Kappa agreement was $Kappa = 0.75$, $IC95\% = (0.68, 0.83)$. A significant association of positive BDR using both criteria was only found with lower FEV1, FVC and FEV1/FVC at diagnosis and lower Methacholine PC20, but not with RV/TLC ratio, an index of lung hyperinflation measured by whole-body plethysmography. There were no significant differences between patients with positive and negative BDR using both criteria in most analyzed items (see Table 1). A significant association of positive BDR using both criteria was only found with lower FEV1, FVC and FEV1/FVC at diagnosis and lower Methacholine PC20, but not with RV/TLC ratio, an index of lung hyperinflation measured by whole-body plethysmography. In Table 1 you'll find the associations of BDR with asthma control and severity, frequency of exacerbations, and inflammatory phenotypes of both criteria.

Conclusions: ERS/ATS has proposed new bronchodilatation criteria that have a high agreement with the former one but are not interchangeable. Bronchodilator response is only related to lower spirometric values and lower methacholine values. However, the former criteria is associated with poor asthma control with the independence of inflammatory biomarkers.

Funding: CIBERES and Sanofi.

23. SUSCEPTIBILITY TO HOSPITALIZATION FOR PNEUMOCOCCAL COMMUNITY-ACQUIRED PNEUMONIA: A GENOME-WIDE ASSOCIATION STUDY

Eva Suarez-Pajes¹, Itahisa Marcelino-Rodríguez^{1,2}, Elisa Hernández Brito³, Eva Tosco-Herrera¹, Luis A. Rubio-Rodríguez⁴, Silvia Gonzalez-Barbuzano¹, **Melody Ramirez-Falcon¹**, José M. Lorenzo-Salazar⁴, María Luisa Briones⁵, Olga Rajas⁶, Luis Borderías⁷, Jose Ferreres^{8,9}, Antoni Payeras¹⁰, Leonardo Lorente¹¹, Javier Aspa⁶, Eurne Carbonell^{8,9}, Jordi Freixinet¹², Felipe Rodríguez de Castro^{13,14}, Jordi Solé Violán^{15,16,17}, Carlos Rodríguez-Gallego^{3,15}, Carlos Flores^{1,4,15,17}

¹Research Unit, Hospital Universitario Nuestra Señora de Candelaria, Santa Cruz de Tenerife, Spain. ²Area of Preventive Medicine and Public Health, Universidad de La Laguna, Santa Cruz de Tenerife, Spain.

³Department of Immunology, Hospital Universitario de Gran Canaria Dr. Negrín, Las Palmas de Gran Canaria, Spain. ⁴Genomics Division, Instituto Tecnológico y de Energías Renovables (ITER), Santa Cruz de Tenerife, Spain. ⁵Department of Respiratory Diseases, Hospital Clínico y Universitario de Valencia, Valencia, Spain. ⁶Department of Respiratory Diseases, Hospital Universitario de la Princesa, Madrid, Spain.

⁷Department of Respiratory Diseases, Hospital San Jorge, Huesca, Spain.

⁸Critical Care Unit, Hospital Clínico de Valencia, Valencia, Spain.

⁹INCLIVA Biomedical Research Institute, Valencia, Spain. ¹⁰Department of Internal Medicine, Hospital Son Llatzer, Palma de Mallorca, Spain.

¹¹Intensive Care Unit, Hospital Universitario de Canarias, Santa Cruz de Tenerife, Spain. ¹²Department of Thoracic Surgery, Hospital Universitario de Gran Canaria Dr. Negrín, Las Palmas de Gran Canaria, Spain.

¹³Department of Respiratory Diseases, Hospital Universitario de Gran Canaria Dr. Negrín, Las Palmas de Gran Canaria, Spain. ¹⁴Department of Medical and Surgical Sciences, School of Medicine, Universidad de Las Palmas de Gran Canaria, Las Palmas de Gran Canaria, Spain. ¹⁵Department of Clinical Sciences, Universidad Fernando Pessoa Canarias, Las Palmas de Gran Canaria, Spain. ¹⁶Critical Care Unit, Hospital Universitario de Gran Canaria Dr. Negrín, Las Palmas de Gran Canaria, Spain. ¹⁷Centro de Investigación Biomédica en Red de Enfermedades Respiratorias (CIBERES), Madrid, Spain.

Introduction: Community-acquired pneumonia (CAP) is an infectious disease that affects the lower respiratory tract and has a high morbidity and hospitalization rate. One of the leading causes of CAP is *Streptococcus pneumoniae* (pneumococcus) infection. Host genetics plays a

critical role in susceptibility and immune response to infectious diseases.

Objectives: To identify genetic susceptibility loci of hospitalization for pneumococcal-induced CAP using a genome-wide association study (GWAS).

Methods: We performed a GWAS in 3,767 Spanish individuals, including 259 adult patients with CAP induced by pneumococcus and 3,508 population controls. Genotyping was performed with the Axiom Spain Biobank Array, and imputation was conducted using Haplotype Reference Consortium release 1.1 as the reference panel. Classical HLA alleles were also imputed. We tested the association of 7,6 million variants using logistic regressions. Subsequently, we prioritized genes based on Bayesian fine-mapping and functional evidence, using the Variant-to-Gene (V2G) tool.

Results: We revealed six independent variants that were genome-wide significant ($p = 5 \times 10^{-8}$), three located on chromosome 6, and one for each of the chromosomes 4, 11, and 20. Based on the highest V2G scores, we prioritized three genes: C4orf33 on chromosome 4, TAPBP for the three variants located on chromosome 6, and ZNF341 on chromosome 20. No gene was prioritized for chromosome 11. Interestingly, TAPBP and ZNF341 deficiencies are known inborn errors of immunity and chromosome 6 variants associate with blood cell count and autoimmune diseases. Associations were all non-significant for the classic HLA alleles.

Conclusions: We performed the first GWAS of pneumococcal-induced CAP hospitalization and identified new susceptibility loci.

Funding: Instituto de Salud Carlos III (PI13/01456 and PI16/00759, PI17/00610, PI19/00141, PI20/00876, FI17/00177) and Ministerio de Ciencia e Innovación (RTC-2017-6471-1; AEI/FEDER), co-financed by the European Regional Development Funds, "Una manera de hacer Europa" from the EU; ITER agreement (OA17/008); Grupo DISA (OA18/017), Fundación Canaria Instituto de Investigación Sanitaria de Canarias (PIFIISC19/43); Fundación Mapfre-Guanarteme (OA19/072); SEPAR (Spanish Society of Pulmonology and Thoracic Surgery-Fundación Española del Pulmón); Cabildo Insular de Tenerife (CGIEU0000219140); and Gobierno de Canarias & Social European Fund "Canarias Avanza con Europa" (TESIS2022010042 and TESIS2021010046). EH-B was supported by a grant from Universidad de Las Palmas de Gran Canaria.

24. A DEEPER ANALYSIS OF FOUR POTENTIAL ASTHMA TRIGGERS AND THEIR SIGNALING PATHWAYS IN LUNG BIOPSIES OF ASTHMATIC AND COPD PATIENTS

Lucía Cremades-Jimeno¹, María López-Ramos¹, Selene Baos¹, Ignacio Mahillo-Fernández², Joaquín Sastre^{3,4}, Blanca Cárdena^{1,4}

¹Immunology Department, IIS-Fundación Jiménez Díaz-UAM, Madrid, Spain. ²Biostatistics and Epidemiology Unit, Fundación Jiménez Díaz, Madrid, Spain. ³Allergy Department, Hospital Universitario Fundación Jiménez Díaz, Madrid, Spain. ⁴Centro de Investigación Biomédica en Red de Enfermedades Respiratorias (CIBERES), Madrid, Spain.

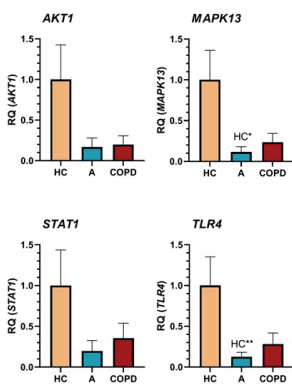
Introduction: Chronic inflammatory respiratory diseases, such as asthma and chronic obstructive pulmonary disease (COPD), are difficult to manage due to the high heterogeneity among patients and the lack of effective treatments. In fact, existing treatments are directed to symptoms, and needed for long periods. With the aim of provide new diagnostic and therapeutic tools, we used systems biology to define and theoretically prioritize potential asthma biomarkers. Also, we identified four potential asthma triggers, AKT1, MAPK13, STAT1 and TLR4; and different elements from their signaling pathways.

Objectives: Analyze the gene and protein expression of the defined asthma triggers, as well as the gene expression of elements in their signaling pathways, in lung samples of asthmatic and COPD patients.

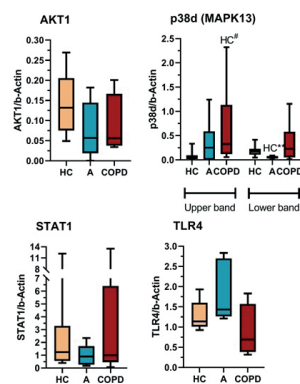
Methods: Lung tissue samples from 10 healthy controls (HC), 9 asthma patients (A), and 10 COPD patients were obtained from the CIBERES biobank. After mechanic homogenization, RNA and protein were extracted using TRIzol method. Gene and protein expression of the four potential triggers were studied by RT-qPCR and Western-Blot, respectively. Additionally, differential expression of 26 related genes was studied through RT-qPCR. Adjusted p-values were calculated with parametric T-Student test.

Results: All of the triggers showed a lower gene expression in both clinical groups, compared to HC, with statistically significant differences between A and HC groups in MAPK13 (adj p = 0.022) and TLR4 (adj p = 0.009). According to protein expression, we only found significant differences in p38d (MAPK13) expression. Two bands were detected, with different behavior: one of them showed differences between HC and A (p = 0.003) and the other between HC and COPD (p = 0.001). Studying the gene expression of elements involved in the four signaling pathways, we found all studied genes (except CCL5 in COPD patients) repressed in both clinical groups, compared to HC subjects; but significance was only reached in the comparison between A and HC groups in ALOX5, BAX, IL13RA1, RELA, and TGFB1; hinting a possible differential protein activation of the four triggers specifically in asthma patients.

A) Gene expression



B) Protein expression



Gene and B) protein expression of the four potential asthma triggers in lung samples of healthy control subjects, asthmatic patients and patients with COPD. Relative quantifications (RQ) of the clinical groups compared to the control group in each sample are represented. Statistically significant differences between the HC and the specified group are shown as: HC⁺ and HC^{**} (p < 0.05 and p < 0.01, respectively). HC: healthy control subjects; A: asthmatic patients; COPD: patients with COPD.

Conclusions: AKT1, MAPK13, STAT1 and TLR4 gene expression is reduced in lungs from patients with asthma and COPD, without significant changes in protein expression. However, differences in elements from their signaling pathways are observed, opening new possibilities in the search of asthma treatments.

Funding: PI20/00903 and PI17/01682 (co-supported by FEDER), CIBERES (ISCIII, 0013) from Fondo de Investigación Sanitaria and Ayudas Fundación SEAC 2018. LCJ supported by Fundación Conchita Rábago, MLR by PEJD-2019-PRE/BMD-16537.

25. IMPACT OF PREVIOUS CANDIDA SPP. COLONIZATION IN PATIENTS WITH CANDIDEMIA ADMITTED IN A TERTIARY CARE HOSPITAL IN MADRID (SPAIN)

Ana Soriano-Martín, Marina Machado, Teresa Vicente, Carlos Sánchez-Carrillo, Elena Reigadas, Agustín Estévez, Roberto Alonso, Luciana Urbina, Celia Sánchez Martínez, Jesús Guinea, Pilar Escribano, Emilio Bouza, Patricia Muñoz

Hospital General Universitario Gregorio Marañón, Madrid, Spain.

Introduction: Multifocal colonization by *Candida* spp. is considered a risk factor for the development of candidemia, especially in patients admitted to intensive care units (ICUs), neonatology and pediatrics services. However, its importance is less described in other hospital units.

Objectives: Our aim was to determine the impact of multifocal *Candida* spp. colonization in all patients with candidemia.

Methods: Single-center, retrospective, observational study in a large tertiary level hospital in Madrid between January 2019-December 2022. Epidemiological, clinical and microbiological variables were collected in a previously designed data collection form for all adult patients hospitalized with candidemia and registered in an anonymized database. A comparative analysis between patients previously colonized and not colonized by *Candida* spp. was performed.

Results: 170 episodes of candidemia were registered in 167 patients (3 had two different episodes, more than 30 days apart); 67 (39.4%) were ICU patients. The incidence of candidemia was 1.08/1,000 admissions. Previous colonization was present in 54.1% and multifocal colonization in 28.3%. Days from colonization to candidemia were 19 (IQR 7.5-54.5). Main colonizing species: 56.4% *Candida albicans*, 14.3% *C. tropicalis*, 12.1% *C. glabrata*, 12.1% *C. parapsilosis* and 4.3% *C. krusei*;

Differences between *Candida* spp. Colonised or not patients with candidemia

	Colonized N = 92 (54.1%)	Non-colonized N = 78 (45.9%)	p
Age – median (IQR)	66 (58.0-74.5)	69.5 (59.0-81.0)	0.21
Comorbidity			
Cardiovascular	57 (62.0)	41 (52.6)	0.22
Gastrointestinal disease	33 (35.9)	35 (32.1)	0.60
Solid tumor	31 (33.7)	33 (42.3)	0.25
Diabetes mellitus	39 (32.6)	30 (38.5)	0.43
Pulmonary disease	27 (29.3)	11 (14.1)	0.02
Chronic kidney disease	22 (23.9)	14 (17.9)	0.34
Hemodialysis	18 (19.6)	4 (5.1)	< 0.01
Liver disease	17 (18.5)	14 (17.9)	0.93
SOT recipients	9 (9.8)	2 (2.6)	0.06
Hematological malignancy	7 (7.6)	4 (5.1)	0.51
HIV	3 (3.3)	4 (5.1)	0.70
Hospital setting at candidemia diagnosis			
Medical ward	25 (27.2)	48 (61.5)	< 0.01
Surgical ward	13 (14.1)	13 (16.7)	0.65
ICU	51 (55.4)	16 (20.5)	< 0.01
Risk factors for candidemia			
Broad-spectrum antibiotics	88 (95.7)	63 (80.8)	< 0.01
Central venous catheter	74 (81.3)	51 (65.4)	0.02
Total parenteral nutrition	72 (78.3)	44 (56.4)	< 0.01
Corticosteroid therapy	54 (58.7)	23 (29.5)	< 0.01
Abdominal surgery	25 (27.2)	18 (23.1)	0.53
Candidemia acquisition			
Nosocomial	82 (89.1)	44 (56.4)	< 0.01
Community	4 (4.3)	15 (19.2)	< 0.01
Health-care	6 (6.5)	19 (24.4)	< 0.01
Origin of candidemia			
Catheter	58 (63.0)	46 (59.0)	0.59
Primary	22 (23.9)	16 (20.5)	0.60
Urinary	6 (6.5)	12 (15.4)	0.06
Abdominal	5 (5.4)	3 (3.8)	0.73
Adequacy of empiric antifungal treatment	7/15 (46.7)	7/9 (77.8)	0.13
Days of hospitalization – median (IQR)	47 (31.0-99.5)	30.5 (15.0-51.0)	< 0.01
Overall mortality	46 (50.0)	30 (38.5)	0.13

HIV: human immunodeficiency virus; ICU: intensive care unit; IQR: interquartile range; SOT: solid organ transplant. P values presented in bold indicate statistical significance (p < 0.05).

isolates were mainly recovered from respiratory tract (62.1%), urinary tract (21.4%), abdomen (7.1%), cutaneous lesions (7.1%) and catheters (2.1%). In 89.1% there was a coincidence between colonizing and etiologic species. The differences between colonized and non-colonized patients are described in the Table. Previously colonized patients had more prior hemodialysis and pulmonary disease, were more frequently in the ICU, had more prolonged stays, more total parenteral nutrition (TPN), central venous catheter (CVC), broad-spectrum antibiotics and corticosteroids.

Conclusions: Previous *Candida* spp. Colonization was declared in only half of the patients with candidemia. Some factors to consider in patients colonized with *Candida* spp. Who developed candidemia include prolonged hospitalizations, antibiotic and corticosteroids use, CVC and TPN disposition, or ICU stays.

Funding: This study was supported by grant PI20/00575 from the Fondo de Investigación Sanitaria (FIS. Instituto de Salud Carlos III; Plan Nacional de I+D+I 2017–2020).

28. PULMONARY VASCULAR PRUNING IN SEVERE PULMONARY HYPERTENSION ASSOCIATED WITH CHRONIC LUNG DISEASES

Agustín Roberto García¹, Ivan Vollmer Torrubiano¹, Isabel Blanco¹, Adelaida Bosacoma Armora¹, Diego Rodriguez-Chiaradía², Clara Martín-Ontiyuelo¹, Fernanda Hernandez-Gonzalez¹, Jesus Ribas³, Xavier Pomares⁴, Maria Molina³, Raul San José Estepar⁵, Joan Albert Barberà¹

¹Hospital Clinic Barcelona, Barcelona, Spain. ²Hospital del Mar, Barcelona, Spain. ³Hospital Universitario Bellvitge, Barcelona, Spain. ⁴Hospital Universitario Parc Taulí, Barcelona, Spain. ⁵Brigham and Women's Hospital, Boston, United States

Introduction: Pulmonary hypertension (PH) is frequently associated with chronic lung disease (CLD), although only a reduced number of patients develop severe PH. The mechanisms underlying the development of severe PH in patients with CLD are unknown. Remodeling and loss of small pulmonary vessels (vascular pruning), evaluated using CT imaging, has been shown in patients with PH and in CLD.

Objectives: We sought to investigate whether patients with severe PH associated with fibrosing idiopathic interstitial pneumonia (FIIP) or chronic obstructive pulmonary disease (COPD) had greater pulmonary vascular pruning than those without or with moderate PH and whether this was associated to the extent of parenchymal derangement.

Methods: We prospectively analyzed 121 patients with CLD: 40 without PH (21 FIIP, 19 COPD), 42 with moderate PH (20 FIIP, 22 COPD) and 34 with severe PH (13 FIIP, 21 COPD); and 39 patients diagnosed with idiopathic pulmonary arterial hypertension (IPAH). Patients with connective tissue disease or other cause of PH were excluded. Volumetric non-contrast chest CT scans, complete pulmonary function testing and right heart catheterization were performed to all patients. Quantitative assessment of pulmonary vascular volumes in CT scans included: total blood volume (TBV), volume of vessels less than 5 mm² in cross-section (BV5), total arterial volume (TAV) and volume of arteries less than 5 mm² in cross-section (BV5art). Densitometric analyses of the extension of fibrosis in patients with FIIP and of the extent of emphysema in COPD were additionally evaluated using the Local Histogram.

Results: The Table shows hemodynamic, lung function and CT imaging measurements in the different groups of patients. Patients with severe PH associated with FIIP or COPD had lower small pulmonary vessels density as shown by reduced BV5/TBV and BV5art/TAV ratios, compared to patients without PH. Patients with severe COPD-PH showed the lowest BV5/TBV and BV5art/TAV values, being significantly lower than in moderate COPD-PH and IPAH. The reduction of small pulmonary vessel density in patients with severe PH was not associated with greater extent of fibrosis in FIIP or emphysema in COPD.

Table: hemodynamic, lung function and CT imaging measurements.

	FIIP			COPD			IPAH (n=38)
	No PH (n=20)	Moderate PH (n=16)	Severe PH (n=18)	No PH (n=17)	Moderate PH (n=18)	Severe PH (n=23)	
mPAP, mmHg	17 ± 3.6*	25 ± 3.7**	36 ± 7**	18 ± 2.4*	27 ± 6**	41 ± 9***	50 ± 13
CI, L/min/m ²	2.7 ± 0.6*	2.6 ± 0.5	2.1 ± 0.4*	2.8 ± 0.4*	2.7 ± 0.6*	2.3 ± 0.6*	2.1 ± 0.6
PVR, dyn·s·cm ⁵	177 ± 51*	304 ± 51*	658 ± 243***	162 ± 43*	287 ± 59*	690 ± 367***	987 ± 474
FVC, %pred	58 ± 18*	63 ± 16*	66 ± 15*	81 ± 19*	69 ± 16*	81 ± 17*	92 ± 13
FEV1, %pred	66 ± 21*	70 ± 14*	72 ± 17*	45 ± 17*	37 ± 19*	55 ± 19*	88 ± 12
TLC, %pred	61 ± 13*	63 ± 10*	64 ± 11*	114 ± 21*	119 ± 23*	97 ± 16**	94 ± 12
Dlco, %pred	39 ± 10*	34 ± 10*	27 ± 12**	46 ± 21*	36 ± 14*	28 ± 10**	61 ± 15
Pulmonary vessel volume measurements							
TBV, mL	107.4 ± 38.5	115.0 ± 30.1	117.9 ± 35.4*	135.9 ± 23.6	145.3 ± 26.4	166.0 ± 41.0**	140.2 ± 30.8
BV5, mL	58.1 ± 20.8	59.2 ± 16.2	59.4 ± 22.4	71.2 ± 11.3	73.8 ± 11.7	74.8 ± 21.9	69.3 ± 15.6
BV5/TBV ratio	0.54 ± 0.03*	0.52 ± 0.04	0.5 ± 0.09*	0.53 ± 0.06	0.52 ± 0.08	0.45 ± 0.07***	0.5 ± 0.05
TAV, mL	65.3 ± 21.9	72.5 ± 22.8	76.5 ± 23.0	78.5 ± 14.3	88.5 ± 19.3	105.5 ± 26.5***	77.8 ± 19.5
BV5art, mL	35.1 ± 10.9	37.1 ± 13.1	35.1 ± 10.3	40.4 ± 7.6	42.7 ± 7.5	44.5 ± 12.3	38.5 ± 9.7
BV5art/TAV ratio	0.54 ± 0.04	0.51 ± 0.06	0.47 ± 0.09*	0.52 ± 0.05	0.49 ± 0.08	0.42 ± 0.07***	0.5 ± 0.06
Fraction of fibrosis	0.65 ± 0.24	0.68 ± 0.15	0.72 ± 0.19	-	-	-	-
Fraction of emphysema	-	-	-	0.48 ± 0.10	0.50 ± 0.13	0.45 ± 0.16	-

* p<0.05 compared with FIIP or COPD without PH; # p<0.05 compared with FIIP and COPD with moderate PH; † p<0.05 compared with IPAH.

FIIP = fibrosing idiopathic interstitial pneumonia; COPD = chronic obstructive pulmonary disease; IPAH=idiopathic pulmonary arterial hypertension; PH=pulmonary hypertension; mPAP= mean pulmonary arterial pressure, CI=cardiac index; PVR=pulmonary vascular resistance; FVC=forced vital capacity; FEV1=forced expiratory volume in the first second; DLco= diffusing capacity for carbon monoxide; TBV= Total blood volume; BV5= pulmonary blood vessel volume in vessels less than 5 mm²; TAV= Total arterial volume; BV5art= pulmonary blood vessel volume in arteries less than 5 mm²

Conclusions: Severe PH in FIIP and COPD is associated with loss of small pulmonary arteries (vascular pruning), which is unrelated to the extent of fibrosis or emphysema.

Funding: Grant PI18/00383 from the Instituto de Salud Carlos III.

29. LIMB MUSCLE DYSFUNCTION IN PATIENTS WITH BRONCHIECTASIS: THE ROLE OF SYSTEMIC INFLAMMATION AND OXIDATIVE STRESS

Adriana Núñez-Robainas^{1,2,3}, Mariela Nieves Alvarado-Miranda^{1,2,3}, Maria Pérez-Peiró^{1,2,3}, Esther Barreiro^{1,2,3}

¹Pulmonology Department, Muscle Wasting and Cachexia in Chronic Respiratory Diseases and Lung Cancer Research Group, IMIM-Hospital del Mar, Parc de Salut Mar, Barcelona, Spain. ²Department of Medicine and Life Sciences (MELIS), Universitat Pompeu Fabra (UPF), Barcelona Biomedical Research Park (PRBB), Barcelona, Spain. ³Centro de Investigación en Red de Enfermedades Respiratorias (CIBERES CB06/06/0043), Instituto de Salud Carlos III (ISCIII), Madrid, Spain.

Introduction: Skeletal muscle dysfunction and nutritional abnormalities are common systemic manifestations in many chronic respiratory diseases such as chronic obstructive pulmonary disease (COPD). Clinical and biological factors including systemic inflammation and oxidative stress are involved in its etiology. Whether systemic inflammation and redox imbalance contribute to these systemic manifestations in bronchiectasis remains to be fully elucidated. Thus, we hypothesized that stable bronchiectasis patients with nutritional abnormalities and muscle dysfunction may exhibit increased systemic levels of inflammation and oxidative stress markers.

Objectives: In stable bronchiectasis patients and control subjects, the main objectives were to assess nutritional, lung and muscle function status, biomarkers of inflammation, oxidative stress (prooxidants and antioxidants), and correlations between biological and clinical variables.

Methods: Twenty stable mild-to-moderate bronchiectasis patients and ten healthy subjects were recruited. In all patients, nutritional status (BMI and FFMI), lung function (FEV1, FEV and FEV1/FVC), upper and lower limb muscle strength and exercise capacity were evaluated. In plasma samples, the following markers were analyzed: myeloperoxidase cyclooxygenase-2, transforming growth factor beta 1 (TGF-β1), vascular endothelial growth factor A (VEGF-A), interleukin 6 (IL-6), protein tyrosine nitration (3-nitrotyrosine), protein carbonylation, malondialdehyde (MDA)-protein adducts, reactive carbonyls, trolox equivalent antioxidant capacity (TEAC), superoxide dismutase (SOD) and catalase activities, and reduced glutathione (GSH). Correlations between clinical and biological variables were assessed using the Pearson's correlation coefficient.

Results: Compared to control subjects, in bronchiectasis patients, BMI, FFMI, FEV1, FVC, FEV1/FVC, handgrip and quadriceps muscle strength were significantly reduced. Plasma levels of myeloperoxidase, TGF- β 1, VEGF-A, IL-6, total protein carbonylation, GSH and SOD levels significantly increased. Among bronchiectasis patients, BMI and FFMI negatively correlated with MDA-protein adduct and GSH plasma levels respectively. Handgrip negatively correlated with IL-6 levels, while quadriceps strength negatively correlated with the proportions of slow-twitch fibers and levels of 3-nitrotyrosine and SOD. Negative associations were also found between the distance walked in the six-minute walk and shuttle tests and TEAC plasma levels.

Conclusions: In patients with mild-to-moderate bronchiectasis, the loss of muscle function takes place in both the upper and the lower limbs along with a reduction in body composition parameters. Levels of systemic inflammatory and oxidative stress parameters were greater in the patients and correlated mainly with the muscle function status of the patients.

Funding: FIS 21/00215 (FEDER, ISC-III), BA21/00003, Intensificación INT19/00002, CIBERES (ISC-III), SEPAR-2020.

30. EFFECT OF EXPOSURE TO DIESEL PARTICLES ON PULMONARY MACROPHAGES

David Soler Segovia^{1,2,3}, Marc Massa Gómez^{1,2,3}, David Espejo Castellanos^{1,2,3}, Xavier Muñoz Gall^{1,2,3,4}, María Jesús Cruz Carmona^{1,2,3}

¹Pulmonology Service, Hospital Universitari Vall d'Hebron, Barcelona, Spain. ²Centro de Investigación Biomédica en Red de Enfermedades Respiratorias (CIBERES), Madrid, Spain. ³Medicine Department, Universitat Autònoma de Barcelona, Barcelona, Spain. ⁴Department of Cell Biology, Physiology and Immunology, Universitat Autònoma de Barcelona, Barcelona, Spain.

Introduction: Diesel exhaust particles (DEP) are an important component of air particulate matter. Macrophages present a key role in immunity due to their ability to phagocytose toxic chemicals, such as DEPs. Nevertheless, studies have shown that the function of macrophages may be impaired by their exposure to DEP.

Objectives: The present study aims to assess the effect of exposure to DEP on pulmonary macrophages in a model of healthy mice.

Methods: BALB/c ByJ mice were randomly divided into five groups. Control group received nasal instillations of saline during 8 days while the experimental groups received nasal instillations of DEP during 8, 17, 26 and 53 days. Bronchoalveolar lavage (BAL) was performed via surgical tracheostomy and lungs were washed with PBS. Bronchoalveolar lavage cytospin slides were examined by leukocytic specific counting and macrophages DEP-uptake analysis (% of loaded macrophages and % of area covered by DEP). Moreover, the lungs were processed to characterize lung immune cells by flow cytometry.

Results: In BAL, inhalation of DEP decreased total macrophages and increased total neutrophils at 17 and 26 days ($p < 0.02$ in all cases). Furthermore, total loaded macrophages increased along exposure ($p < 0.0017$ for all groups). The % of macrophages area covered by DEP show an acute increase at 8 days ($p = 0.0005$) which is maintained for 26 and 53 days ($p = 0.006$ and $p = 0.027$ respectively). Moreover, inhalation of DEP produced an acute decrease of total monocytes in lung at 8 days ($p = 0.001$) and an increase in total dendritic cells (DCs) ($p < 0.022$).

Conclusions: The results demonstrated that macrophages are the main cells involved in clearance of DEPs after exposure. The results demonstrated that DEP exposure activates the innate immune response during short exposure but this progresses to an adaptive response if the exposure remains.

Funding: Study supported by Instituto de Salud Carlos III (PI18/00344) and FEDER.

33. ASSESSMENT OF THE IMPACT OF OBSTRUCTIVE SLEEP APNEA ON BLOOD PRESSURE IN PEDIATRIC PATIENTS

Esther Solano Pérez¹, Carlota Coso¹, María Castillo García¹, Laura Silgado Martínez¹, Leticia Álvarez Balado¹, María Esther Viejo Ayuso¹, Sofía Romero Peralta¹, Rosa Mediano San Andrés¹, Alfonso Ortigado¹, Ainhoa Álvarez², Carlos Egea², Genoveva del Río³, Fernanda Troncoso³, Carolina Díaz⁴, Alejandra Roncero⁵, Olga Mediano⁶

¹Hospital Universitario de Guadalajara, Guadalajara, Spain. ²Hospital Universitario de Araba, Vitoria, Spain. ³Fundación Jiménez Díaz, Madrid, Spain. ⁴Hospital Universitario Santa Lucía, Cartagena, Spain. ⁵Hospital Universitario San Pedro, La Rioja, Spain. ⁶Hospital Universitario de Guadalajara, Guadalajara, Spain.

Introduction: Obstructive sleep apnea (OSA) has an impact on blood pressure (BP) in children. Values close to normal have shown to be predictors of high blood pressure (HBP), cardiovascular risk (CV) and coronary disease in the future. In adults, it has been shown that patients with OSA more frequently suffer from a non-dipper pattern, related to a higher CV risk. NCT03696654.

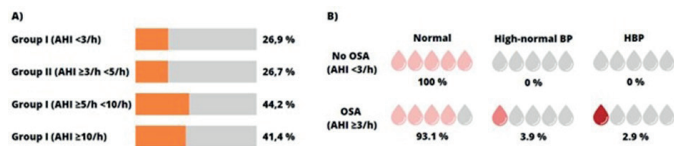
Description of the sample

General characteristics	Continuous variables		
	n	Mean \pm SD	Median (P25-P75)
Age	132	8.9 \pm 3.5	
Height percentile	126		57 (27-83)
Weight percentile	126		60 (32-93)
Mean systolic blood pressure	132	102.5 \pm 10.7	
Mean diastolic blood pressure	132	64.2 \pm 8.1	
Mean global blood pressure	132	75.8 \pm 5.5	
		Categoric variables	
Sex (male)	132	74 (56.1%)	
Chervin	132		
Negative (normal)		82 (62.1%)	
Positive (abnormal)		50 (37.9%)	
Tonsils	129		
I (0-25%)		9 (7.0%)	
II (26-50%)		35 (27.1%)	
III (51-75%)		57 (44.2%)	
IV (76-100%)		28 (21.7%)	
Palate	128		
Normal		89 (69.5%)	
Ojival		39 (30.5%)	
Mandible	130		
Normal		89 (69.5%)	
Abnormal		39 (30.5%)	
Bite	43		
Class III		14 (32.6%)	
Class II		19 (44.2%)	
Open		8 (19.6%)	
Asymmetry		2 (4.6%)	
Mallampati classification	130		
Class I		28 (21.5%)	
Class II		68 (52.3%)	
Class III		29 (22.3%)	
Class IV		5 (3.8%)	
OSA severity	132		
Group I (AHI < 3/h)		32 (24.2%)	
Group II (AHI \geq 3/h < 5/h)		28 (21.2%)	
Group III (AHI \geq 5/h < 10/h)		42 (31.8%)	
Group IV (AHI \geq 10/h)		30 (22.7%)	

Objectives: To explore the relationship between the severity of OSA (apnea/hypopnea index-AHI) and non-dipper pattern in 24h BP monitoring (ABPM).

Methods: Prospective study that included 132 children (4-18 years) with suspected OSA (pilot study from the Kids Trial Study). Clinical/anthropometric variables were collected, polysomnography was performed to assess OSA and ABPM study for assessing BP. Four groups were established based on OSA severity: 1) No OSA: AHI < 3/h; 2) Mild OSA: AHI ≥ 3/h – < 5/h; 3) Moderate OSA: ≥ 5/h – < 10/h; 4) Severe OSA: ≥ 10/h. Mean global BP, the presence or absence of a non-dipper pattern (< 10% decrease in BP values during sleep compared to awake) and the diagnosis of HBP (European guides of 2016). The relationship between OSA severity and BP was determined using a parametric mean difference analysis (ANOVA). The frequency of appearance (%) of the non-dipper pattern and the diagnosis of HBP in the different groups were evaluated.

Results: The Table shows the baseline characteristics of the population and the sleep study. The mean global BP was not statistically significant different between groups (ANOVA p-value = 0.402). The non-dipper pattern showed a possible trend of increased prevalence depending on the OSA severity (Group I: 26.9%; Group II: 26.7%; Group III: 44.2%; Group IV: 41.4%) (Figure A). All the diagnoses of high/normal BP and HBP were made in the OSA group (Figure B).



A) Frequency of non-dipper pattern according to obstructive sleep apnea (OSA) severity. B) Relationship between high blood pressure (HBP) and OSA. AHI: apnea/hypopnea index; BP: blood pressure.

Conclusions: There could be a relationship between OSA and the higher frequency of non-dipper pattern and the diagnosis of HBP in children. Studies with larger populations are needed to explore these findings.

Funding: Funds received by ISCIII (PI18/00565 y PI22/01653), SEPAR (535-2018 y 1073-2020), unconditional grant from Menarini laboratories and awarded by NEUMOMADRID.

34. ASSESSMENT OF THE IMPACT OF OBSTRUCTIVE SLEEP APNEA ON THE CARDIAC STRUCTURE IN THE PEDIATRIC PATIENT MEASURED BY ECHOCARDIOGRAPHY

Carlota Coso¹, Esther Solano Pérez¹, María Castillo García¹, Laura Silgado Martínez¹, Leticia Álvarez Balado¹, María Esther Viejo Ayuso¹, Sofía Romero Peralta¹, Rosa Mediano San Andrés¹, Alfonso Ortigado¹, Ainhoa Álvarez², Carlos Egea², Genoveva del Río³, Fernanda Troncoso³, Carolina Díaz⁴, Alejandra Roncero⁵, Olga Mediano¹

¹Hospital Universitario de Guadalajara, Guadalajara, Spain. ²Hospital Universitario de Araba, Vitoria, Spain. ³Fundación Jiménez Díaz, Madrid, Spain. ⁴Hospital Universitario Santa Lucía, Cartagena, Spain. ⁵Hospital Universitario San Pedro, La Rioja, Spain.

Introduction: Changes in intrathoracic pressure caused by respiratory events produced by obstructive sleep apnea (OSA) have an impact on hemodynamics and cardiac structure. Different studies have shown an increase in the interventricular septum and the dimensions of the left ventricle in patients with OSA. These intermediate consequences mean that OSA can contribute independently to cardiovascular disease.

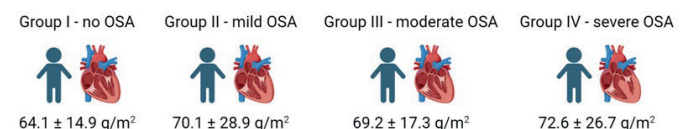
Objectives: To evaluate the impact of OSA on the cardiac structure of the pediatric patient measured by Left Ventricular Hypertrophy (LVH) by echocardiography. NCT03696654.

Methods: Multicenter, longitudinal and prospective study. Preliminary data from a pilot study from the Kids Trial study are presented. A total of 132 children between the ages of 4 and 18 referred for suspected OSA were included. Clinical and anthropometric variables (Table) were collected and polysomnography (PSG) was performed on all of them, classifying them into the following OSA severity groups: 1. No OSA: AHI < 3/h; 2. Mild OSA: AHI ≥ 3/h – < 5/h; 3. Moderate OSA: ≥ 5/h – < 10/h; 4. Severe OSA: ≥ 10/h. In 83 of the participants, it was possible to assess the presence of organic damage by echocardiography, measuring LVH (g/m²). The possible alterations in LVH between the OSA severity groups were analyzed using the difference in the means obtained.

Results: Baseline characteristics and sleep study of the participants are shown in the Table. LVH measurements showed an increasing trend depending on the OSA severity groups (Group I: 64.1 ± 14.9; Group II: 70.1 ± 28.9; Group III: 69.2 ± 17.3; Group IV: 72.6 ± 26.7), although without a statistically significant difference (Figure).

Description of the sample

	n	Continuous variables	
		Mean ± SD	Median (P25-P75)
Age	132	8.9 ± 3.5	
Height percentile	126		57 (27-83)
Weight percentile	126		60 (32-93)
Left ventricle hypertrophy	83		62.7 (54.5-81.7)
		Categoric variables	
Sex (male)	132	74 (56.1%)	
Cherwin	132		
Negative (normal)		82 (62.1%)	
Positive (abnormal)		50 (37.9%)	
Tonsils	129		
I (0-25%)		9 (7.0%)	
II (26-50%)		35 (27.1%)	
III (51-75%)		57 (44.2%)	
IV (76-100%)		28 (21.7%)	
Palate	128		
Normal		89 (69.5%)	
Ojival		39 (30.5%)	
Mandible	130		
Normal		89 (69.5%)	
Abnormal		39 (30.5%)	
Bite	132		
Class III		14 (10.6%)	
Class II		19 (14.4%)	
Open		8 (6.1%)	
Asymmetry		2 (1.5%)	
Mallampati classification	130		
Class I		28 (21.5%)	
Class II		68 (52.3%)	
Class III		29 (22.3%)	
Class IV		5 (3.8%)	
OSA severity	132		
Group I (AHI < 3/h)		32 (24.2%)	
Group II (AHI ≥ 3/h < 5/h)		28 (21.2%)	
Group III (AHI ≥ 5/h < 10/h)		42 (31.8%)	
Group IV (AHI ≥ 10/h)		30 (22.7%)	



Relationship between OSA severity and LVH.

Conclusions: There could be an impact on the cardiac structure of children suffering from OSA, as measured by LVH. A study in a larger population is needed to confirm this possibility.

Funding: Funds received by ISCIII (PI18/00565 y PI22/01653), SEPAR (535-2018 y 1073-2020), unconditional grant from Menarini laboratories and awarded by NEUMOMADRID.

38. GENOME-WIDE ANALYSIS OF HAEMOPHILUS INFLUENZAE GENES REVEALS DAM MEDIATED EPIGENETIC REGULATION OF THE FORMATE-DEPENDENT NITRITE REDUCTASE (FNR) REGULON

Celia Gil-Campillo^{1,2}, Gabriel Gutiérrez³, Begoña Euba¹, Irene Rodríguez-Arce¹, Jeroen D. Langereis⁴, María Antonia Sánchez-Romero⁵, Junkal Garmendia^{1,2}

¹Institute Of Agrobiotechnology, Spanish Research Council (idab-csic)-Government of Navarra, Mutilva Baja, Spain. ²Centro de Investigación Biomédica en Red de Enfermedades Respiratorias (CIBERES), Madrid, Spain. ³Department of Genetics, Faculty of Biology, University of Seville, Seville, Spain. ⁴Section Pediatric Infectious Diseases, Laboratory of Medical Immunology, Radboud Institute for Molecular Life Sciences and Radboud Center for Infectious diseases, Radboudumc, Nijmegen, The Netherlands. ⁵Department of Microbiology and Parasitology, Faculty of Pharmacy, University of Seville, Seville, Spain.

Introduction: *Haemophilus influenzae* is a human-adapted pathogen causing chronic lower airway infections and recurrent exacerbations in chronic obstructive pulmonary disease (COPD) patients. Unraveling *H. influenzae* virulence mechanisms will result in identifying targets for drug development. By using transposon insertion sequencing (Tnseq), we screened bacterial genes required for infection in a murine model of airway infection, identified and validated the methyltransferase Dam.

Objectives: To study the role of Dam GATC methylation in the regulation of *H. influenzae* gene expression, and the contribution of such epigenetic regulation to this host-pathogen interplay.

Methods: We followed two complementary approaches: (i) RNA sequencing (RNA-seq) to profile differential gene expression when comparing WT and dam mutant strains. (ii) methylome analysis in a panel of *H. influenzae* PacBio clinical strain genomes to screen hypo/hemi-methylated GATC sites in non-coding regions, as potential elements of epigenetic regulation of gene expression.

Results: The oxygen sensitive fumarate nitrate (FNR) encoding gene, together with the FNR regulon genes ytfE, dmsA and cydD, were over-expressed upon dam inactivation. Further analysis identified GATC motifs in the fnr, dmsA and cydD promoter regions, and Dam methylation of these sites was confirmed. Conversely, methylome analyses recurrently showed GATC hypo/hemi-methylation in a region con-

taining two GATC motifs upstream of the high temperature protein G (htpG) encoding gene, the proximal one overlapping with a putative FNR binding site. Analysis of such GATC sites revealed possible phenotypic heterogeneity in the above mentioned proximal motif, further tested by ad hoc generation of fluorescent reporter strains for single-cell analyses.

Conclusions: Together, our results shed light on Dam methyltransferase contribution to *H. influenzae* pulmonary infection, highlight epigenetic regulation of the *H. influenzae* FNR regulon and its likely involvement in airway infection and bacterial response to environment stress conditions.

Funding: C.G.-C. is funded by PhD studentship PRE2019-088382. This work has been funded by grant MICIU RTI2018-096369-B-I00 and PID2021-125947OB-I00 to J.G. CIBER is an initiative from ISCIII.

41. RELATIONSHIP BETWEEN ASYNCHRONIES AND SLEEP ARCHITECTURE IN MECHANICALLY VENTILATED PATIENTS

Montserrat Batlle Solà

Althaia, Xarxa Assistencial Universitària de Manresa, Manresa, Spain.

Introduction: Sleep quality in ICU is poor. The Odds Ratio Product (ORP) is a continuous index based on EEG. The ORP-Sleep Architecture can be described according to the % of total recording time (TRT) during the sleep study spent in deep sleep (ORP < 0.5) and the % of TRT in full wakefulness (ORP > 2.25). The asynchronies during MV are common and might be related to sedation. It's unknown the relationship between sleep and asynchronies during MV in ICU.

Objectives: To describe the night sleep patterns using ORP and its relationship with sedation, the MV modality and the amount and type of asynchronies in a cohort of mechanically ventilated patients.

Methods: Prospective observational study in a single ICU from a University Hospital in Spain. A Sleep study using Prodigy[®] was performed in a stable phase after ICU admission. The waveforms from the ventilator were recorded using BetterCare[®] to detect asynchronies.

Results: 41 patients were included: Age 64 yo (54-76), Females 29%, APACHE II 9 (6-14). At sleep study: RASS -5 (-3 to -5), duration of MV 3 days (2-4.75), VCV (68%), PSV (19%). Propofol (54%), midazolam (32%), dexmedetomidine (12%). Almost all patients with fentanyl infusion (85%). The amount of deep sleep was 41% "little", 20% "normal" and 39% "excessive". The amount of full wakefulness was 78% "little", 15% "normal" and 7% "excessive". No differences were found between the sleep patterns and the mode of MV. Lightly sedated patients tended to spend less time in deep sleep and more in unstable sleep and in full wakefulness (p = ns). Compared to propofol, midazolam increased the amount of ORP-superficial sleep (p = 0,03) but not the ORP-deep

41. communication

	Little deep sleep (n = 17)	Normal deep sleep (n = 8)	Excessive deep sleep (n = 16)	p
IEE, % breaths; median (IQR)	0.2% (0-0.8)	0.38% (0-0.9)	0.15% (0-0.25)	0.2
DT, % breaths; median (IQR)	0.5% (0.1-1.1)	0.77% (0.26-1.1)	0.6% (0.3-0.82)	0.98
SC, % breath; median (IQR)	0.1% (0-0.3)	0.2% (0.1-0.4)	0.2% (0-0.3)	0.69
RT, % breath; median (IQR)	2.3% (0.7-6)	1.3% (0.15-3)	8% (4-18%)	0.001
PC, % breath; median (IQR)	0	0	0% (0-0.005)	0.74
	Little full wakefulness (n = 32)	Normal full wakefulness (n = 6)	Excessive full wakefulness (n = 3)	p
IEE, % breaths; median (IQR)	0.18% (0-0.4)	0.57% (0.2-0.79)	0.02% (0-0.4)	0.18
DT, % breaths; median (IQR)	0.5% (0.14-1.1)	0.77% (0.25-1.1)	0.6% (0.3-0.8)	0.48
SC, % breath; median (IQR)	0.1% (0-0.26)	0.25% (0.14-0.4)	0.1% (0-0.26)	0.02
RT, % breath; median (IQR)	4.6% (1.2-10)	1.6% (0.7-3.5)	0.75% (0.56-4.6)	0.17
PC, % breath; median (IQR)	0	0.06% (0-0.14)	0	0.006

Amount of each asynchrony according to time in deep sleep (above) and in full wakefulness (below). IEE: Ineffective expiratory efforts; DT: Double trigger; SC: Short cycling; RT: Reverse trigger; PC: Prolonged cycling. Deep Sleep: ORP < 0.5. Little Deep Sleep: < 10% of TRT; Normal Deep Sleep 10-28% of TRT; Excessive Deep Sleep > 28% of TRT. Full wakefulness: ORP > 2.25. Little full wakefulness: < 3% of TRT; Normal full wakefulness: 3-12% of TRT; Excessive full wakefulness > 12% of TRT.

sleep (restorative, $p = 0.42$). No differences were found between low incidence of asynchronies (AI < 10%) and high incidence (AI > 10%) in deep sleep and full wakefulness. Two asynchronies were related to at least normal full wakefulness: Short Cycling (SC) ($p = 0.02$) and Prolonged Cycling (PC) ($p = 0.006$). The reverse trigger asynchrony (RT) was related to excessive deep sleep ($p = 0.001$).

Conclusions: Most patients had either insufficient or excessive amount of deep sleep, but very little time in full wakefulness. Patients with midazolam spent more time in superficial sleep than those in propofol. The global incidence of asynchronies (AI) was not related with sleep patterns, but the asynchronies related to inspiratory time and flow were associated with wakefulness, and reverse triggering with an excessive amount of deep sleep.

42. DIFFERENTIAL HOST TRANSCRIPTOMIC RESPONSE TO VIRAL AND BACTERIAL PNEUMONIAS

Sandra Viz-Lasheras¹, Alberto Gomez-Carballa¹, Jacobo Pardo-Seco¹, Sara Pischedda¹, Irene Rivero-Calle¹, Myrsini Kaforou^{2,3}, Heather Jackson^{2,3}, Dominic Habgood-Coote^{2,3}, Mike Levin^{2,3}, Federico Martín-Torres¹, Antonio Salas¹

¹Genetics, Vaccines, Infectious Diseases and Pediatrics Research Group, Instituto de Investigación Sanitaria de Santiago, Universidad de Santiago de Compostela, Santiago de Compostela, Spain. ²Section of Paediatric Infectious Disease, Faculty of Medicine, Imperial College London, London, United Kingdom. ³Centre for Paediatric and Child Health, Imperial College London, London, United Kingdom

Introduction: Pneumonia is one of the largest causes of death in children younger than 5 years old outside the neonatal period. Pneumonia can be caused by a wide variety of micro-organisms. Diagnosis remains challenging and is based on clinical or microbiological criteria that are often inaccurate, slow and remain unreliable for therapy and prognosis. We investigate host transcriptomic biomarkers in blood from children with viral and bacterial pneumonia and healthy controls, aiming at identifying a gene-expression signature that could help diagnosis and management of the disease.

Objectives: We aim to describe the host transcriptomic response to a pneumonia infection in children and to identify the minimum molecular signature to differentiate viral and bacterial pneumonia, helping to reduce the use of unnecessary antibiotic prescription.

Methods: RNA-seq data was obtained from blood of patients and controls. Data normalisation and differential expression (DE) analysis were carried out using DESeq2. We used the Reactome and GO pathway database to examine biological pathways associated with the DE genes (DEG) in pneumonia patients vs. controls and in children with a bacterial infection vs. children with viral infections. We investigated a minimum specific transcript signature to differentiate between viral/bacterial pneumonia using Parallel Regularised Regression Model Search.

Results: We identified several DEGs in the comparisons controls vs. pneumonia and viral vs. bacterial pneumonias. Functional enrichment analysis showed pathways significantly altered mostly related to the immune system response in both comparisons. Preliminary findings show a minimum host transcriptomic signature allowing to differentiate viral from bacterial pneumonias.

Conclusions: We found different mechanisms and genes involved in the specific response to bacterial and viral pneumonias. Our results suggest that host transcriptomic signatures could be helpful to stratify severe pneumonia condition according to its bacterial or viral origin and contribute to reduce unnecessary antibiotic prescriptions in children with respiratory infections.

Funding: EUCLIDS received funding from the European Union's Seventh Framework Program under grant no. 279185 and PERFORM received funding from the European Union's Horizon 2020 research and innovation program under grant no. 668303.

43. PREDICTIVE BIOMARKERS OF BENIGN PULMONARY NODULES IN LUNG CANCER SCREENING

Carolina Gotera, Javier Alfayate, Elena Cabezas, Diana Sánchez Mellado, Abdulkader El Hachem Debek, Fernanda Troncoso, Laura Nuñez, Marcel Rodríguez, Javier Pinillos, Laura Sánchez, Adele Cardeñosa, Rafael Santana, María Jesús Rodríguez Nieto, Germán Peces-Barba

IIS-Fundación Jiménez Díaz, ISCIII-CIBERES, Madrid, Spain.

Introduction: The National Lung Screening Trial (NLST) demonstrated a 20% reduction in lung cancer (LC) mortality with low-dose CT (LDCT). However, the false positive rate reported after additional testing, including surgery in those suspicious pulmonary nodules (PN) that could not be accessed by bronchoscopy, was high (27%). Studies

General characteristics

	(n = 1,514)
Gender, men, n (%)	947 (56.03)
Age, mean ±	62.91 ± 5.99
BMI, mean ±	27.62 ± 5.41
Current smoker, n (%)	1120 (68.58)
Pack-years index (PYI), mean ±	51.0 ± 22.29
History of CVD or arrhythmias, n (%)	151 (9.97)
Family history of lung cancer, n (%)	205 (13.54)
Spirometry (pre-BD), mean ±	
FVC (L)	3.15 ± 0.88
FVC (%)	95.36 ± 17.87
FEV ₁ (L)	2.16 ± 0.72
FEV ₁ (%)	81.02 ± 20.96
FEV ₁ /FVC	68.22 ± 11.78
Spirometry (post-BD), mean ±	
FVC (L)	3.25 ± 0.91
FVC (%)	98.06 ± 17.71
FEV ₁ (L)	2.21 ± 0.73
FEV ₁ (%)	82.30 ± 20.79
FEV ₁ /FVC	67.72 ± 12.57
Lung diffusion capacity (DLCO) test, mean ±	84.67 ± 21.33
Dyspnoea mMRC scale, n (%)	
0-I	1,469 (86,92)
II-IV	161 (13,07)
COPD, n (%)	790 (48,98)
GOLD GRADE, n (%)	
I	273 (34,55)
II	425 (53,79)
III	85 (10,75)
IV	7 (0,88)
GOLD RISK, n (%)	
A	601 (76,95)
B	102 (12,9)
E	87 (11,01)
Emphysema, n (%)	1,258 (83,09)
Bronchodilator therapy, n (%)	1,063 (62,97)
SAMA	636 (38,99)
LABA	616 (37,81)
LAMA	644 (39,53)
ICS	314 (19,28)
LABA/LAMA/ICS	152 (9,33)

Plus-minus values are means ± SD. BMI: Body mass index; CVD: Cardiovascular disease; pre-BD: prebronchodilator; post-BD: postbronchodilator; FEV₁: forced expiratory volume in 1 second; FVC: forced vital capacity; GOLD: Global Initiative for Chronic Obstructive Lung Disease; COPD: Chronic obstructive pulmonary disease; mMRC: Medical Research Council; SABA: short-acting beta-agonist; SAMA: short-acting muscarinic antagonists; LAMA: long-acting muscarinic antagonist; LABA: long-acting beta-agonists; ICS: Inhaled corticosteroid.

have identified serum biomarkers (BM) associated with the risk of developing several types of cancer, including LC.

Objectives: Determine serum BM capable of identifying benign pulmonary nodules.

Methods: We conducted a cross-sectional analysis of a prospective cohort of patients from 1 January 2014 to 31 January 2023 from the Fundación Jiménez Díaz lung cancer screening (LCS) program. Patients underwent LDCT, pulmonary function tests and blood tests per protocol. For LDCT findings: indeterminate or suspicious PN were considered non-calcified nodules ≥ 6 mm. Those that remained stable at follow-up or with negative results after additional testing were considered for BNP. Suspicious PN waiting for results were excluded.

Results: A total of 1,514 patients were included. Of these, 944 were male (55.92%) with a mean age of 62.91 ± 5.99 years, and most were smokers with COPD and/or Emphysema. The prevalence of LC was 4.16/100 person-years. The general characteristics of the population are described in the Table. An indeterminate or suspicious finding was described in 13% of LDCTs, which required further testing, and in 49.4% of these, LC was confirmed. Our analysis showed statistically significant differences in serum BM in indeterminate PN with benign type at follow-up: lowest serum eosinophil levels, both absolute and percentile (177.92 SD 107.14 vs 235.61 SD 181.20 $P = 0.0022$; (2.42% SD 1.42 vs 3.06% SD 2.10; $P = 0.0154$) and higher pro-BNP levels (155.83 SD 173.57 vs 91.83 SD 282.97; $P = 0.0059$). We found no differences in the other serum biomarkers analyzed: neutrophils, CRP and fibrinogen.

Conclusions: The prevalence of indeterminate nasal polyps in the at-risk population is high, with almost 50% of LCs detected. Our series has found a significant relationship between serum eosinophil and BNP values capable of identifying benign nasal polyps. In addition, these BMs are relatively inexpensive and easy to collect and analyse, which will allow future lines of research to validate these results.

44. LUNG CANCER SCREENING PROGRAM WITH LOW-DOSE CT IN SELECTED COPD-EMPHYSEMA POPULATION

Carolina Gotera¹, Javier Alfayate¹, Elena Cabezas¹, Diana Sánchez Mellado¹, Abdulkhader El Hachem Debek¹, Laura Núñez², Fernanda Troncoso¹, Marcel Rodríguez¹, Borja Recalde^{1,2}, Andrés Giménez¹, Adele Cardeñosa¹, Laura Sánchez¹, Rafael Santana¹, Patricia Lazo², Ivonne Cabrejos², Noelia Cubero², María Jesús Rodríguez Nieto^{1,2}, Germán Peces-Barba¹

¹IIS-Fundación Jiménez Díaz, ISCIII-CIBERES, Madrid, Spain. ²Hospital General de Villalba, Madrid, Spain.

Introduction: Lung cancer (LC) is the leading cause of cancer death worldwide (18%). Five-year survival for LC is 12-18% due to late detection.

Objectives: To analyse the LCS program in a selected population,

Methods: We conducted a transversal analysis of a prospective cohort of patients included in our LCS registry from January 2014 to January 2023 at the Fundación Jiménez Díaz and General de Villalba Hospital, Madrid (Spain). Inclusion criteria: 55-75 years, smoking history of more than 30 pack-years and being a current smoker or former smoker in the last 15 years and COPD or emphysema. Exclusion criteria were evidence of any cancer in the past 15 years, signs or symptoms that could be attributable to malignancy or medical conditions that pose a significant risk of mortality at inclusion.

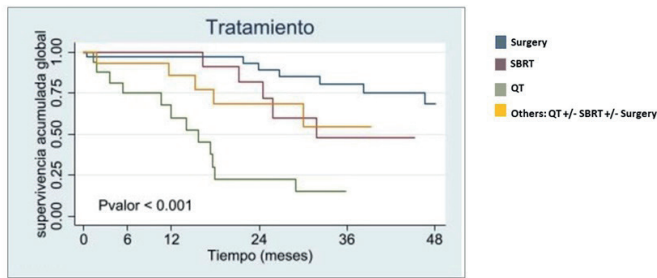
Results: In total, 1,514 individuals underwent LDCT. Of these, 944 were male (55.92%) with a mean age of 62.91 ± 5.99 years, and the majority were smokers (1,120 [68.29%]) with a mean PYI of 51 ± 22.29 . More than 50% had COPD with predominantly mild-moderate airflow limitation, less symptomatic, and low risk of future exacerbations

(GOLD Group A). Emphysema was observed in 81.63% of LDCT with a marked centrilobular pattern followed by centroacinar and paraseptal (625 [48.82%]; 394 [30.78%]; 232 [18.12%], respectively). The general characteristics of the population are described in Table 1. To date, 85 cancers have been detected, of which 58 (68.2%) were diagnosed early (cancer prevalence 4.16/100 person-years). Adenocarcinoma is the most frequent histological type (55.29%), with surgery being the treatment of choice. The mean follow-up until LC diagnosis was 2.15 years (SD 1.95). Furthermore, a statistically significant association between COPD (60 [70.59%] vs 743 [48.12%]; $p \leq 0.001$) and Emphysema (76 [88.41%] vs 1,203 [77.41%]; $p 0.009$) was observed in patients with LC. A significant difference in mortality was observed according to the stage and oncological treatment. Mortality was lower in patients treated with surgery or SBRT (Figure). We found no significant difference in mortality in patients with Emphysema with or without COPD or according to airflow obstruction in COPD.

General characteristics

	All (n = 1,514)
Gender, men, n (%)	947 (56.03)
Age, mean \pm	62.91 \pm 5.99
BMI, mean \pm	27.62 \pm 5.41
Current smoker, n (%)	1120 (68.58)
Pack-years index (PYI), mean \pm	51.0 \pm 22.29
History of CVD or arrhythmias, n (%)	151 (9.97)
Family history of lung cancer, n (%)	205 (13.54)
Spirometry (pre-BD), mean \pm	
FVC (L)	3.15 \pm 0.88
FVC (%)	95.36 \pm 17.87
FEV1 (L)	2.16 \pm 0.72
FEV1 (%)	81.02 \pm 20.96
FEV1 /FVC	68.22 \pm 11.78
Spirometry (post-BD), mean \pm	
FVC (L)	3.25 \pm 0.91
FVC (%)	98.06 \pm 17.71
FEV1 (L)	2.21 \pm 0.73
FEV1 (%)	82.30 \pm 20.79
FEV1 /FVC	67.72 \pm 12.57
Lung diffusion capacity (DLCO) test, mean \pm	84.67 \pm 21.33
Dyspnoea mMRC scale, n (%)	
0-I	1,469 (86.92)
II-IV	161 (13.07)
COPD, n (%)	790 (48.98)
GOLD GRADE, n (%)	
I	273 (34.55)
II	425 (53.79)
III	85 (10.75)
IV	7 (0.88)
GOLD RISK, n (%)	
A	601 (76.95)
B	102 (12.9)
E	87 (11.01)
Emphysema, n (%)	1,258 (83.09)
Bronchodilator therapy, n (%)	1,063 (62.97)
SAMA	636 (38.99)
LABA	616 (37.81)
LAMA	644 (39.53)
ICS	314 (19.28)
LABA/LAMA/ICS	152 (9.33)

Plus-minus values are means \pm SD. BMI: Body mass index; CVD: Cardiovascular disease; pre-BD: prebronchodilator; post-BD: postbronchodilator; FEV1: forced expiratory volume in 1 second; FVC: forced vital capacity; GOLD: Global Initiative for Chronic Obstructive Lung Disease; COPD: Chronic obstructive pulmonary disease; mMRC: Medical Research Council; SABA: short-acting beta-agonist; SAMA: short-acting muscarinic antagonists; LABA: long-acting muscarinic antagonist; LABA: long-acting beta-agonists; ICS: Inhaled corticosteroid.



Conclusions: Our prevalence confirms that LCS with LDCT is more efficient in a selected high-risk population. In addition, LC detected at early stages (I-II) treated with SBRT (non-candidates for surgical treatment due to airflow limitation), we observed a similar to surgery.

46. CHARACTERIZATION OF MACROLIDE-RESISTANT *STREPTOCOCCUS PNEUMONIAE* CAUSING PNEUMOCOCCAL PNEUMONIA IN BARCELONA AMONG 2011-2019

Sara Calvo-Silveria^{1,2}, Lucía Fernández-Delgado¹, Paula Sánchez-Cañibano¹, Aida González-Díaz^{1,2}, Fe Tubau^{1,2}, Dàmaris Berbel^{1,2}, Irene Cadenas-Jiménez¹, Lucía Saiz-Escobedo¹, José Yuste^{2,3}, Sara Martí^{1,2,4}, Carmen Ardanuy^{1,2,5}

¹Hospital de Bellvitge, Hospitalet de Llobregat, Spain. ²Centro de Investigación Biomédica en Red de Enfermedades Respiratorias (CIBERES), Madrid, Spain. ³Pneumococcal Reference Laboratory, Madrid, Spain. ⁴Department of Medicine (UB), Barcelona, Spain. ⁵Department of Pathology (UB), Barcelona, Spain.

Introduction: *Streptococcus pneumoniae* is the main etiologic agent in adult pneumonia, being the polysaccharide capsule its main virulence factor. Macrolides are used in pneumonia treatment, especially in patients allergic to other antibiotics or in combination treatment. Antibiotic pressure has been associated with resistant-strains selection related to the acquisition of transposons carrying resistance genes.

Objectives: The aim was to characterize the mechanisms of resistance to macrolides in strains causing pneumococcal pneumonia (PP) in adults.

Methods: All isolates causing PP in patients ≥ 18 years of age resistant to macrolides (EUCAST) treated at the Bellvitge University Hospital among 2011-2019 were included. Three periods were established (2011-2013, 2014-2016 and 2017-2019). The strains were serotyped by Quellung and/or PCR. Genes related to macrolide resistance [erm(B) and mef] and tetracycline [tet(M)] were detected by PCR. Transposon characterization was performed by PCR detection of int, xis, tnpR and tnpA genes.

Results: Macrolide-resistance frequency over the three periods analyzed was 31.0%, 28.0% and 30.0%, respectively. The resistant strains (n = 186) were isolated mainly from men (63.4%) and the patients mean age was 69.6 (SD \pm 14.0). The cMLS phenotype was the majority in the three periods with a frequency of 92.5% (n = 74), 81.0% (n = 47) and 83.3% (n = 40), respectively. All strains of the cMLS phenotype carried the erm(B) gene, alone (n = 22) or combined with tet(M) (n = 111), with mef(E) (n = 3), or with both (n = 25). The most frequent transposon were: Tn6002 (n = 71) and Tn3872 (n = 25) associated with erm(B)+tet(M); Tn2010 (n = 31) related to erm(B)+mef(E)+tet(M); and Tn917 (n = 10) associated with erm(B). The most frequent serotypes among cMLS were: 19A (n = 34), 6C (n = 24) and 15A (n = 21). The most frequent genotypes were ST320 of serotype 19A (n = 32), ST315 of serotype 6C (n = 23) and ST63 of serotype 15A (n = 18). The M phenotype was detected in 25 isolates (13.4%) associated with the presence of the mef(E) gene, alone (MEGA element, n = 17) or com-

bined with tet(M) (Tn2009, n = 8), and mainly to ST62 genotype of serotype 11A (n = 8).

Conclusions: Resistance to macrolides is high in PP isolates from adults in our area. The cMLS phenotype associated with erm(B) gene is the most frequent. The Tn6002 is more frequent conferring resistance to macrolides, lincosamides [erm(B)], and tetracyclines [tet(M)]. Lineages associated with serotype 19A, included in the 13-serotype conjugate vaccine, are the most frequent among macrolide-resistant strains. Adult vaccination strategies with the new broad-spectrum conjugate vaccines can help control macrolide resistance in pneumococci.

Funding: This study has been funded FIS18/00339.

47. ACTIVE VIRAL REPLICATION IN THE LUNG DURING THE FIRST 11 DAYS OF SYMPTOMS PREDICTS MORTALITY IN CRITICALLY ILL COVID-19 PATIENTS

Ángel Estella¹, Nadia García Mateo^{2,3}, Alicia Ortega^{2,3}, David de Gonzalo-Calvo^{4,3}, Antoni Torres^{5,3}, Ferrán Barbé^{4,3}, Jesús F. Bermejo-Martin^{2,3,6}, Ana P. Tedim^{2,3}

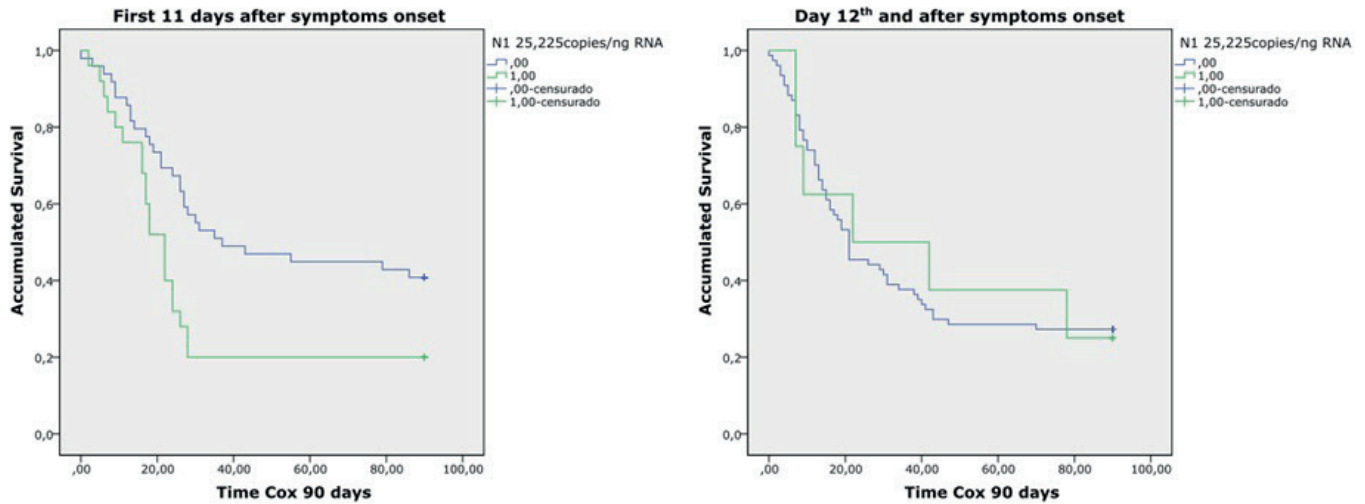
¹Intensive Care Unit, Hospital Universitario de Jerez, Departamento de Medicina Universidad de Cádiz, INIBICA, Cádiz, Spain. ²Group for Biomedical Research in Sepsis (BioSepsis), Instituto de Investigación Biomédica de Salamanca, Gerencia Regional de Salud de Castilla y León, Salamanca, Spain. ³Centro de Investigación Biomédica en Red de Enfermedades Respiratorias (CIBERES), Madrid, Spain. ⁴Translational Research in Respiratory Medicine, University Hospital Arnau de Vilanova and Santa Maria, Lleida, Spain. ⁵Department of Pulmonology, Hospital Clinic de Barcelona, Institut D Investigacions August Pi I Sunyer (IDIBAPS), Universidad de Barcelona, Barcelona, Spain. ⁶School of Medicine, Universidad de Salamanca, Salamanca, Spain.

Introduction: Bronchoalveolar lavage (BAL) fluid obtained from routine bronchoscopic procedures in the ICU may provide significant information for the management of SARS-CoV-2 pneumonia.

Objectives: The aim of this study was to determine the viral load of SARS-CoV-2 in BAL fluids and correlated these results with clinical patients' data.

Methods: 159 ICU patients (≥ 18 years) previously diagnosed with COVID-19 (nasopharyngeal swab PCR) were recruited (March 2020-March 2022, Hospital Universitario de Jerez de la Frontera). BAL fluids were obtained as routine procedures for microbiology laboratory analysis in the first 24h after intubation and frozen after an initial quality check at -80 °C for further analysis. SARS-CoV-2 RNA was extracted from 140 μ l of BAL fluid using the QIAamp® Viral RNA Mini Kit, according to manufacturer instructions. RNA concentration was determined using Qubit™ RNA High Sensitivity quantification kit and Invitrogen™ Qubit™ 4 Fluorometer. Droplet digital PCR (ddPCR) was performed with 3 μ l (1/0.03/0.01 ng) RNA solution using the Bio-Rad SARS-CoV-2 ddPCR kit (N1, N2, and RNase P genes) according to the manufacturer's instructions on a QX-200 ddPCR platform. In-house ddPCR assays were also performed to quantify genomic (E) and subgenomic (sE) RNA for the SARS-CoV-2 E gene. Survival analysis was performed using Kaplan-Meier curves (p < 0.05). Differences in viral load between groups were assessed using the Mann-Whitney U test (p < 0.05).

Results: Approximately 82% of BAL fluid samples were positive for genomic RNA of N1 (n = 129), N2 and E (n = 130, each) and 67% (n = 106) were positive for subgenomic RNA of gene E RNA. Kaplan-Meier curves evidenced that patients with high viral load (N1 $\geq 25,225$, N2 $\geq 24,616$, E $\geq 24,354$, sE ≥ 441 copies/ng RNA) in BAL fluids obtained in the first 11 days after symptoms onset had a decreased survival mean-time compared to those with lower viral loads: [N1 (31.5 vs 51.7 days, p = 0.017 (Figure)), N2 (31.5 vs 51.7 days p = 0.017), E (33.6 vs 51.0 days p = 0.047) and sE (35.2 vs 50.8 days p = 0.05)]. Viral load in BAL



Kaplan-Meier curves indicating differences in survival for N1 gene in patients with BAL fluid obtained in the first 11 days of symptoms onset and BAL fluids obtained after the 11th day of symptoms onset.

showed no impact on survival in those samples collected beyond day 11. BAL samples collected in the first 11 days showed a significantly higher viral load than BAL collected later [(N1-5,167 copies/ng RNA [IQR: 42,964] vs 104 copies/ng RNA [IQR: 2,761]; N2-5,282 copies/ng RNA [IQR: 44,549] vs 96 copies/ng RNA [IQR: 2,829]; E-4,853 copies/ng RNA [IQR: 50,694] vs 91 copies/ng RNA [IQR: 1,808]; sE-108 copies/ng RNA [IQR: 817] vs 3 copies/ng RNA [IQR: 43], $p < 0.001$ all comparisons).

Conclusions: Quantification of viral load of SARS-CoV-2 in BAL fluids in the first 11 days of symptoms predicts mortality.

Funding: Factores de riesgo, pronóstico personalizado y seguimiento de los enfermos ingresados en las unidades de Cuidados Intensivos Españolas infectados por el virus SARS-CoV2; CIBERESUCICOVID-PLUS (Programa de donaciones “estar preparados” – UNESPA, ES21PE07).

50. INCIPIID (EARLY DIFFUSE INTERSTITIAL DISEASE PROGRAM) A STUDY OF PROGNOSTIC BIOMARKERS AND PULMONARY FIBROSIS PROGRESSION

Elena Cabezas, Carolina Gotera, Laura Sánchez, Adele Cardeñosa, Germán Peces-Barba, María Jesús Rodríguez Nieto

IIS-Fundación Jiménez Díaz, ISCIII-CIBERES, Madrid, Spain.

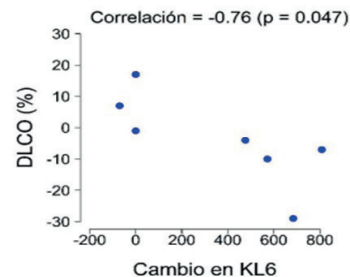
Introduction: Progressive fibrosing interstitial lung diseases a marked clinical and functional deterioration that affects morbidity, mortality and quality of life.

Objectives: (1) To evaluate the utility of serum BM in the diagnosis and follow-up of patients with ILAs in an LCS. (2) To study the correlation between serum BM and clinical parameters, the type of radiological effects and the role of functional parameters in the diagnosis and in a follow-up period.

Methods: This prospective investigation aimed to study subjects with incipient interstitial alterations in LDCT in LCS at the Hospital Fundación Jiménez Díaz and Hospital General de Villalba. Inclusion criteria: 55-75 years, active smokers or those who had quit smoking in the last 15 years with a PYI (pack year index) > 30 , emphysema and/or COPD. Respiratory function tests and LDCT were performed. Blood work was performed to measure inflammatory BM (CRP, leukocytes, fibrinogen, ferritin). In patients with interstitial alterations, KL-6 determination was extended. The relationship between the serum KL-6 value and the rest of the analytical variables, marked in 2020, and the functional and radiological progression was studied. In addition, the

change in KL-6 value (from 2020 to 2022) was compared with the functional progression of these patients.

Results: A good correlation (-0.76) has been observed between the increase in the value of KL-6 from 2020 to 2022 and a statistically significant decrease in DLCO (%) ($p < 0.047$), that is, the increase in KL-6 is related to functional progression, with a decrease in DLCO (%). Likewise, there is a trend similar to that observed in diffusion with a moderate correlation between the increase in the KL-6 and the decrease in FVC (%), but it does not reach statistical significance. In addition, there could be a certain relationship between the values of KL-6 and other analytical values such as LDH and ferritin, with some of the variables that measure functional progression FEV1 (%) and FVC (%).



Conclusions: Increased KL-6 may be useful for predicting functional progression in patients with early interstitial abnormalities detected in LCS. Moreover, there may be a certain relationship between the values of KL-6 and other analytical values such as LDH and ferritin, with some of the variables that measure functional progression of FEV1 (%) and FVC (%).

Funding: Roche Scholarships 2019.

51. A FAST AND RELIABLE GENETIC BARCODING STRATEGY TO CONFIRM ANTIBIOTIC RESISTANCE GENOTYPE-PHENOTYPES IN MYCOBACTERIUM ABSCESSUS

Juan Calvet-Seral^{1,2}, Estefanía Crespo-Yuste^{1,2}, Carlos Martín Montañés^{1,2}, Anandi Martín^{3,4}, Jesús Gonzalo-Asensio^{1,2}

¹Universidad de Zaragoza, Zaragoza, Spain. ²Centro de Investigación Biomédica en Red de Enfermedades Respiratorias (CIBERES), Madrid, Spain. ³University of Louvain, Bruselas, Belgium. ⁴Syngulon, Bruselas, Belgium.

Introduction: Infections caused by nontuberculous mycobacteria are increasing worldwide¹. Of those, *Mycobacterium abscessus* is the major cause of infections, especially in patients with cystic fibrosis or chronic obstructive disease^{2,3}. Similarly to multidrug-resistant (MDR) tuberculosis, *M. abscessus* diseases are difficult to treat due to the limited therapeutic arsenal and development of drug resistance⁴, resulting in a treatment success rate less than 50%⁵. A clinical isolate of *M. abscessus* showing bedaquiline resistance was sequenced, and a novel mutation in the *atpE* gene was identified.

Objectives: To establish a direct genotype-phenotype relationship of the D29A mutation, we developed a recombineering-based method⁶ consisting of the specific replacement of the desired mutation in the chromosome of the *M. abscessus* ATCC19977 reference strain.

Methods: The substrate used in recombineering carried a genetic barcode consisting of silent mutations in codons flanking the *atpE* D29A mutation.

Results: After selection of bedaquiline resistant colonies, transformed with substrates, carrying either the sole D29A mutation, or the mutation with the barcode, we obtained similar numbers of bedaquiline resistant transformants. These colonies were confirmed by Sanger sequencing and allele-specific PCR, demonstrating the presence of the genetic barcode in its specific location in the chromosome. All recombinant strains displayed the same profile of bedaquiline resistance compared to the original clinical isolate from which the D29A mutation was identified. In addition, we also demonstrate the suitability of this method to directly assess an unrelated mutation in the *atpE* gene, A64P, also conferring bedaquiline resistance. To confirm the reproducibility of this technique, we successfully reproduced results of the D29A and A64P mutations using two independent reference strains of *M. abscessus*. Analogs of these two mutations have been reported also in *M. tuberculosis*⁷.

Conclusions: Overall, our genetic barcoding strategy represents a fast and reliable approach to confirm potential antibiotic resistance mutations identified by current genome sequencing techniques, as facilitates allele confirmation by PCR without need of Sanger sequencing, shortening times. We envisage a potential extension of this technique to mycobacteria other than *M. abscessus*, and also its application to study virulence, physiology and biological traits of the *Mycobacterium* genus.

Funding: This work was supported by grants from “Gobierno de Aragón-Fondo Europeo de Desarrollo Regional (FEDER) 2014-2020: Construyendo Europa Desde Aragón” to J.C.-S., grant PRE2020-096507 funded by MCIN/AEI 10.13039/501100011033 to E.C.-Y., and by grant PID2019-104690RB-I00 funded by MCIN/AEI/10.13039/501100011033 to J.G.-A.

References

1. Ratnatunga CN, et al. (2020). PMID: 32194556.
2. Griffith DE, et al. (2022). PMID: 34314673.
3. Floto RA, et al. (2016). PMID: 26666259.
4. Nessar R, et al. (2012). PMID: 22290346.
5. Victoria L, et al. (2021). PMID: 33981630.
6. van Kessel JC, et al. (2008). PMID: 18923412.
7. Segala E, et al. (2012). PMID: 22354303.

54. COMBINED CELL THERAPY AND ANTICOAGULANTS AS A TREATMENT FOR AN *IN VIVO* MODEL OF ACUTE LUNG INJURY

Marta Camprubí-Rimblas^{1,2}, Aina Areny-Balagueró^{1,2}, Elena Campaña-Duel^{1,2}, Luis Morales-Quinteros^{1,2,3}, Sara Quero², Adrian Ceccato¹, Luis Blanch^{1,2}, Antonio Artigas^{1,2}

¹Critical Care Research Center, Parc Taulí Hospital Universitari, Institut d'Investigació i Innovació Parc Taulí (I³PT-CERCA), Universitat Autònoma de Barcelona, Sabadell, Spain. ²Centro de Investigación Biomedica En Red de Enfermedades Respiratorias (CIBERES), Madrid,

Spain. ³Intensive Care, Hospital de la Santa Creu i Sant Pau, Barcelona, Spain.

Introduction: Evidence suggests the beneficial effects of cell therapies or nebulized anticoagulants for the treatment of patients with acute respiratory distress syndrome (ARDS). A combined treatment of the supernatant of mesenchymal stem cells (snMSC) together with nebulized antithrombin (AT), might be a good antiinflammatory, anticoagulant and antimicrobial option for ARDS patients.

Objectives: To evaluate the potential therapeutic effects of a combined cell therapy (snMSC) with nebulized AT in an acute lung injury (ALI) model at 72h.

Methods: The ALI model was induced in Sprague-Dawley rats (~250 g) by the intratracheal administration of 300 µl HCl (0.1 M) and 2 h later 500 µl Lipopolysaccharide (LPS 30 µg/g body weight). Nine hours after the injury 500 µl of the snMSC was intratracheally administered. Some animals also were treated with nebulized AT (500 IU/Kg body weight, AeronexPro System Aerogen Limited) 28h and 52h after injury. Control animals received saline. Animals were sacrificed at 72h. Proinflammatory, chemoattractant, procoagulant and fibrinolytic mediators were evaluated in lung tissue homogenates (mRNA) in the multilobular lungs. The unilobular lungs were embedded in paraffin to obtain histological sections and stain them with hematoxylin-eosin. Lung injury score (LIS) was quantified obtaining the sum of each of the independent variables (hemorrhage, peribronchial infiltration, interstitial edema, pneumocyte hyperplasia, and intra-alveolar infiltration). One-Way-ANOVA and Newman Keuls *post hoc* test (Statistical significance: $p \leq 0.05$).

Results: snMSC or snMSC+AT significantly decreased tissue factor (TF) and plasminogen activator inhibitor-1 (PAI-1) in the lung tissue of injured animals at 72h (Fig. a). Both therapies reduced the mediator of de novo monocytes recruitment (CCL2) and neutrophils recruitment (CXCL1), and the same pattern was followed by IL-1 β . From a histological perspective (Fig. b), lung damage caused by the HCl/LPS administration was evidenced, and snMSC or snMSC+AT significantly decreased the LIS proving recovery of the lung structure compared to injured non-treated animals.

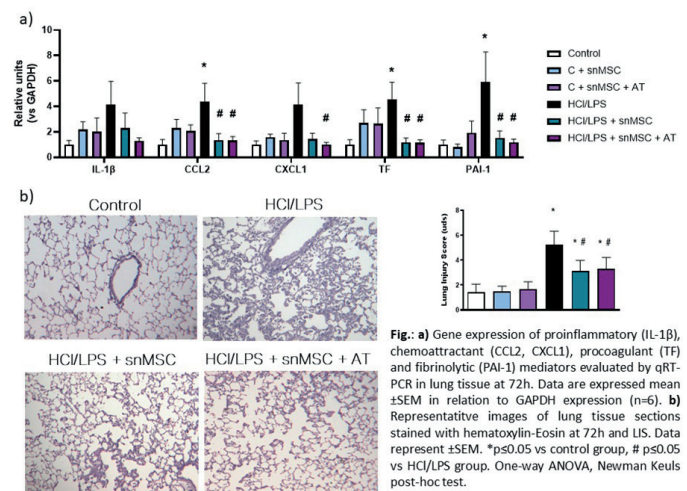


Fig.: a) Gene expression of proinflammatory (IL-1 β), chemoattractant (CCL2, CXCL1), procoagulant (TF) and fibrinolytic (PAI-1) mediators evaluated by qRT-PCR in lung tissue at 72h. Data are expressed mean \pm SEM in relation to GAPDH expression (n=6). b) Representative images of lung tissue sections stained with hematoxylin-Eosin at 72h and LIS. Data represent \pm SEM. * $p \leq 0.05$ vs control group, # $p \leq 0.05$ vs HCl/LPS group. One-way ANOVA, Newman Keuls *post-hoc* test.

Conclusions: snMSC alone or combined with nebulized AT decrease lung injury in an ALI model at 72. Both therapies reduce inflammation, neutrophils and monocytes recruitment, coagulation and promote the activation of fibrinolysis in an ALI model at 72h. These results suggest a possible local therapeutic option for the treatment of ARDS, however, further investigation is required to evaluate the effects of snMSC and its combination with AT in ALI/ARDS.

Funding: This project was supported by Ministerio de Economía y Competitividad - Instituto de Salud Carlos III (PI18/00677 for A Artigas

and PFIS FI19/00102 for L Morales-Quinteros), Fundació Acadèmia de Ciències Mèdiques i de la Salut de Catalunya i de Balears (for A Artigas), Institut d'investigació i Innovació Parc Taulí (I3PT)(CIR2019/035, for M Camprubí-Rimblas) and CIBER de Enfermedades Respiratorias (CIBERes).

55. COVID-19 VACCINE EFFECTIVENESS IN THE PEDIATRIC POPULATION IN GALICIA, NORTHWEST SPAIN. A POPULATION-BASED STUDY

Narmeen Mallah^{1,2,3,4}, Jacobo Pardo-Seco^{1,2,3}, Sonia Ares-Gómez^{1,2,3}, Luis-Ricardo López-Pérez⁵, Juan-Manuel González-Pérez⁵, Benigno Rosón⁵, María-Teresa Otero-Barros⁶, Carmen Durán-Parrondo⁶, Victoria Nartallo-Penas⁶, Susana Mirás-Carballal⁶, Carmen Rodríguez-Tenreiro-Sánchez^{1,2,3}, Irene Rivero-Calle^{1,2,3,7}, Alberto Gómez-Carballa^{1,2,3}, Antonio Salas^{1,2,3,8}, Federico Martín-Torres^{1,2,3,7}

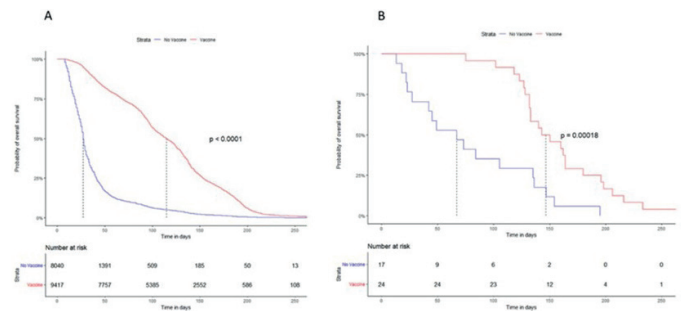
¹Genetics, Vaccines and Pediatric Infectious Diseases Research Group (GENVIP), Instituto de Investigación Sanitaria de Santiago (IDIS), Santiago de Compostela, Galicia, Spain. ²WHO Collaborating Centre for Vaccine Safety, Santiago de Compostela, Spain. ³Centro de Investigación Biomédica en Red de Enfermedades Respiratorias (CIBERES), Madrid, Spain. ⁴Department of Preventive Medicine, University of Santiago de Compostela (USC), Santiago de Compostela, Spain. ⁵Subdirección de Sistemas y Tecnologías de la Información, Servizo Galego de Saude, Galicia, Spain. ⁶Dirección Xeral de Saude Pública, Consellería de Sanidade, Xunta de Galicia, Galicia, Spain. ⁷Translational Pediatrics and Infectious Diseases, Hospital Clínico Universitario and University of Santiago de Compostela (USC), Santiago de Compostela, Spain. ⁸Unidade de Xenética, Instituto de Ciencias Forenses, Facultade de Medicina, Universidade de Santiago de Compostela (USC), and GenPoB Research Group, Instituto de Investigación Sanitaria (IDIS), Hospital Clínico Universitario de Santiago, Servizo Galego de Saude, Galicia, Spain.

Objectives: We aimed to evaluate vaccine effectiveness (VE) against SARS-CoV-2 in two age groups, 5-11 and ≥ 12 -year-old children, in Galicia-Northwest Spain.

Methods: Under collaboration with the Galician Directorate of Public Health, we undertook a population-based test-negative control study in Galicia-Spain. We estimated adjusted odds ratios (OR) and their 95% confidence intervals (CI) using multiple logistic regression models, and then calculated VE as $(1-OR) \times 100$. In our settings, children aged between five and 11 years were vaccinated with the Comirnaty® (Pfizer, US) vaccine, while those aged 12 years or above received either the Comirnaty® (Pfizer, US) or the SpikeVax® (ModernaTX, Inc) vaccine. Fully vaccinated children were defined as those who had received two doses of the vaccine, with 14 days counted from the administration of the second dose. We performed stratified and sensitivity analyses.

Results: 26,984 positive and 27,256 negative SARS-CoV-2 test results from children aged 5-11 during the Omicron circulation fulfilled the inclusion criteria and were entered into the analysis. In the fully vaccinated 5-11-year-old children, VE was 44% (95%CI: 38%-49%). 41,264 SARS-CoV-2 test results corresponding to children 12 years or older were eligible for the analysis. Of the 41,264 test results, 38,205 (92.58%) were undertaken during the Delta variant circulation period, of which 3,856 (10.09%) were positive. The remaining 3,061 (7.42%) SARS-CoV-2 tests were performed during the Omicron variant predominance period and 1,301 (42.50%) of them were positive. VE in fully vaccinated ≥ 12 -year-old individuals was 83% (95%CI: 81%-85%) against Delta and 75% (95%CI: 59%-85%) against Omicron. Stratified analyses revealed that Comirnaty® and SpikeVax® vaccines showed a similar magnitude of VE [Comirnaty® VE: 82%; 95%CI: 79%-84% and SpikeVax® VE: 85%; 95%CI: 82%-88%]. VE was maintained in all age

subgroups in both pediatric populations, but the effectiveness declined over time.



Survival analysis of SARS-CoV-2 infection (A) and hospitalization for COVID-19 (B).

Conclusions: In our settings, along with data from other studies, mRNA VE was moderate against SARS-CoV-2 infections in the 5-11-year-old populations, but high in older children. VE declined over time, suggesting a potential need for booster dose schedules.

56. SIMPLIFIED STRATEGY TO UPDATE THE POST-PANDEMIC TUBERCULOSIS TRANSMISSION SITUATION IN MADRID BY STREAMLINING MOLECULAR AND GENOMIC ANALYSIS

Cristina Rodríguez-Grande¹, Amadeo Sanz-Pérez¹, Andrea Molero-Salinas¹, Marta Herranz², Álvaro Martínez¹, Rosalía Palomino-Cabrera¹, Sergio Buenestado-Serrano¹, Patricia Muñoz^{1,3,4}, Laura Pérez-Lago¹, Darío García de Viedma^{2,3,1}, Mycobacteria Infections Madrid Study Group²

¹Instituto de Investigación Sanitaria Gregorio Marañón, Madrid, Spain.

²Hospital General Universitario Gregorio Marañón, Madrid, Spain.

³Centro de Investigación Biomédica en Red de Enfermedades Respiratorias (CIBERES), Madrid, Spain. ⁴Universidad Complutense de Madrid, Madrid, Spain.

Introduction: Molecular epidemiology and genomic strategies have been essential to provide us with a more precise understanding of the transmission dynamics of *Mycobacterium tuberculosis* (MTB). In Madrid, an effort was made in 2018 to centralise the strain archive of all 24 hospitals as a first step for a population-based approach to survey transmission. A pilot study during 2019 allowed the characterisation of transmission clusters (involving 10% of the total cases), which was halted due to COVID-19 pandemic.

Objectives: This work aims to evaluate an alternative strategy to a faster update the epidemiological situation during and after the pandemic, through a rationalised tandem use of genotypic and genomic analysis.

Methods: 1) Preliminary screening of potential clusters: Simplified genotyping by a 6 loci MIRU reduced panel (MIRU6). 2) Likely clusters: Extended genotyping with MIRU24 on MIRU6 clusters. 3) Confirmed recent transmission clusters: Whole genome sequencing confirmation of the MIRU24 clusters. 4) Identification of strain-specific SNPs from the strains involved in confirmed clusters. 5) Nanopore sequencing of multiple amplicons including strain marker SNPs to track/update the presence of these strains before, during and after the COVID-19 pandemic.

Results: In order to identify the most discriminatory set of MIRU-VN-TR loci for the MTB strains circulating in our population, we analysed the discriminatory power (HGDMI index) of each of the 24 MIRU loci in a collection of 100 isolates representative of clustered/orphan strains. The combinations of the loci 10, 16, 31, Qub11b, 1995 and Q26 offered the highest discriminatory power and were selected (MIRU6). The application of MIRU6 on 246 MTB isolates obtained in 2021 identified 156 (63%) orphan cases, which were ruled out from our subse-

quent analysis. The remaining 90 cases were analysed by MIRU24; 22.2% of which were considered as likely clusters. WGS analysis will lead to the identification of strain marker SNPs to be targeted by multiplex PCR to track/update the presence of the strains.

Conclusions: The first-line application of the MIRU6 discriminatory panel allowed us to identify cases not involved in chains of transmission and thus to dedicate the resources of discriminatory genotyping only to those cases most likely corresponding to active clusters. WGS characterisation of the strains involved in confirmed clusters is an alternative for updating the TB epidemiological information gaps during the pandemic.

Funding: ISCIII (PI21/01823, PI19/00331), PFIS contract (FI20/00129), and European Regional Development Funds (FEDER) from the European Commission, "A way of making Europe".

58. IMPACT OF AN ANTIMICROBIAL STEWARDSHIP PROGRAMME ON THE QUALITY OF ANTIBIOTIC TREATMENTS

Carlos Disdier Gómez^{1,2}, Cristina Caba^{3,4}, Ricardo Pereira^{1,5}, Juan Luengo^{3,6}, María Isabel Martín^{3,6}, Jaime Corral^{1,7}, Luis Carlos Fernández⁴

¹Centro de Investigación Biomédica en Red de Enfermedades Respiratorias (CIBERES), Madrid, Spain. ²Fundosalud, Mérida, Spain. ³PROA-Complejo Hospitalario Universitario de Cáceres, Cáceres, Spain. ⁴Servicio de Farmacia, Complejo Hospitalario Universitario de Cáceres, Cáceres, Spain. ⁵INUBE, Badajoz, Spain. ⁶Servicio de Medicina Interna, Complejo Hospitalario Universitario de Cáceres, Cáceres, Spain. ⁷Servicio de Neumología, Complejo Hospitalario Universitario de Cáceres, Cáceres, Spain.

Introduction: The appropriate use of antibiotics has a clear impact on the clinical course of patients, on the development of bacterial resistance, on adverse reactions and on the cost of care. Drug utilization studies make it possible to detect deviations in their use.

Objectives: To analyze the change in the adequacy of hospital antibiotic treatment before and after the implementation of an antimicrobial stewardship programme (ASP).

Methods: We performed an observational, transversal study to compare the percentage of antibiotic treatments considered adequate before and after the implementation of our ASP at the University Hospital Complex of Cáceres. Adequate treatment was defined as that which met all of the following characteristics: 1) be active against the pathogen causing the infection; 2) correct dose, duration and route of administration; 3) adhere to the recommendations of the current antimicrobial therapeutic guide of the national health system.

Results: We included a total of 348 in-patients with antibiotic treatments, 183 of these during March 2022 and before starting the ASP, and 165 of these during March 2023, 1 year after starting the ASP.

69.7% of the antibiotic treatments were considered adequate after the implementation of the ASP compared to 55.2% in the previous period. In relation to empirical antibiotic treatments, 63% of them were adequate after the ASP compared to 54% before the ASP, while 77% of targeted treatments were adequate after the ASP compared to 73% before this. Finally, the surgical prophylaxis improved 35.5% after the ASP implementation (43.2% of adequate treatments before starting the ASP vs 78.7% after 1 year of its implementation). The most frequent sources of infection were pneumonia (35.7%), urinary tract infection (23.5%) and intra-abdominal infection (10.4%). The most frequent causes of treatment inadequacy were: excessive duration (28.6%), unnecessary antibiotic (22.4%), and antibiotic with a broader spectrum than necessary (18.4%).

Causes of inappropriate treatments

Excessive duration	28.6%
Unnecessary antibiotic	22.4%
Antibiotic with a broader spectrum than necessary	18.4%
Inadequate antibiotic	18.4%
Inadequate dose	8.2%
Inappropriate route of administration	4.1%

Conclusions: The implementation of an antimicrobial stewardship programme produces an improvement in the adequacy of these therapies, especially in surgical prophylaxis (mainly due to the updating of the protocols in our hospital complex). However, there is still a 30% of inadequate treatment, which indicates that the program must be improved.

60. IMMUNOLOGICAL PROFILE OF LUNG TISSUE OF PATIENTS WITH HYPERSENSITIVITY PNEUMONITIS

Marc Massa Gómez^{1,2}, Silvia Sánchez Díez^{1,2}, David Soler Segovia¹, David Espejo Castellanos^{1,2}, Iñigo Ojanguren Arranz^{1,2}, Christian Romero Mesones¹, Xavier Muñoz Gall^{1,2}, María Jesús Cruz Carmona^{1,2}

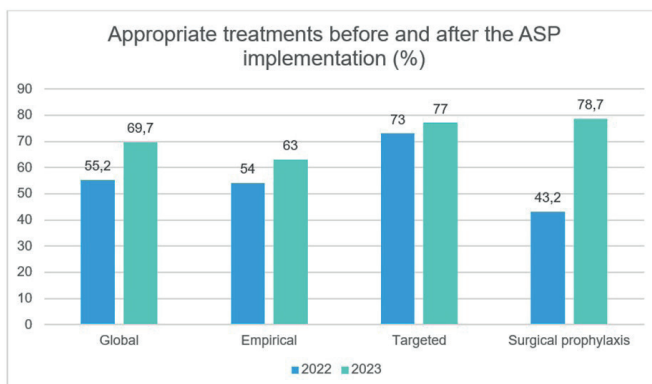
¹Pulmonology Service, Department of Medicine, Vall d'Hebron University Hospital, Barcelona, Spain. ²Centro de Investigación Biomédica en Red de Enfermedades Respiratorias (CIBERES), Madrid, Spain.

Introduction: Hypersensitivity pneumonitis (HP) is an interstitial lung disease characterized by a bronchoalveolar inflammation after the inhalation of organic or inorganic compounds in genetically predisposed individuals. It is known that up to 40% of cases of HP progress to pulmonary fibrosis, so that patients suffer a significant loss of lung function which may require a lung transplant to avoid death as consequence of respiratory failure.

Objectives: The aim of this study was to identify potential biomarkers involved in the innate and immune responses that lead to pulmonary fibrosis in patients who underwent lung transplant due to advanced fibrotic HP.

Methods: Cross-sectional study conducted in 18 patients diagnosed with fibrotic HP and 10 patients diagnosed with idiopathic pulmonary fibrosis (IPF) who underwent lung transplantation. Healthy donors (n = 8) were included as control groups. Lung samples were obtained from Vall d'Hebron and Ciberes Biobanks. Cytokines with a Th1, Th2 and Th17 profile were determined in the tissue homogenate supernatant and pre-transplant serum samples.

Results: Fifty per cent of patients with fibrotic HP had a more pronounced Th2 profile with higher levels of IL-5 and IL-6 in lung tissue homogenate. This group of patients also had increased levels of IL-1 β , IL-8, G-CSF and MCP-1, and lower levels of GM-CSF and IL-23 compared to HP patients with a no Th2 profile. HP patients with a Th2 profile also had higher levels of TNF α while the others exhibited in-



Appropriate treatments before and after the ASP implementation (%).

creased levels of IL-2 compared to healthy controls. Cytokines levels in serum do not show significant differences between groups with the exception of IL-10 which was higher in HP patients with Th2 profile compared to IPF patients. Patients with fibrotic HP and IPF had higher levels of IL-7, IL-13, IL-17 and IL-23 compared to healthy donors, while the levels of IL-1 β and GM-CSF were increased in patients with fibrotic HP but not in patients with IPF.

Conclusions: Results suggest that there are two phenotypes of the disease (Th2-high and Th2-low profiles). In this sense the immunological response in HP patients with a more Th2-high profile seems to indicate a more pronounced activation of the adaptive immune response with high production of cytokines involved in the recruitment of granulocytes.

Funding: Study funded by ISCIII (PI18/00345), CIBERES, FEDER and FUCAP.

61. INCIDENCE OF PATIENT-VENTILATOR ASYNCHRONIES IN SEVERE ARDS COVID-19 PATIENTS

Alba Xifra-Porxas^{1,2}, Leonardo Sarlabous^{1,2}, Verónica Santos-Pulpón^{1,2}, Rudys Magrans³, Rafael Fernández^{4,2}, Gastón Murias⁵, Guillermo Muñoz-Albaiceta^{6,2}, Sol Fernández-Gonzalo^{1,7,8}, Guillem Navarra^{1,2}, Gemma Gomà^{1,2}, Sara Nogales-Herranz¹, Oriol Roca¹, Josefina López-Aguilar^{1,2}, Lluís Blanch^{1,2}, Candelaria de Haro^{1,2}

¹Critical Care Center, Hospital Universitari Parc Taulí, Institut d'Investigació i Innovació Parc Taulí I3PT, Sabadell, Spain. ²Centro de Investigación Biomédica en Red de Enfermedades Respiratorias (CIBERES), Madrid, Spain. ³Better Care, S. L, Barcelona, Spain. ⁴Intensive Care Unit, Fundación Althaia, Universitat Internacional de Catalunya, Manresa, Spain. ⁵Servicio de Terapia Intensiva del Hospital Británico de Buenos Aires, Buenos Aires, Argentina. ⁶Unidad de Cuidados Intensivos, Hospital Universitario Central de Asturias, Departamento de Biología Funcional, Universidad de Oviedo, Oviedo, Spain. ⁷Centro de Investigación Biomédica En Red de Salud Mental (CIBERSAM), Madrid, Spain. ⁸Department of Clinical and Health Psychology, Universitat Autònoma de Barcelona, Barcelona, Spain.

Introduction: Patient-ventilator asynchronies are routinely observed in up to 80% of mechanically ventilated patients, which originate from a mismatch between the patient's inspiratory effort and the programmed gas delivery of the ventilator. They occur throughout the duration of mechanical ventilation and in seemingly apneic patients. Observational studies have consistently associated patient-ventilator asynchronies with adverse clinical outcomes, such as longer duration of ventilator support and higher mortality, and even long-term emotional and cognitive sequelae.

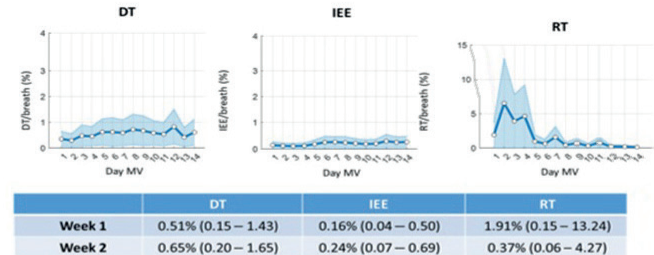
Objectives: To characterize the incidence and evolution of double triggering (DT), ineffective inspiratory efforts during expiration (IEE) and reverse triggering (RT) during invasive mechanical ventilation (IMV) in ARDS COVID-19 patients, as well as the effect of neuromuscular blockers (NMBs) on these asynchronies.

Methods: Observational study from a prospective real-world data cohort from two hospitals (Sabadell and Manresa). Paw and Flow signals were continuously recorded using a dedicated software (Better Care S.L.) during the first 14 days of IMV. We analysed the incidence during all this period and also we compared the incidence during the first 7 days (week 1) and the following days until day 14th (week 2). To investigate the effect of NMBs on asynchronies, a within-subject analysis was performed on the subset of patients that had signals from days with and without NMBs.

Results: We analysed 19,489,119 breaths from 85 patients. Overall, DT events were identified in all patients, IEE events in 98.8% of patients, and RT events in 97.7% of patients. In terms of asynchrony incidence per breath, the median DT was 0.62% [0.22%-1.32%], the median IEE

was 0.22% [0.07%-0.62%], and the median RT was 0.97% [0.18%-4.62%]. The incidence of DT and IEE did not change from week 1 to week 2, whereas the incidence of RT decreased from week 1 to week 2 (Figure a). Although the use of NMBs significantly reduced DT and IEE, they were not completely abolished. On the other hand, there was no significant reduction in RT with the use of NMBs (Figure b).

(a) Evolution of patient-ventilator asynchronies in COVID19 patients



(b) Effect of muscle relaxation on patient-ventilator asynchronies

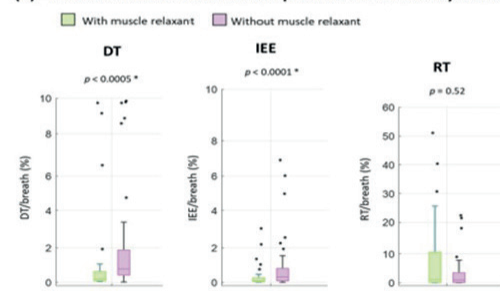


Figure 1. (a) The upper three graphs show the evolution of DT, IEE and RT events throughout the first 14 days of mechanical ventilation. The white dots represent the median across patients, and the shaded blue area is the standard error of the median. The table indicates the median (IQR) across patients for week 1 and week 2, for each asynchrony. (b) The graphs show the effect of muscle relaxation on DT, IEE and RT events. Each graph includes two boxplots, one that represents the median asynchrony with muscle relaxant across patients (green), and the other that represents the median asynchrony without muscle relaxant across patients (purple). The black dots are outliers. To test for statistical significance, we used the Wilcoxon signed rank test.

Conclusions: RT is the most frequent asynchrony in ARDS COVID-19 patients during the first 7 days, followed by DT. Our findings suggest that the use of NMBs does not modify the incidence of RT, and results in a reduction of DT and IEE without completely eliminating them.

Funding: This work was funded by project IDI-20210060 (CDTI/CIEN), CIBER Enfermedades Respiratorias, and Fundació Parc Taulí. Dr. Sarlabous is supported by Pla Estratègic de Recerca i Innovació en Salut program from the Health Department of Generalitat de Catalunya, Spain.

62. UNDERSTANDING COPD UNDERDIAGNOSIS IN THE POST-COVID ERA

Tamara Alonso Pérez¹, Elena Ávalos Pérez-Urría¹, María Rodrigo-García¹, Adrián Peláez Laderas¹, Elena García Castillo¹, Rosa María Girón Moreno¹, Joan B. Soriano¹, Julio Ancochea Bermúdez¹, Esteve Fernández Muñoz²

¹Hospital Universitario La Princesa, Madrid, Spain. ²Instituto Catalán de Oncología, Barcelona, Spain.

Introduction: COPD underdiagnosis remains a global concern, reaching 74.7% in Spain according to EPISCAN II. The COVID-19 pandemic collapsed many pneumology services from 2020 and onwards.

Objectives: We aimed to characterize COPD within our post-COVID external consultation and explore its underdiagnosis.

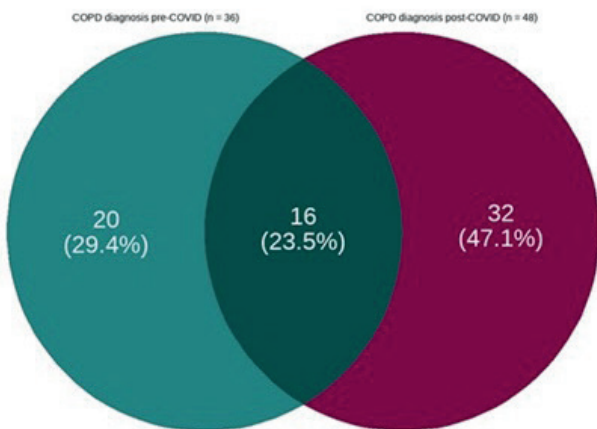
Methods: We evaluated patients seen in our post-COVID external consultation between April 2020 and December 2022, and performed a descriptive analysis of their clinical and functional variables. We compared those with or without a previous diagnosis of COPD ac-

ording to clinical history, and their most recent spirometry, defining COPD as a post-BD FEV₁/FVC < 0.7.

Results: From a total of 473 patients, 287 (60.8%) were men and 186 (39.2%) were women with a mean ± SD age of 65.3 ± 13.2 and 65.3 ± 14.6 yrs., respectively. Overall, 420 (88.8%) patients performed spirometry during follow-up. From those 420 patients, 31 (7.4%) had a previous diagnosis of COPD according to clinical history, while 48 (11.4%) had COPD by spirometric criteria. Correct COPD diagnosis was 33.3%, underdiagnosis 66.6%, and overdiagnosis 4.0%. By gender, COPD underdiagnosis was 58.3% in women and 69.4% in men (p > 0.05). We found significant differences (p < 0.05) between COPD sub-populations (under-, over- and well- diagnosed), in the number of comorbidities (lower in underdiagnosed patients), and their characteristics (underdiagnosed had less smoking habit and lower pack-year index, among other).

COPD subpopulations (under-, over-, well-diagnosed)

Total (n = 420)	FEV ₁ /FVC ratio	
	FEV ₁ /FVC < 0.7 n = 48 (11.4%)	FEV ₁ /FVC ≥ 0.7 n = 372 (88.6%)
Previous diagnosis of COPD n = 31 (7.4%)	16 (33.3%)	15 (4.0%)
No previous diagnosis of COPD n = 389 (92.6%)	32 (66.7%)	357 (96.0%)
Men (n = 259)		
FEV ₁ /FVC ratio		
FEV ₁ /FVC < 0.7 FEV ₁ /FVC ≥ 0.7		
n = 36 (13.9%) n = 223 (86.1%)		
Previous diagnosis of COPD n = 22 (8.5%)	11 (30.6%)	11 (4.9%)
No previous diagnosis of COPD n = 237 (91.5%)	25 (69.4%)	212 (95.1%)
Women (n = 161)		
FEV ₁ /FVC ratio		
FEV ₁ /FVC < 0.7 FEV ₁ /FVC ≥ 0.7		
n = 12 (7.5%) n = 149 (92.5%)		
Previous diagnosis of COPD n = 9 (5.6%)	5 (41.7%)	4 (2.7%)
No previous diagnosis of COPD n = 152 (94.4%)	7 (58.3%)	145 (97.3%)



Venn's diagram. COPD diagnosis.

Conclusions: In our post-COVID external consultation 11.2% of patients were incorrectly diagnosed of COPD (either over- or underdiagnosed). Underdiagnosed patients had less comorbidities and less smoking. More comprehensive screening and diagnostic protocols for COPD are still needed, especially during the post-COVID era.

67. COMPARATIVE STUDY OF THE ETIOLOGY OF NOSOCOMIAL BACTEREMIC PNEUMONIA IN VENTILATED AND NON-VENTILATED PATIENTS: A 10-YEAR EXPERIENCE IN AN INSTITUTION

Emilio Bouza, Helmuth Guillen-Zabala, Adriana Rojas, Gabriela Cañada, Emilia Cercenado, Carlos Sánchez-Carrillo, Pablo Martín-Rabadán, Cristina Diez, Luis Puente, Patricia Muñoz, Alicia Galar

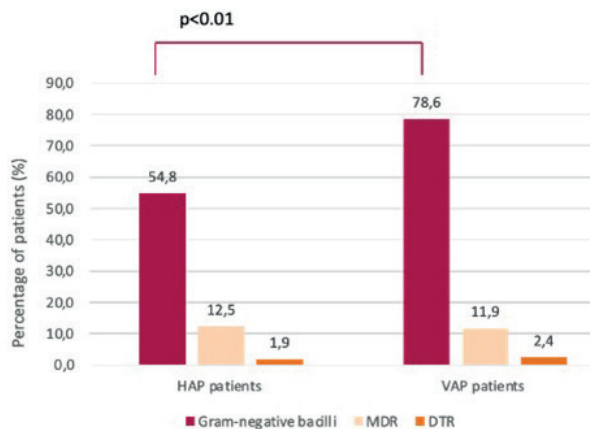
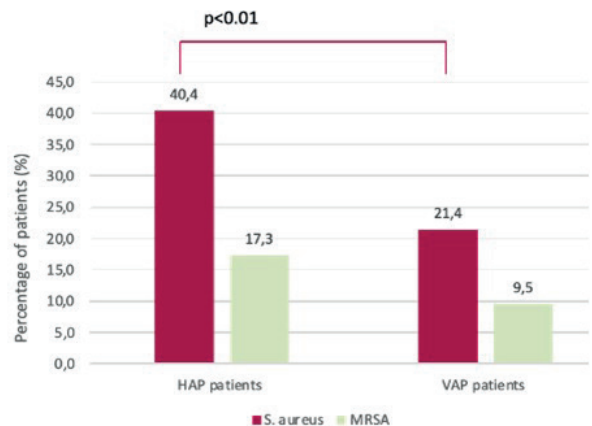
Hospital General Universitario Gregorio Marañón, Madrid, Spain.

Introduction: The etiology of nosocomial pneumonia (NP) of the mechanically-nonventilated patients (HAP) is poorly understood because of the difficulties in obtaining reliable respiratory tract samples. It is assumed that it might be similar to that of mechanically-ventilated patients (VAP) but studies comparing the etiology of both groups are scarce.

Objectives: We compared the etiology of bacteremic NP (bNP) episodes in HAP and VAP in our institution over a 10-year period.

Methods: We defined NP in adults according to ATS criteria. bNP episodes were those with significant isolates obtained in one/more blood cultures concordant with one/more respiratory pathogens isolated with less than 7 days of difference.

Results: During 2010-2019, 188 patients were included. Comparison between HAP (n = 104)/VAP (n = 84) was: male (80.8%/63.1%; p < 0.01); median age (69.3/67.8 years old; p = 0.602); etiology: *Staphylococcus aureus* (40.49%/21.4%; p < 0.01), *Enterobacteriales* (35.6%/39.3%; p = 0.601), and *Pseudomonas aeruginosa* (14.4%/34.5%; p < 0.01). Microorganisms were considered MDR in 29.8%/21.4% of cases respectively (p = 0.193). Median days of hospital stay in HAP/VAP were 45.0/53.5 days (p = 0.255), mortality 55.8%/53.6% (p = 0.770) and related mortality 45.2%/35.7% (p = 0.233).



Comparison of nosocomial bacteremic pneumonia episodes caused by S. aureus and Gram-negative bacilli in HAP and VAP patients.

Conclusions: The etiology of bNP in hospitalized patients is similar but not identical between HAP/VAP. It shows some differences, such higher prevalence of *S. aureus* in HAP and *P. aeruginosa* in VAP. Overall, bNP is a dreadful disease with mortalities over 40%.

Funding: This study was supported by the grants PI20/01350 from Fondo de Investigación Sanitaria (FIS, Instituto de Salud Carlos III; Plan Nacional de I+D+I 2013-2016) and Juan Rodés CM18/00030 from Instituto de Salud Carlos III, partially financed by the European Social Fund (FSE). The study was co-funded by the European Regional Development Fund (FEDER) 'A way of making Europe.'

68. ANALYSIS OF DIFFERENTIALLY EXPRESSED MICRORNAS AND THEIR TARGET GENES IN LUNG TISSUE FROM ASTHMATIC INDIVIDUALS

Marta Gil Martínez^{1,2}, Clara Lorente-Sorolla Martínez-Acitores¹, José Manuel Rodrigo Muñoz^{1,2}, Sara Naharro González¹, Joaquín Sastre Domínguez^{3,2}, Victoria del Pozo Abejón^{3,2}

¹Immunology Department, IIS-Fundación Jiménez Díaz, Madrid, Spain. ²Centro de Investigación Biomédica en Red de Enfermedades Respiratorias (CIBERES), Madrid, Spain. ³Allergy Department, Hospital Universitario Fundación Jiménez Díaz, Madrid, Spain.

Introduction: Asthma is a chronic inflammatory disease of the airways with a complex pathophysiology, being one of the most prevalent chronic diseases. There is a broad spectrum of disease severity among individuals with asthma. Moreover, asthma includes several disease variants and can be stratified into phenotypes and endotypes, thus facilitating responsiveness to treatment, specify the pathogenic mechanisms, and anticipate risks. Reliable biomarkers to identify severe asthma patients and treat them properly, are needed. For this matter, microRNAs (miRNAs) can be a useful tool.

Objectives: The main aim of this study was to analyse the expression of miRNAs and their target genes in lung tissue.

Methods: This study was performed with lung biopsy samples of sixteen asthmatic and twenty non-asthmatic individuals. First, RNA was obtained and then was used to analyse the expression of seven miRNAs, which were previously described in serum and categorised asthma according to the inflammatory component and use of oral corticosteroids, and seven target genes by reverse transcription and semi quantitative real time PCR (RT-qPCR). Statistical analysis included unpaired comparative and correlation tests. Pathway enrichment analysis of deregulated miRNAs, for target gene selection, was performed using DIANA-miRPath v3.0.

Results: Of the seven miRNAs analysed, hsa-miR-26a-1-3p, hsa-miR-376a-3p and hsa-miR-769-5p were found differentially expressed in lung biopsies from asthmatic and non-asthmatic individuals. Expression levels of these three miRNAs were higher in asthmatic patients. Furthermore, in silico pathway analysis showed that these three miRNAs regulate signaling pathways that be related with asthma pathogenesis, from which some target genes were selected for study, involved in the regulation of several crucial pathways: extracellular matrix (ECM)-receptor interaction (COL3A1, COL6A2, COL1A1 and COL6A3), non-small cell lung cancer (CDK6 and CCND1) and p53 signaling pathway (CDK6, CCND1 and IGFBP3). Of these, IGFBP3 were identified as differentially expressed in lung biopsy samples from asthmatic and non-asthmatic subjects, showing greater expression in asthmatic patients.

Conclusions: In this study, we observed a significant altered expression of three miRNAs (hsa-miR-26a-1-3p, hsa-miR-376a-3p and hsa-miR-769-5p) and we conclude that could be used as markers to differentiate asthmatic and control individuals, and play a role in immune regulation of asthma pathogenesis.

Funding: This study was supported by Fondo de Investigación Sanitaria and Fondo Europeo de Desarrollo Regional (FIS and FEDER) [PI18/00044]; for Biomedical Network of Respiratory Diseases (CIBERES), Instituto de Salud Carlos III (ISCIII). M.G.-M. was supported by a Contrato predoctoral de formación en investigación (PFIS) contract (FI19/00067) from the FIS (Ministerio de Sanidad y Consumo, Spain).

69. NOVEL REPURPOSING STRATEGIES FOR ANTIMICROBIAL DEVELOPMENT IN *KLEBSIELLA PNEUMONIAE*

Marta Gómara-Lomero¹, José Antonio Aínsa^{1,2}, Santiago Ramón-García^{1,2,3}

¹Grupo de Genética de Micobacterias, Universidad de Zaragoza, Zaragoza, Spain. ²Centro de Investigación Biomédica en Red de Enfermedades Respiratorias (CIBERES), Madrid, Spain. ³Fundación Agencia Aragonesa para la Investigación y el Desarrollo (ARAID), Zaragoza, Spain.

Introduction: Treatment of infections caused by multi-drug resistant (MDR) *Klebsiella pneumoniae* remains challenging due to the limited therapeutic options. Drug repurposing could accelerate the development of urgently needed successful interventions.

Objectives: This work aimed to identify and characterise novel drug combinations against *Klebsiella pneumoniae* based on the concepts of synergy and drug repurposing.

Methods: Firstly, we performed a semi-qualitative high-throughput synergy screen (sHTSS) with tigecycline, colistin and fosfomicin (last-line antibiotics against MDR *Enterobacteriaceae*) combined with an FDA-library containing 1,430 clinically approved drugs. Selected hits were further validated by secondary checkerboard (CBA) and time-kill (TKA) assays. Synergistic and killing effects were evaluated at different time points (8, 24 & 48 hours) to obtain a priority list of combinations. Secondly, we explored the *in vitro* validation process of combinations based on two drugs identified in the previous screening: zidovudine and azithromycin, respectively, against a panel of twelve MDR/XDR *K. pneumoniae* strains and their activities confronted with those combinations currently used for MDR enterobacteria treatment (meropenem/ertapenem, meropenem/colistin, fosfomicin/colistin, fosfomicin/tigecycline). Moreover, we evaluated cytotoxicity of novel combinations against Hep G2 cell line.

Results: We identified 109 hits by sHTSS that enhanced any of the three antibiotics, most of them known antimicrobials (Figure). Further validation showed 15.09% and 65.85% confirmation rates by CBA and TKA respectively. As a result, six novel combinations based on non-antibiotic drugs were identified, and several synergistic combinations with clinical-translational potential were prioritized. For novel zidovudine- and azithromycin-based combinations, we obtained better bactericidal activities than usual treatments without added cytotoxicity. Zidovudine plus ceftazidime-avibactam, zidovudine plus fosfomicin, azithromycin plus fosfomicin and azithromycin plus colistin were the most potent combinations (Table).

Conclusions: sHTSS paired to TKA are powerful tools for the identification and characterization of novel synergistic drug combinations against *K. pneumoniae*. Both zidovudine and azithromycin were demonstrated to act *in vitro* as good candidates in combination therapies with clinically used antibiotics against *K. pneumoniae*. Further pre-clinical studies might support the translational potential of zidovudine- and azithromycin-based combinations for the treatment of these infections.

Funding: This work was supported by a fellowship from the Government of Aragon (Gobierno de Aragón y Fondos FEDER de la Unión Europea "Construyendo Europa desde Aragón") to M.G.-L., and a grant from the Government of Aragon, Spain (Ref. LMP132_18) (Gobierno de Aragón y Fondos Feder de la Unión Europea "Construyendo Europa desde Aragón") to S.R.-G.

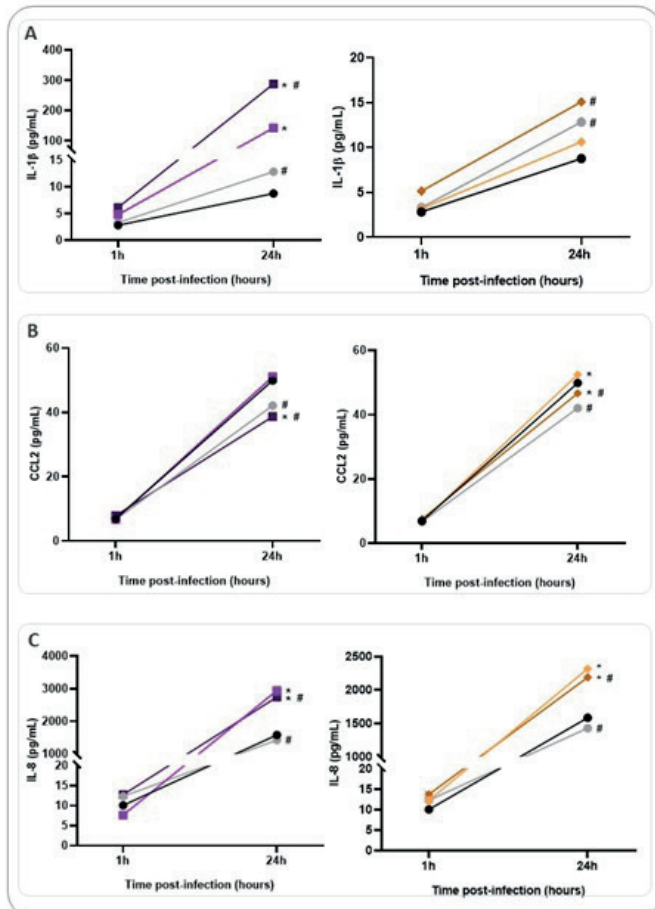


Figure 1.1. Protein concentration in cell culture supernatant of proinflammatory (IL-1 β) (A) and chemoattractant mediators CCL2 and IL-8 (B, C) 1 h and 24 h post-infection with *P. aeruginosa* or *S. pneumoniae* of the HPAEpiC and THP-1 cells co-culture. n=5-12. Data represented as mean \pm SEM. * p<0.05 vs the respective control group (control group at 5% or control group at 15% of CO₂); †p=0.05 vs the respective group at 5% of CO₂ (control group at 5% or PA group at 5%); # p<0.05 vs the respective group at 5% of CO₂ (control group at 5% or PA group at 5%).

1. Protein concentration in cell culture supernatant of proinflammatory (IL-1 β) (A) and chemoattractant mediators CCL2 and IL-8 (B, C) 1 h and 24 h post-infection with *P. aeruginosa* or *S. pneumoniae* of the HPAEpiC and THP-1 cells co-culture. n = 5-12. Data represented as mean \pm SEM. *p = 0.05 vs the respective control group (control group at 5% or control group at 15% of CO₂); †p = 0.05 vs the respective group at 5% of CO₂ (control group at 5% or PA group at 5%). 2. Protein concentration in cell culture supernatant of occludin (D) and ZO-1 (E) in total intracellular protein 1 h and 24 h post-infection with *P. aeruginosa* or *S. pneumoniae* of the HPAEpiC and THP-1 cells co-culture. n = 5-12. Data represented as mean \pm SEM. *p = 0.05 vs the respective group evaluated at 1 hour post-infection. ZO-1: zonula occludens 1.

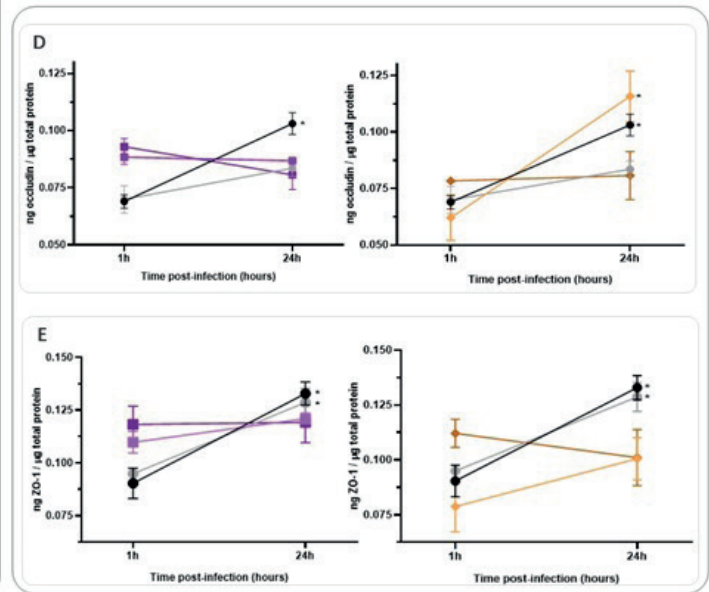


Figure 1.2. Protein concentration in cell culture supernatant of occludin (D) and ZO-1 (E) in total intracellular protein 1 h and 24 h post-infection with *P. aeruginosa* or *S. pneumoniae* of the HPAEpiC and THP-1 cells co-culture. n=5-12. Data represented as mean \pm SEM. * p<0.05 vs the respective group evaluated at 1 hour post-infection. ZO-1: zonula occludens 1.

Conclusions: The hypercapnic condition on bacterial-infection response could play a detrimental in the course of PA and SPN infection. **Funding:** This project was supported by Sociedad Española de Neumología y Cirugía Torácica (SEPAR); European Society of Intensive Care Medicine (ESICM); Parc Taulí Hospital Universitari, Institut d'Investigació i Innovació Parc Taulí (I3PT) and Centro de Investigación Biomédica en Red de Enfermedades Respiratorias (CIBERES).

73. FILAGGRIN AND CYTOKINES IN RESPIRATORY SAMPLES OF PRETERM INFANTS AT RISK FOR RESPIRATORY VIRAL INFECTION

José Manuel Rodrigo-Muñoz¹, Beatriz Sastre¹, Laura Sánchez-García², María Luz García-García³, Ersilia González-Carrasco⁴, Celia Fabra², Marta Gil-Martínez¹, Clara Lorente-Sorolla⁵, Sara Naharro-González⁵, Zahara García de Castro⁵, Sonia Alcolea⁶, Inmaculada Casas⁷, Cristina Calvo⁸, Victoria del Pozo¹

¹Department of Immunology, IIS-Fundación Jiménez Díaz, Centro de Investigación Biomédica en Red de Enfermedades Respiratorias (CIBERES), Madrid, Spain. ²Neonatology Department, Hospital Universitario La Paz, Madrid, Spain. ³Pediatrics Department, Hospital Severo Ochoa, Translational Research Network in Pediatric Infectious

Diseases (RITIP), Centro de Investigación Biomédica en Red de Enfermedades Infecciosas (CIBERINFEC), Madrid, Spain. ⁴Neonatology Department, Hospital Severo Ochoa, Madrid, Spain. ⁵Department of Immunology, IIS-Fundación Jiménez Díaz, Madrid, Spain. ⁶Pediatric Infectious Diseases Department, Hospital Universitario La Paz, Fundación IdiPaz, CIBERINFEC, Madrid, Spain. ⁷Respiratory Virus and Influenza Unit, National Microbiology Center (ISCIII), Centro de Investigación Biomédica en Red de Epidemiología y Salud Pública (CIBERESP), Madrid, Spain. ⁸Pediatric Infectious Diseases Department, Hospital Universitario La Paz, Fundación IdiPaz, Translational Research Network in Pediatric Infectious Diseases (RITIP), CIBERINFEC, Madrid, Spain.

Introduction: Preterm and very low birth weight infants are highly vulnerable to respiratory viral infections (RVIs). These respiratory infections are very frequent in Neonatal Intensive Care Units (NICUs), and have been shown to be determinant of poorer respiratory outcomes in children. Immune response and respiratory barriers are key defense elements against viral insults in premature infants admitted to NICUs; and thus, further research is needed to fully characterize preterm infants' immune response to acute respiratory viral infections.

Objectives: Our main goals were to describe the local immune response in respiratory secretions of preterm infants with RVIs during NICU admission and to evaluate the expression and synthesis of lung barrier regulators, both in respiratory samples and *in vitro* models

Methods: Nasopharyngeal aspirate (NPA) was obtained, separating cells from supernatants. Viral detection was performed by nested PCR and gene expression by qPCR. Proteins were detected by western blot and ELISA or Luminex. Small airway epithelial cells (SAEC) were stimulated with Poly:IC and/or wounding.

Results: Samples from preterm infants that went on to develop RVIs had lower filaggrin gene and protein levels at cellular level were compared to never-infected neonates (controls). Filaggrin, MIP-1 α /CCL3 and MCP-1 levels were higher in pre-infection supernatants from compared to non infected controls, being molecules related with modulation of risk infection. In contrast, samples from children who later developed IVR had lower frequency of filaggrin expression and lower protein levels. Filaggrin, HIF-1 α , VEGF, RANTES/CCL5, IL-17A, IL-1 β , MIP-1 α and MIP-1 β /CCL5 levels were higher during and after infection. ROC curve and logistic regression analysis shows that these molecules could be used as infection risk biomarkers. SAECs stimulated by poly:IC reduced filaggrin expression and increased its levels in the supernatant. Finally, stimulation of SAECs with poly:IC increased TLR3 and TSLP expression, and reduced AREG expression.

Conclusions: We conclude that filaggrin expression and protein quantity decrease at the ANP cellular level, whereas its secreted levels increased in basal samples from infected neonates and in poly:IC-stimulated SAECs. Our findings highlight the importance of filaggrin as a facilitating factor of RVIs.

Funding: This study has been partially supported by ISCIII-Instituto de Salud Carlos III, FIS (Fondo de Investigación Sanitaria-Spanish HealthResearch Fund) grants FI19/00067, PI18/00167, PI21/00896, PI18CIII/00009 and FEDER funds (Fondo Europeo de Desarrollo Regional); Sociedad Española de Alergología e Inmunología Clínica (SEAC) Beca19A04_Valverde; Alfonso X El Sabio University Grant: VIII Convocatoria Santander-UAX; CIBER de Enfermedades Respiratorias (CIBERES), CIBER de Enfermedades Infecciosas (CIBERINFEC) y CIBER de Epidemiología y Salud Pública. (CIBERESP) a Carlos III Institute of Health Initiative.

74. THERAPEUTIC EFFICACY OF MTBVAC AGAINST ESTABLISHED EXPERIMENTAL ASTHMA BY SYSTEMIC DESENSITIZATION

Silvia Calvo García¹, Santiago Uranga Maíz¹, Ana Belén Gómez Aguirre¹, Jose Manuel Rodrigo Muñoz², Victoria del Pozo Abejón², Carlos Martín Montañés¹, Nacho Aguiló Anento¹

¹Universidad de Zaragoza, Grupo Genética de Micobacterias, Zaragoza, Spain. ²Fundación Jiménez Díaz, Madrid, Spain.

Introduction: Asthma is one of the most common pulmonary diseases in the world, and its incidence continues increasing, generating a huge economic burden in public health. Asthma is often associated with an exacerbated type 2 inflammation. Allergen-specific Th2 lymphocytes produce cytokines which are responsible of some of the clinical symptoms. Thus, therapies targeting asthma-associated type 2 responses have demonstrated to be highly promising. MTBVAC is a novel live attenuated tuberculosis vaccine currently under clinical evaluation as tuberculosis vaccine. Intradermal MTBVAC has been widely tested in preclinical and clinical trials, and it just starts efficacy trials in newborns this year. Due to its Th1 response-promoting activity, the pulmonary administration of the MTBVAC has been shown to have strong therapeutic efficacy.

Objectives: 1. To study the mechanism of intravenous MTBVAC against asthma. 2. To implement efficacy studies of MTBVAC against allergic asthma. 3. To undermine the effect of MTBVAC incubation on human peripheral blood mononuclear cells (PBMCs).

Methods: For animal models, mice were subjected to different allergy protocols, using ovalbumin and house dust mite like allergens. Results showed here correspond to cytometry flow, ELISA tests and histolog-

ical analysis. Human PBMCs were incubated in presence of MTBVAC and subjected to proliferation assay. The resulted supernatant was analysed by ELISA and genes measured by qPCR.

Results: Here, considering the systemic character of endovenous administration of vaccines, we explore this route with MTBVAC to study how its mechanism against allergies works. Results show that the endovenous administration of MTBVAC is capable of desensitizing (reduction of antigen specific Th2 cytokines) in spleen, also in absence of established symptoms, such as eosinophilia. In addition, MTBVAC produces IFN γ , which is not necessary for reducing eosinophils in BAL and lung. According to efficacy studies, MTBVAC has a long-term protection against asthma, as therapeutic effect is maintained six months post vaccination. To translate this study into clinical research, we have analyzed the effects of MTBVAC incubation on PBMCs from asthmatic patients. Results suggest that MTBVAC reduces the clonal proliferation of allergen-specific cells and reduces the production of allergen-induced Th2 cytokines.

Conclusions: Our data showed strong therapeutic efficacy of MTBVAC intravenous administration in a scenario of established disease, not only in animal models but also in human PBMCs.

Funding: Ministerio de ciencia, innovación y universidades. Gobierno de España. Ayudas para contratos predoctorales 2019. Ayuda movilidad CIBER 2022.

78. LUNG-ON-A-CHIP PHYSIOMIMETIC MODEL TO IMPROVE THE STUDY OF THE EFFECTS OF INFECTIONS IN CULTURED CELLS

Esther Marhuenda^{1,2}, Alvaro Villarino¹, Raimon Sunyer^{1,3,4}, Nuria Gavara^{1,5,4}, Ramon Farre^{1,2,6,4}, Isaac Almendros^{1,2,6}, Jorge Otero^{1,2,5,4}

¹Universitat de Barcelona, Barcelona, Spain. ²Centro de Investigación Biomédica en Red de Enfermedades Respiratorias (CIBERES), Madrid, Spain. ³Centro de Investigación Biomédica en Red de Bioingeniería, Biomateriales y Nanomedicina, Madrid, Spain. ⁴IN²UB, Barcelona, Spain. ⁵IBEC, Barcelona, Spain. ⁶IDIBAPS, Barcelona, Spain.

Introduction: Current *in vitro* models do not realistically recreate the complex pathophysiology of bacterial/endotoxin-mediated lung injury.

Objectives: To develop an advanced physiomic model of lung injury based on the use of 3D extracellular matrix hydrogels and lung-on-a-chip devices.

Methods: Monolayers of rat primary alveolar epithelial cells were cultured on top of decellularized lung hydrogels¹ containing primary lung mesenchymal stromal cells. These 3D structures were then cultured on the flexible membranes of lung-on-a-chip devices where cyclic stretch was applied to mimic breathing. An inflammatory response was induced by using a lipopolysaccharide bacteriotoxin hit. A conventional 2D culture on plastic plates was used as control. The secretion of the most relevant inflammatory cytokines was assessed by ELISA.

Results: Cytokine analysis (Figure) showed that the developed advanced model presented a more reduced inflammatory response than traditional models (2D cultures in plastic), which is in line with what is expected from the response commonly observed in patients. Further, from the individual analysis of the different stimuli, it was observed that the use of extracellular matrix hydrogels obtained from decellularized lungs had the most significant impact on the change of the inflammatory response².

Conclusions: The developed advanced model showed a better-adjusted response to a bacteriotoxin-mediated hit than the classic cell culture setting. For studying infections in organs other than the lung the hydrogel can be made by decellularizing the corresponding organ. Therefore, this novel physiomic model is a potential platform to obtain more robust results when testing different drugs or cell therapy for lung injury.

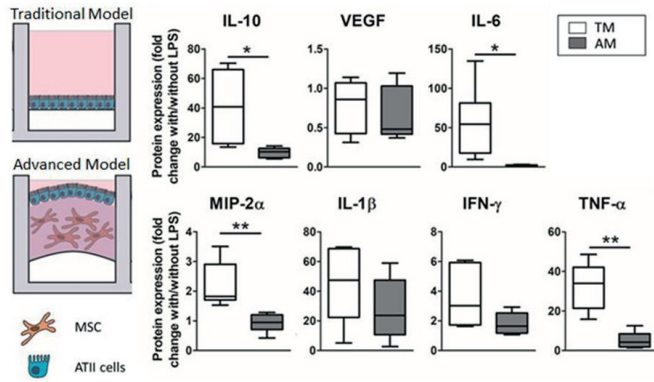


Figure 1. Different magnitude response of the advanced model (ATII cultured on hydrogels with 3D-cultured LMSC inside) compared to a traditional 2D culture model (ATII cell cultured on PDMS). Results were expressed as the ratio of cytokines expressed with/out the LPS hit, for either the traditional model (TM) or the advanced model (AM).

Funding: This research was funded by the Spanish Ministry of Science, Innovation and Universities, grants numbers PID2019-108958RB-I00, PGC2018-097323-A-I00, and PID2021-128674OB-I00.

References

1. Marhuenda *et al.* IJMS. 2022.
2. Marhuenda *et al.* Front Pharmac. 2023.

83. LOW ANTI-S1 ANTIBODIES AND ANTIGENEMIA AT EMERGENCY ROOM ADMISSION PREDICT HOSPITALIZATION IN COVID-19 DURING AN OMICRON-PREDOMINANT WAVE

Amanda de la Fuente^{1,2}, Tamara Postigo¹, Alicia Ortega^{1,2}, Marta Dominguez-Gil González^{3,2}, Raúl López Izquierdo^{4,2}, Jesus F Bermejo-Martin^{1,2}

¹Group for Biomedical Research in Sepsis (BioSepsis), Instituto de Investigación Biomédica de Salamanca (IBSAL), Gerencia Regional de Salud de Castilla y León, Salamanca, Spain. ²Centro de Investigación Biomédica en Red de Enfermedades Respiratorias (CIBERES, CB22/06/00035), Instituto de Salud Carlos III, Madrid, Spain. ³Microbiology Service, Hospital Universitario Río Hortega, Valladolid, Spain. ⁴Emergency Department, Hospital Universitario Río Hortega, Valladolid, Spain.

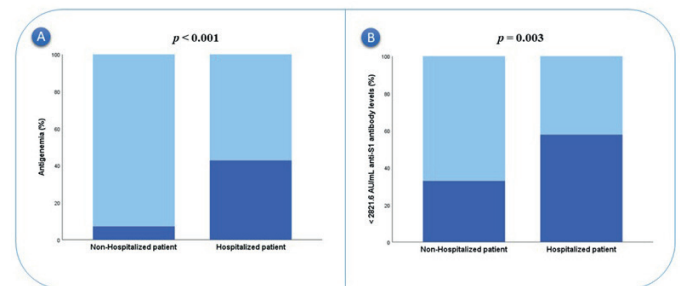
Introduction: The current pandemic of SARS-CoV-2 remains a global concern. Therefore, detection of frail patients with the highest likelihood of deterioration is needed. Detection of viral antigens and/or RNA in plasma has been shown to be associated with severe disease.

In critically ill patients, our group had previously evidenced that presence of N-antigenemia at ICU admission is associated with increased mortality. This evidence supports the monitoring of antigenemia in hosts, since it can be used as a tool to identify patients at higher risk of deterioration.

Objectives: To profile the presence of N-antigenemia along with the concentration of anti-SARS-CoV-2 S1 antibodies in plasma of patients with COVID-19 at admission to the ER to assess their ability to predict hospitalization.

Methods: The presence of N-antigenemia and anti-SARS-CoV-2 IgG titers (anti-N and anti-S1) were evaluated in the first 24 hours following ER admission in 146 COVID-19 patients, by using the Panbio® COVID-19 Ag Rapid Test Device and the SARS-CoV-2 IgG II Quant and SARS-CoV-2 IgG assays on an Alinity platform from Abbott (Chicago, IL, USA), respectively. Statistical analysis was performed using IBM SPSS Statistics 25.0. Differences between independent groups were assessed using the chi-square test or Fisher's Exact Test for categorical variables and the Mann-Whitney U test for continuous variables. Multivariate logistic binary regression was employed to evaluate the association between antigenemia and hospital admission.

Results: The presence of N-antigenemia at ER admission was more commonly observed in those patients who were hospitalized (43% vs 7%, $p < 0.001$) (Figure, panel A). Patients who required hospitalization lacked more often and lower levels of anti-SARS-CoV-2 S1 IgG antibodies (25% vs 10%, $p = 0.014$) (1154 vs 8435 AU/mL in median, $p = 0.002$). [anti-SARS-CoV-2 S1 IgG] yielded an overall AUC of 0.648 to predict hospitalization in our cohort, with an OOP of 2821 AU/mL (Sensitivity 58%; Specificity: 67%). The proportion of patients with anti-SARS-CoV-2 S1 antibodies below the OOP was higher in the group of hospitalized patients (58% vs 33%, $p = 0.003$) (Figure, panel B). The multivariate analysis revealed that those patients with N-antigenemia, as well as those with [anti-SARS-CoV-2 S1 IgG] less than 2821 AU/mL, were at increased risk of hospitalization (HR [CI95%], p) (5.29 [1.31-21.43], 0.020) (9.79 [2.23-42.92], 0.002) respectively (Table).



Panel A. Frequency of N-antigenemia in non-hospitalized and hospitalized patients. Panel B. Frequencies of patients with anti-S1 antibody levels < 2821.6 AU/mL in each group.

Univariate and multivariate logistic regression analysis to predict hospitalization

	Univariate				Multivariate (N = 146)				Multivariate (N = 146)			
	OR	95%CI		p	OR	95%CI		p	OR	95%CI		p
Age (years)	1.06	1.04	1.09	< 0.001	1.06	1.02	1.11	0.002	1.09	1.04	1.14	< 0.001
Male	2.94	1.50	5.79	0.002	2.48	0.79	7.78	0.120	2.18	0.68	7.00	0.192
Institutionalized	6.80	1.85	25.03	0.004	0.68	0.08	6.26	0.736	0.79	0.09	7.18	0.834
Charlson Comorbidity Index	2.86	1.92	4.29	< 0.001	2.24	1.29	3.86	0.004	2.67	1.43	4.99	0.002
Hypertension	3.55	1.60	7.85	0.002	0.15	0.03	0.82	0.029	0.16	0.03	0.89	0.036
Vaccination (≥ 2 doses)	0.311	0.13	0.75	0.009	0.42	0.10	1.74	0.233	0.56	0.12	2.70	0.473
Altered state of consciousness	4.97	0.99	24.82	0.050	0.19	0.01	3.40	0.259	0.19	0.01	3.34	0.253
SpO2/FIO2 ratio	0.95	0.93	0.97	< 0.001	0.98	0.95	1.01	0.053	0.98	0.95	1.01	0.117
Respiration rate	1.36	1.18	1.55	< 0.001	1.31	1.08	1.58	0.005	1.22	1.03	1.45	0.025
Mean Arterial Pressure	0.98	0.96	0.99	0.035	0.96	0.93	0.99	0.043	0.97	0.93	1.01	0.055
[Antigenemia]	9.62	3.65	25.37	< 0.001	5.29	1.31	21.43	0.020	-	-	-	-
[Anti-S1 antibody levels] (< 2,821.6 AU/mL)	2.79	1.42	5.49	0.003	-	-	-	-	9.79	2.23	42.92	0.002

Conclusions: Profiling anti-SARS-CoV-2 S antibody levels and N-antigenemia upon entry to the ER could contribute to identify those patients at risk of deterioration who will need to be hospitalized.

Funding: AdIF contract is financially supported by Instituto de Salud Carlos III (ISCIII) and co-funded by the European Union (PFIS: FI20/00278).

85. GENERATION OF A SARS-COV-2 AEROSOL INFECTION MODEL IN HUMANIZED MICE K18-HACE2: ONE STEP FURTHER IN THE STUDY OF RESPIRATORY COINFECTIONS

Pablo Soldevilla^{1,2,3}, María Vidal^{1,2}, Jorge Diaz⁴, Yaiza Rosales⁴, Mireia Martínez⁴, Daniel Pérez-Zsolt⁵, Jordana Muñoz-Basagoiti⁵, Marçal Gallemí⁵, Dàlia Raïch-Regué⁵, Elisa Molina⁵, Alexia Paris⁶, Ana Blanco⁶, Gustavo Tapia⁷, Nuria Izquierdo-Useros^{1,5,8}, Pere-Joan Cardona^{1,2,3,6,9}, Cristina Vilaplana^{1,2,3,9,10}

¹Germans Trias i Pujol Research Institute (IGTP), Badalona, Spain.

²Unitat de Tuberculosi Experimental (UTE), Badalona, Spain. ³Centro de Investigación Biomédica en Red de Enfermedades Respiratorias (CIBERES), Madrid, Spain. ⁴Centre de Medicina Comparativa I Bioimatge de Catalunya (CMCiB), Badalona, Spain. ⁵IrsiCaixa AIDS Research Institute, Badalona, Spain. ⁶Servei de Microbiologia, Laboratori Clínic Metropolitana Nord (LCMN), Hospital Universitari Germans Trias i Pujol, Badalona, Spain. ⁷Servei d'Anatomia Patològica, Hospital Universitari Germans Trias i Pujol, Badalona, Spain. ⁸Centro de Investigación Biomédica en Red de Enfermedades Infecciosas (CIBERINFEC), Madrid, Spain. ⁹Departament de Genètica i Microbiologia, Universitat Autònoma de Barcelona, Bellaterra, Spain. ¹⁰Direcció Clínica Territorial de Malalties Infeccioses i Salut Internacional de Gerència Territorial Metropolitana Nord, Institut Català de la Salut, Barcelona, Spain.

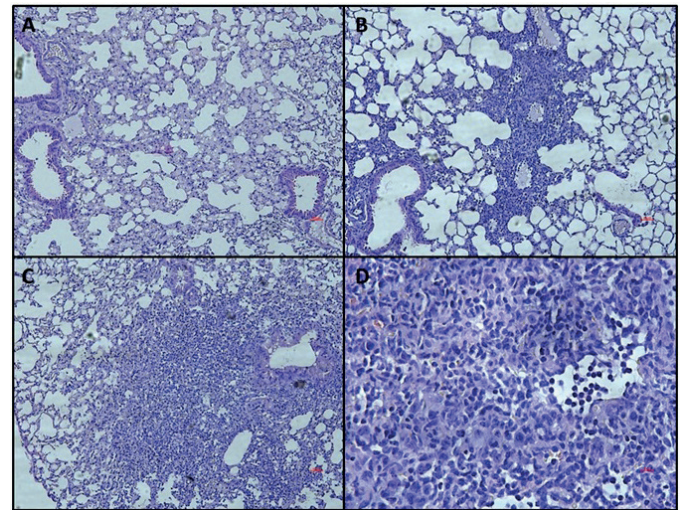
Introduction: The similarities between *Mycobacterium tuberculosis* and SARS-CoV-2 in terms of transmission, immunomodulatory capacities and inflammatory pathogenicity, make us think about the possible existence of a positive synergism between both microbes in a situation of coinfection. In this scenario, an appropriate animal model to study the pathogenicity of the coinfection needs to be established. Due to its genetic characteristics, the mouse strain K18-hACE2, which can be infected by the two pathogens, could be the answer to that problem. According to bibliography, in these mice, intranasal SARS-CoV-2 administration leads to early death of the animals. However, the aerosol administration could be potentially the best option to study the coinfection.

Objectives: Under this context, our group has the objective of establish the SARS-CoV-2 aerosol infection model using this mice strain, in order to perform the future M. tuberculosis-SARS-CoV-2 coinfection studies.

Methods: A total number of 24 mice K18-hACE2 (12 males/12 females) were randomly distributed in three experimental groups. Each group was exposed to a different SARS-CoV-2 concentration (1×10^4 , 1×10^5 and 5×10^5 TCID₅₀/mL) in an aerosol generating machine. Immediately after the exposition (day 0), two animals of each sex per group were euthanized to determine viral load in lung, brain, nostrils and nasal swab by quantitative PCR. The rest were followed for a week to register any possible sign of disease progression. After the week, these animals were euthanized to repeat the same assays as the animals in day 0. Lung samples for hematoxylin-eosin studies were also taken.

Results: No significant weight loss was registered during the week in none of the experimental groups. In all the lung samples a relation between dose and number of positives at day 0. The infection progressed in all animals independently of the dose. All the animals of 5×10^5 TCID₅₀/mL dose were infected by the end of the week. The histopathological analysis showed clear signs of infection, represent-

ed by vasculitis, perivascular inflammatory infiltration and elevated lymphocytic presence (Figure).



Pulmonary pathology caused by SARS-CoV-2 infection in K18-hACE2 after aerosol infection. The animals developed alveolar wall inflammation with interalveolar edema (A), lymphocytic inflammatory infiltration (B and C) and alveolar lymphocytic infiltration (D). Data not published.

Conclusions: The aerosol administration delivers correctly the SARS-CoV-2 inoculum to the animal lung, without compromising its survival rate, like the intranasal route does. It also recreates the pathogeny of pulmonary COVID-19 infection. So, this model presents potential to be applied in future M. tuberculosis-SARS-CoV-2 coinfection studies. It also could be used to study other coinfections or to test treatments and vaccines efficacy.

Funding: CIBER Enfermedades Respiratorias CB06/06/0031; 2021 SGR 00920.

86. LUNG EXTRACELLULAR MATRIX HYDROGELS DERIVED MATRIKINES INDUCE ALVEOLAR EPITHELIAL INFLAMMATION

Anna Ulldemolins, Carolina Herranz-Diez, Ramon Farré, Nuria Gavara, Isaac Almendros, Raimon Sunyer, Jorge Otero

Universitat de Barcelona, Barcelona, Spain.

Introduction: Decellularized extracellular matrix (ECM) hydrogels provide a more realistic scaffold preserving tissue-specific chemical and biochemical cues. However, these natural-derived hydrogels can release matrikines, small peptides generated during ECM proteolysis. Considering that lung ECM-derived hydrogels are being used to maintain pulmonary cells in culture, it is important to better understand the potential effects of ECM-derived matrikines on pulmonary cells.

Objectives: Here, we aim to investigate the inflammatory effects of matrikines on lung epithelial cells.

Methods: The kinetics of matrikine release from porcine lung dECM was evaluated for 3 weeks. Total protein concentration was determined by bicinchoninic acid (BCA) assay, and the released matrikines were identified by liquid mass spectroscopy. The inflammatory response of rat lung epithelial cells after 24h of exposure to matrikines released from hydrogels was determined.

Results: The matrikine release presented a peak after 24 hours of hydrogel preparation followed by a reduction until day 7. After one week, the matrikine release was negligible. The expression of interleukin (IL)-6 and tumor necrosis factor (TNF)- α showed a 34-fold and 77-fold increase in comparison to controls, respectively. This inflammatory response was avoided by rinsing the hydrogels prior to cell culture.

Conclusions: Our findings suggest that the presence of matrikines by using natural-derived hydrogels in cell culture can promote an inflammatory response in pulmonary cells. This inflammatory effect can be minimized by washing the hydrogels before using them for cell culture.

Funding: Ministerio de Ciencia e Innovación (PID2019-108958RB-I00/AEI/10.13039/501100011033), CIBERES and SEPAR.

89. IDENTIFYING COVID-19 VARIABLES ASSOCIATED WITH LONG COVID USING REGRESSION AND MACHINE LEARNING METHODS

Adrián Peláez^{1,2}, Miguel Ángel Spínola Tena³, María Rodrigo-García³, Elena García Castillo^{1,2}, Tamara Alonso^{1,2}, Rosa M^a Girón Moreno¹, Guillermo J. Ortega³, Joan B. Soriano^{1,2}, Esteve Fernández^{4,5,6,2}, Julio Ancochea^{1,7,2}

¹Servicio de Neumología, Hospital Universitario de la Princesa, Madrid, Spain. ²Centro de Investigación en Red de Enfermedades Respiratorias (CIBERES), Madrid, Spain. ³Hospital Universitario de la Princesa, Madrid, Spain. ⁴Unidad de Control del Tabaco, Centro Colaborador de la OMS para el Control del Tabaco, Institut Català d'Oncologia, L'Hospitalet de Llobregat, Barcelona, Spain. ⁵Grupo de Investigación en Control del Tabaco, Institut d'Investigació Biomèdica de Bellvitge-IDIBELL, L'Hospitalet de Llobregat, Barcelona, Spain. ⁶Facultad de Medicina y Ciencias de la Salud, Campus de Bellvitge, Universitat de Barcelona, L'Hospitalet del Llobregat, Barcelona, Spain. ⁷Facultad de Medicina, Universidad Autónoma de Madrid, Madrid, Spain.

Introduction: Approximately one sixth of patients who suffered from acute COVID-19 develop persistent symptoms consistent with long COVID. These symptoms can persist for months and have a significant impact on quality of life. The exact causes of long COVID are not fully understood, and research is ongoing to determine the underlying mechanisms and potential treatments.

Objectives: To determine critical variables during COVID-19 associated with the development of long COVID.

Methods: This is a retrospective, single-centre cohort of patients admitted at the Hospital de la Princesa (Madrid) with acute COVID-19, of whom some were later identified with long COVID as per the WHO definition and seen in a dedicated consultation. The outcome variable was "long COVID". Critical variables were selected by using both a univariate logistic regression and the machine learning algorithm Random Forest. Logistic regression was used to find the best model to explain the outcome, and the Gradient Boosting, a Random-For-est-like algorithm, was employed as a predictive method. A comparison of predictions between the logistic regression and the Gradient Boosting was performed.

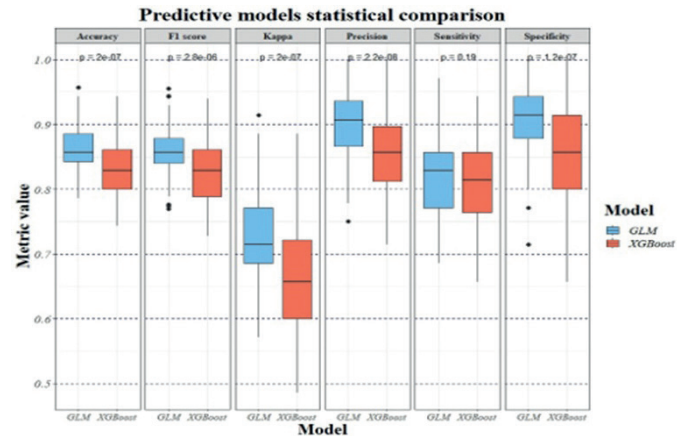
Results: Out of 4,703 patients admitted with acute COVID-19 from March 2020 to December 2022, 473 attended a dedicated external

Logistic regression of the final model using the variables selected with a backward-forward AIC

	Odds Ratio	95%CI	p-value
Stay (13, 341]	3.7	1.4 -9.9	0.008 **
NIMV	16.3	3.7 -126.8	0.001 **
LDH on admission	1.0	1.0 -1.0	0.087
Lymphocytes at discharge	1.0	1.0 -1.1	0.024 *
CPD	5.9	1.9 -19.6	0.003 **
Corticosteroids	3.5	1.2 -11.6	0.028 *
Immunosuppressants	5.1	1.5 -18.9	0.010 *
ICU Group	6.3	1.6 -29.0	0.011 *

Stay: Duration of hospitalization, NIMV: use of NIMV, LDH on admission: admission level of lactate dehydrogenase; LIN outcome: level of lymphocytes at discharge, CPD: cardiopulmonary disease, Corticosteroids: need for parenteral steroids, Immunosuppressant: need for parenteral immunosuppressants, ICU Group: ICU admission). Significance codes: *p<0.05; **p<0.001.

consultation, of whom 143 (30.2%) fulfilled the WHO definition of long-COVID. By using as a reference group 4,230 COVID-19 patients which have not attended the post COVID consultation, a logistic regression yielded a final model, selected with a backward-forward Akaike Information Criterion (AIC), with the variables described in the Table. A comparison of predictions between the logistic regression and the Gradient Boosting method, cross validated in 100 different random samples, showed sensitivity = 82.8% and specificity = 87.9% for the logistic regression and sensitivity = 80.7% and specificity = 85.8% for the Gradient Boosting (Figure).



Comparison of predictions yield between logistic regression and XGBoost, cross validated in 100 different random samples.

Conclusions: This study identifies critical variables related to the development of long COVID in admitted patients who had COVID-19. Identifying these variables can help healthcare professionals to identify patients at higher risk of developing long COVID and take appropriate measures to prevent it or earlier interventions to potentially improving outcomes.

90. NEW EPIGENETIC PREDICTOR OF CHRONIC THROMBOEMBOLIC PULMONARY HYPERTENSION

Verónica Sánchez-López^{1,2}, Julia Oto³, Olga Tura-Ceide^{4,5}, David Hervás⁶, Elena Arellano¹, Isabel Blanco^{7,2}, Víctor Peinado^{7,2}, Pilar Medina⁸, Joan Albert Barberá^{4,2}, Remedios Otero-Candelera^{1,2}

¹Instituto de Biomedicina de Sevilla (IBiS). Hospital Universitario Virgen del Rocío/CSIC/Universidad de Sevilla, Seville, Spain. ²Centro de Investigación Biomédica en Red de Enfermedades Respiratorias (CIBERES), Madrid, Spain. ³Haemostasis, Thrombosis, Arteriosclerosis and Vascular Biology Research Group, Medical Research Institute Hospital La Fe, Valencia, Spain. ⁴Hospital Clínic-Institut d'Investigacions Biomèdiques August Pi i Sunyer (IDIBAPS); University of Barcelona Barcelona, Spain, Barcelona, Spain. ⁵Biomedical Research Institute-IDIBGI, Gerona, Spain. ⁶Departamento de Estadística e Investigación Operativa Aplicadas y Calidad, Universitat Politècnica de València, Valencia, Spain. ⁷Hospital Clínic-Institut d'Investigacions Biomèdiques August Pi i Sunyer (IDIBAPS); University of Barcelona, Barcelona, Spain. ⁸Haemostasis, Thrombosis, Arteriosclerosis and Vascular Biology Research Group, Medical Research Institute Hospital La Fe; Valencia, Spain.

Introduction: Early recognition towards chronic thromboembolic pulmonary hypertension (CTEPH) after a pulmonary embolism (PE) is very complex due to the insidious nature of the disease and the lack of effective biomarkers. Experts support the application of basic research to develop more agile and faster diagnostic algorithms.

Objectives: To identify a panel of miRNAs that differentiates patients with PE from patients with CTEPH.

Methods: Twenty-two patients with CTEPH, 13 with PE and no diagnosis of either CTEPH or cancer at 2 years-follow-up, and 19 controls were prospectively recruited. Total plasma RNA was isolated and the expression of 179 miRs was quantified. Expression levels were normalized using the most stable miR selected by BestRef.

Results: A panel of 8 plasma miRNAs was differentially expressed in CTEPH and PE: miR-574-3p, miR-146b-5p, miR-193a-5p, miR-885-5p, miR-122-5p, miR-365a-3p, miR-142-3p and miR-192-5p that we have named as chronic pulmonary thromboepigen (CPT). We obtained a predictive model of CTEPH with the CPT miRNA panel as predictor (AUC = 0,843 (95%CI: 0.758-0.927)).

Conclusions: The CPT panel could be integrated into the CTEPH algorithm for qualitatively improve diagnosis. CPT panel was registered in the Spanish Patent and Trademark Office (OEPM)[P202231096]. More data from large independent and international cohorts about its diagnostic ability are needed for its full generalization.

Funding: Instituto de Salud Carlos III (PI15/01085, PI15/00582, CPII15/00002 and CP17/00114), SETH and SEPAR 164/2016.

91. HARVESTING PULMONARY ENDOTHELIAL CELLS FROM THE SWAN-GANZ PULMONARY ARTERY CATHETER

Anna Sardiné^{1,2}, Clara Martín¹, Àngela Veà¹, Ylenia Roger^{1,2}, Isabel Blanco^{1,2}, Ana Ramírez¹, Aránzazu Rosado³, Alberto Benguría³, Ana Dopazo^{3,4}, Olga Tura-Ceide⁵, Joan Albert Barberà^{1,2}

¹Department of Pulmonary Medicine, Hospital Clínic-University of Barcelona, Institut d'Investigacions Biomèdiques August Pi i Sunyer (IDIBAPS), Barcelona, Spain. ²Centro de Investigación Biomédica en Red de Enfermedades Respiratorias (CIBERES), Madrid, Spain. ³Genomics Unit, Centro Nacional de Investigaciones Cardiovasculares (CNIC), Madrid, Spain. ⁴Centro de Investigación Biomédica en Red en Enfermedades Cardiovasculares (CIBERCV), Madrid, Spain. ⁵Department of Pulmonary Medicine, Dr. Josep Trueta University Hospital de Girona, Santa Caterina Hospital de Salt and the Girona Biomedical Research Institut (IDIBGI), Girona, Spain.

Introduction: Endothelial dysfunction plays a relevant role in the development of pulmonary arterial hypertension (PAH). However, it is difficult to directly assess the state of the pulmonary endothelium and the impact that treatment has on it. A new methodology to obtain pulmonary artery endothelial cells (PAEC) from cells adhered to the tip of the pulmonary artery catheter (Swan-Ganz) used for the hemodynamic diagnosis of PAH has been recently reported (J Vis Exp. 2019 Jan 23;(143)).

Objectives: The objective of the study was to evaluate the performance of this methodology in obtaining PAEC and the viability of isolated cells for RNA sequencing.

Methods: Three methodological approaches were evaluated in pilot studies. In the first study, cells were harvested by scraping the balloon of the catheter tip (n = 21). Cell counting and RNA extraction were performed. Harvested cells (n = 3) were characterized by flow cytometry. In the second study, two methods of cell harvesting were evaluated. Cells were detached using trypsin or scraping the balloon and subsequently used for bulk RNA sequencing (n = 9). In the third study, cells were detached using trypsin and cultured until passage 0 (n = 12) for subsequent single cell RNA sequencing.

Results: The number of cells obtained in the first pilot was variable (6×10^4 to $1,8 \times 10^6$). The mean concentration of RNA recovered was 6.4 ± 6.7 ng/ μ L, with a 260/280 nm ratio of 1.43. The proportion of mature endothelial cells was 20.6% of viable cells in the sample. In the second study, the RNA obtained was undetectable using both detachment methods. In the third study, PAECs were successfully cultured in 8 of 12 cases (viability for culture 67%). The number of cells obtained (6×10^5) is optimal for single cell RNA sequencing.

Conclusions: This methodological development study shows that it is feasible to isolate and grow in culture PAEC harvested from the tip of pulmonary artery catheters used for the hemodynamic diagnosis of PAH. Single cell RNA sequencing is only feasible in PAEC that have been grown up in culture.

Funding: ISCIII (PI 21/00403), SEPAR (2022/1277), FUCAP (2022) and CP17/00114. A. Sardiné was the recipient of a mobility grant from the CIBERES.

94. PATHOGENICITY MECHANISMS OF PNEUMOCOCCAL SEROTYPE 8 AS AN IMPORTANT CAUSE OF INVASIVE DISEASE

Covadonga Pérez García¹, Julio Sempere García^{1,2}, Sara de Miguel^{3,4,2}, Samantha Hita¹, Erick J. Vidal¹, Aída Úbeda¹, Pilar Membrillo⁵, Juan Carlos Sanz^{6,7}, Carmen Ardanuy^{8,2}, Mirian Domenech Lucas^{5,1,2}, Jose Yuste Lobo^{1,2}

¹Spanish Pneumococcal Reference Laboratory, National Center for Microbiology, Instituto de Salud Carlos III, Madrid, Spain. ²Centro de Investigación Biomédica en Red de Enfermedades Respiratorias (CIBERES), Madrid, Spain. ³Epidemiology Department, Directorate General of Public Health, Regional Ministry of Health of Madrid, Madrid, Spain. ⁴Department of Preventive Medicine, University Hospital 12 de Octubre, Madrid, Spain. ⁵Department of Genetics, Physiology, and Microbiology, Faculty of Biology, Complutense University of Madrid, Madrid, Spain, Madrid, Spain. ⁶Clinical Microbiology Unit, Public Health Regional Laboratory of the Community of Madrid, Directorate General of Public Health, Regional Ministry of Health of Madrid, Madrid, Spain. ⁷Centro de Investigación Biomédica en Red de Epidemiología y Salud Pública (CIBERESP), Madrid, Spain. ⁸Department of Microbiology, Hospital Universitari de Bellvitge-University of Barcelona-IDIBELL, Barcelona, Spain.

Introduction: Invasive pneumococcal disease (IPD) is associated with high morbidity and mortality rates. The use of pneumococcal conjugate vaccines (PCVs) has been an excellent prophylactic measure to reduce the number of IPD cases due to vaccine serotypes. However, serotypes not included in PCV-13 have occupied the niche left by vaccine serotypes. With this phenomenon of serotype replacement, we have seen how in recent years that serotype 8 has become one of the main non-vaccine serotypes causing IPD in both pediatric and adult populations.

Objectives: We analyzed the national evolution of IPD cases by serotype 8 from 2008-2022. Within this period, 111 strains were selected from the Community of Madrid to know the circulating sequence-types (STs). Adhesion assays to lung cells and evasion of the host immune response including opsonophagocytosis (OPA) assays were performed to determine variations among STs that could explain the current evolution.

Methods: The evolution of IPD cases was obtained from the cases registered at the National Center of Microbiology. PCR-MLST was performed to analyze the genotype of the selected strains. The A549 and HL-60 cell lines were used for adhesion and opsonophagocytosis assays respectively using with rabbit serum. Biofilm formation was also tested.

Results: The number IPD cases due to serotype 8 has exponentially increased since 2011, when PCV13 was introduced in Spain in the private market. This rise was interrupted between 2020-2021 due to the SARS-CoV-2 pandemic. However, in 2022 we found partial recovery with similar values to the pre-pandemic period confirming the importance of serotype 8 as a major cause of IPD in children and adults. The circulating genotypes are shown in the Table. ST53 was temporarily replaced by ST63, a multidrug-resistant clone from a capsular switching (15A-ST63 and 8-ST53). Our results confirmed that ST1110 is more resistant to opsonophagocytosis whereas ST53 showed higher infection rates of lung cells and forms a better biofilm.

YEAR	% ST53	% ST1110	% ST63	% ST404
2008	14.29	-	71.43	14.29
2009	16.67	16.67	66.67	-
2010	25.00	-	75.00	-
2011	50.00	25.00	25.00	-
2012	20.00	40.00	40.00	-
2013	50.00	50.00	-	-
2014	42.86	28.57	14.29	14.29
2015	25.00	75.00	-	-
2016	35.00	55.00	-	10.00
2017	46.15	46.15	-	7.69
2018	45.45	50.00	4.55	-
2019	-	100.00	-	-
2020	38.46	53.85	-	7.69

Circulating genotypes from 2008-2020. ST53 and ST1110 belong to the same clonal complex (CC53).

Conclusions: Since the introduction of PCV-13, Serotype 8 has been one of the most prevalent serotypes causing IPD, both in the pediatric and adult population. Despite the advantage of ST63, a unique clone from Spain, it has finally been replaced by ST53 and ST1110 (both within the CC53). There must be other factors, independent of the CC53 capsule that make it more advantageous than multidrug-resistant ST63. Better immune evasion by ST1110 and better adhesion and biofilm formation rates by ST53 could explain why CC53 is now the predominant within Serotype 8.

Funding: This study was funded by grant PID2020-119298RB-I00 from MICINN.

95. IDENTIFICATION OF EARLY METABOLIC BIOMARKERS IN AN ANIMAL MODEL OF CHRONIC KIDNEY DISEASE

Pilar Alonso-Moreno¹, Marina Caño-Fernández¹, Ana K. Guzmán-Aguayo¹, María S. Fernández-Alfonso¹, Jose L. Izquierdo-García^{1,2}

¹Instituto Pluridisciplinar and Facultad de Farmacia, Universidad Complutense de Madrid, Madrid, Spain. ²Centro de Investigación Biomédica en Red de Enfermedades Respiratorias (CIBERES), Madrid, Spain.

Introduction: Patients with chronic kidney disease (CKD) are at high risk of developing critical illness that leads to admission to intensive care units (ICU). However, current diagnostic parameters, such as albuminuria, estimated glomerular filtration rate (eGFR), or kidney damage markers, are insufficient to detect CKD at early stages since patients are often asymptomatic. Nuclear magnetic resonance (NMR)-based metabolomics provides a unique fingerprint of the disease's metabolic status, making it a promising tool to anticipate early CKD diagnosis.

Objectives: This study aims to identify early metabolic biomarkers for the diagnosis of CKD in its early stages and to understand the disease's progression in diabetic patients.

Methods: Three types of rats were used in this animal model: control Wistar rats (W), Munich Wistar Frömter (MWF) rats with spontaneous CKD, and MWF rats with induced diabetes (MWF-D). A metabolomic study of 46 serum samples was conducted using nuclear magnetic resonance, and multivariate statistical analyses were performed on the results.

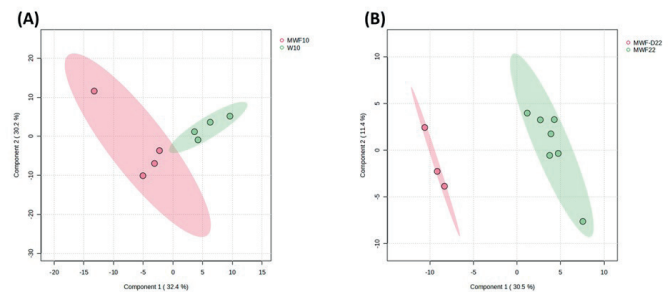
Results: We compared the different models over three time periods: 10, 16, and 22 weeks. Control rats demonstrated metabolic changes over the weeks due to natural aging, but no such changes were observed in MWF and MWF-D rats. The comparison between W and MWF at 10 weeks showed the evolution of the disease, as we were able to distinguish between the two groups based on their metabolic profile (Figure A) and identify early diagnostic biomarkers (Table). At

the same week, MWF-D rats demonstrated high glucose levels. However, when comparing the two disease groups, their metabolic profiles varied greatly (Figure B). At week 10, MWF rats had a diverse metabolic profile, while MWF-D rats had considerably high glucose levels. By week 22, glucose, glycerol, ethanol, and amino acids were overexpressed in MWF rats, while glucose dominated in MWF-D rats.

Statistically significant spectral position to discriminate W and MWF groups at 10 weeks

Frequency (ppm)	Metabolites	W or MWF	p-value
1.31587	Lactate	W	0.0002
1.47592	Lysine, Alanine	W	0.002
4.13672	Lactate, Proline, 3-Hydroxybutyrate	W	0.04
3.67658	Ethanol, Glycerol, Glucose	MWF	0.02
3.56655	Glycerol	MWF	0.03
3.57655	Glycerol	MWF	0.04
3.80662	Glucose, Glycerol	MWF	0.05
3.79661	Glucose, Glycerol	MWF	0.01

W: control Wistar rats; MWF: Munich Wistar Frömter rats.



Partial Least Squares (PLS) score plots of serum spectra analyzed by Nuclear Magnetic Resonance spectroscopy of (A) W (n = 4) and MWF rats (n = 4) at 10 weeks (Accuracy = 0.8, R2 = 0.74445, Q2 = 0.17667); (B) MWF (n = 7) and MWF-D rats (n = 3) at 22 weeks (Accuracy = 1.0, R2 = 0.93618, Q2 = 0.65729). W = control Wistar rats. MWF = Munich Wistar Frömter rats. MWF-D = Diabetic MWF rats.

Conclusions: Our study identified possible diagnostic metabolic biomarkers for CKD, including glucose, glycerol, and ethanol. Additionally, we found that diabetes causes changes in metabolites, which could be due to the MWF and MWF-D rats already being aged at 10 weeks. Further studies are needed to fully understand the disease's progression in these patients.

Funding: This research was supported by grants: (i) PID2019-10656RJ-I00 from the Spanish Ministry of Science and Innovation and (ii) MINDSHIFT - MARIE Skłodowska-CURIE ACTIONS Innovative Training Networks) and Grupos Santander Universidad Complutense de Madrid [grant number GR-921641].

97. THE RELATIONSHIP BETWEEN SPUTUM COLOUR AND QUALITY OF LIFE IN PATIENTS WITH BRONCHIECTASIS

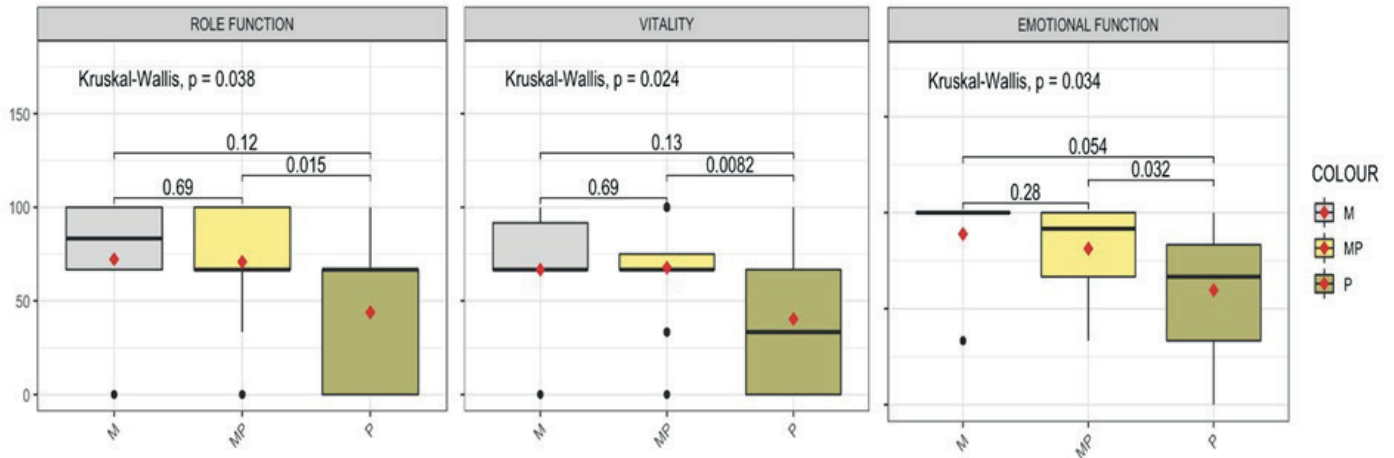
Leticia Bueno Freire^{1,2,3,4}, Rubén López Aladid^{1,2}, Patricia Oscanoa Huamán^{1,2,3,4}, Victoria Alcaraz Serrano⁵, Andrea Catalina Palomeque^{1,2,3}, Roberto Cabrera Ortega^{1,2,3}, Rosanel Amaro Rodríguez³, Laia Fernández Barat^{1,2,4}, Antoni Torres Martí^{1,2,3,4}

¹Fundació Clínic per a la Recerca Biomèdica (FCRB) - Institut de Investigacions Biomèdiques August Pi i Sunyer (IDIBAPS), Barcelona, Spain. ²Centro de Investigación Biomédica en Red de Enfermedades Respiratorias (CIBERES), Madrid, Spain. ³Hospital Clínic de Barcelona, Barcelona, Spain. ⁴Universitat de Barcelona (UB), Barcelona, Spain. ⁵Instituto de Salud Global de Barcelona (ISGlobal), Barcelona, Spain.

Introduction: Sputum colour is a useful clinical tool for evaluating and monitoring non-cystic fibrosis bronchiectasis (BE) (Murray et al.

Health-related quality of life according to the sputum colour (n = 57). Data is presented as n (%) or median (P25-P75). P-values in bold were statistically significant

	Mucoid	Mucopurulent	Purulent	p-value
	6 (10.53)	32 (56.14)	19 (33.33)	
QOL-B				
Physical Function	50.00 (33.33-66.67)	66.67 (33.33-66.67)	33.33 (33.33-66.67)	0.257
Role Function	83.33 (66.67-100.00)	66.67 (66.67-100.00)	66.67 (0.00-66.67)	0.038*
Vitality	66.67 (66.67-91.67)	66.67 (66.67-75.00)	33.33 (0.00-66.67)	0.024*
Emotional Function	100.00 (100.00-100.00)	91.67 (66.67-100.00)	66.67 (33.33-83.33)	0.034*
Social Function	75.00 (37.50-100.00)	50.00 (25.00-83.33)	33.33 (0.00-66.67)	0.517
Treatment Burden	66.67 (66.67-100.00)	83.33 (66.67-100.00)	66.67 (33.33-100.00)	0.156
Health Perceptions	25.00 (16.67-58.33)	33.33 (16.67-66.67)	16.67 (0.00-33.33)	0.057
Respiratory Symptoms	83.33 (66.67-100.00)	66.67 (66.67-66.67)	66.67 (33.33-66.67)	0.063



Quality of life domains with significant differences according to the sputum colour. Figure shows boxplots of the three quality of life domains with significant differences according to the sputum colour. The line inside the boxplot represents the median, whereas the red diamond stands for the mean. The dots show the outliers and individual sample values. Statistical testing showed significant differences between the mucopurulent and purulent samples. Abbreviations: M: mucoid; MP: mucopurulent; P: purulent.

2009), but its ability to capture health-related quality of life (QoL) has barely been explored.

Objectives: The aim of this study was to assess the relationship between sputum colour and QoL in BE patients colonized by *Pseudomonas aeruginosa* (PA).

Methods: In this cross-sectional observational study involving BE patients colonized by PA, demographic characteristics, sputum microbiology, and pulmonary function (FEV1, FVC, FEV1/FVC) were recorded. Sputum colour was assessed using Murray's scale, which classifies sputum into three categories: mucoid (clear), mucopurulent (pale yellow/pale green), and purulent (dark yellow/dark green). QoL was measured using the Quality of Life Questionnaire-Bronchiectasis v3.1 (QOL-B) (Quittner et al. 2015). This questionnaire consists of 37 questions distributed across 8 domains, where each domain has a score ranging from 0 to 100, and higher scores indicate better QoL. Fisher's exact test and Kruskal-Wallis were used in the univariate analysis, whilst ordinal logistic regression was applied in the multivariate.

Results: A total of 57 patients were included (23 women, 67,53 ± 16,96 years). The Table shows QoL according to the sputum colour. Purulent samples showed significantly worse QoL in 3 out of 8 domains (role function, vitality, and emotional function) compared to those mucopurulent (Figure). Further, sputum colour and culture were significantly associated (mixed flora vs. non-mucoid PA vs. mucoid PA vs. other pathogenic microorganisms, $p = 0,04$). No significant differences were found in relation to sex, disease phase (exacerbation vs. stable), Bronchiectasis Severity Index (BSI), years of PA colonization, and lung function. These results were kept when considering sputum colour and culture concurrently.

Conclusions: Sputum colour is a validated and simple tool that could be useful in BE patients colonized by PA to quickly identify a worsen-

ing of QoL, regardless of the phase of the disease. While these findings are in line with previous literature, their validation would require future studies with a larger and more heterogeneous population.

Funding: ISCIII-FEDER (Code: PI18/00145) grant awarded to AT and LFB; Intramural CIBER project 2018 (ES18PI01X1-2021) awarded to AT and LFB; ISCIII-FOS (F119/00090) grant awarded to RLA, CB06/06/0028 del CIBER de Enfermedades Respiratorias (CIBERES); ICREA Academy/ Institució Catalana de Recerca i Estudis Avançats awarded to AT; 2.603/IDIBAPS, SGR/Generalitat de Catalunya awarded to AT; SEPAR grants 2016 (Code:208) and 2019 (Code: 628) awarded to LFB.

99. DYNAMIC TRENDS OF NEW VACCINE SEROTYPES 22F AND 33F DURING COVID-19 IN SPAIN

Julio Sempere¹, Samantha Hita Díaz², Covadonga Pérez-García², Pilar Membrillo Solbes², Erick Vidal Alcántara², Aída Úbeda², Mirian Domenech³, Jose Yuste¹

¹National Center for Microbiology, Instituto de Salud Carlos III; Centro de Investigación Biomédica en Red de Enfermedades Respiratorias (CIBERES), Madrid, Spain. ²National Center for Microbiology, Instituto de Salud Carlos III, Madrid, Spain. ³Faculty of Biology, Universidad Complutense de Madrid; Centro de Investigación Biomédica en Red de Enfermedades Respiratorias (CIBERES), Madrid, Spain.

Introduction: The best strategy to fight *Streptococcus pneumoniae* infections, and especially, invasive pneumococcal disease (IPD), is the use of preventive measures such as the administration of pneumococcal vaccines targeting the pediatric and elderly populations as risk groups. Serotype replacement by non-vaccine serotypes due to high diversity in *S. pneumoniae* is worrisome.

Objectives: The main objective of this work is to evaluate the impact of 13-valent pneumococcal conjugate vaccine (PCV13) and COVID-19 in the epidemiology of 22F and 33F serotypes, as they are included in the recently approved PCV15 and PCV20 vaccines.

Methods: We evaluated more than 30,000 clinical isolates in both pediatric and adult population during the period 2009-2022. Serotyping was performed by dot-blot and PCR-sequencing. MLST genotyping of selected strains was performed by PCR-sequencing and cgMLST genotyping of selected strains was performed by NGS.

Results: Since the introduction of PCV13, IPD cases by serotypes 22F and 33F have increased in all population, especially in adults (from 64 cases in 2009 to 133 cases in 2019 for serotype 22F; from 26 cases in 2009 to 70 cases in 2019 for serotype 33F), being specially significant for adults ≥ 65 years. The main circulating clones are ST43322F and ST71733F, but 33F has bigger clonality without differences between adult and pediatric isolates, whereas 22F has two different groups differentiating pediatric isolates vs adult isolates. Since the beginning of COVID-19 pandemic, the incidence of 22F and 33F serotypes has diminished notably (from 133 in 2019 to 76 cases in both years 2020/21 for serotype 22F; from 70 cases in 2019 to 46 cases in both years 2020/21 for serotype 33F). However, the proportion of IPD cases by both serotypes have not, indicating a decrease of general IPD during the pandemic. In the re-opening (2022), we have recovered pre-pandemic cases by both serotypes in the pediatric population, and we have an increase in cases by both serotypes in the adult population.

Conclusions: Even with the decrease of IPD cases by serotypes 22F and 33F thanks to COVID-19 pandemic, they are still both relevant in IPD in Spain. To this day, serotype 22F remains the third cause of IPD in adults. Funding: This work was supported by Ministerio de Ciencia e Innovación (MICINN) (PID2020-119298RB-I00) and by MSD (MVP-132/21).

101. REARRANGEMENT OF CELL TYPES IN THE RAT CAROTID BODY NEUROGENIC NICHE INDUCED BY CHRONIC INTERMITTENT HYPOXIA

Candelaria Caballero Eraso^{1,2,3}, Olaia Colinas^{4,5,6}, Lin Gao^{4,7}, Jose Lopez Barneo^{4,7,6}

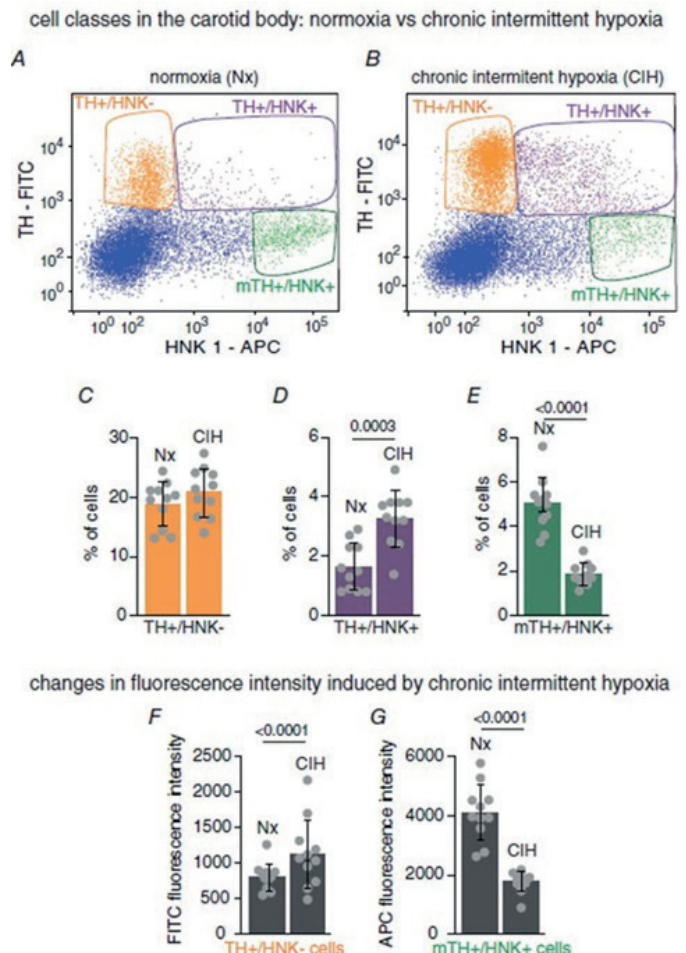
¹Instituto de Biomedicina de Sevilla (IBIS), Hospital Universitario Virgen del Rocío/CSIC/Universidad de Sevilla, Sevilla, Spain. ²Unidad Médico Quirúrgica de Enfermedades Respiratorias, Hospital Universitario Virgen del Rocío/IBIS, Sevilla, Spain. ³Centro de Investigación Biomédica en Red de Enfermedades Respiratorias (CIBERES), Madrid, Spain. ⁴Instituto de Biomedicina de Sevilla (IBIS), Hospital Universitario Virgen del Rocío/CSIC/Universidad de Sevilla, Sevilla, Spain. ⁵Centro de Investigación Biomédica en Red de Enfermedades Neurodegenerativas (CIBERNED), Madrid, Spain. ⁶Departamento de Fisiología Médica y Biofísica, Facultad de Medicina, Universidad de Sevilla, Sevilla, Spain. ⁷Centro de Investigación Biomédica en Red de Enfermedades Neurodegenerativas (CIBERNED), Madrid, Spain.

Introduction: Obstructive sleep apnea is a frequent condition in the human population that predisposes to severe cardiovascular and metabolic alterations. Overactivation of the carotid body (CB), the main arterial oxygen (O₂)-sensing chemoreceptor, by repeated episodes of hypoxaemia is believed to contribute to the pathogenesis of sympathetic hyperactivity present in sleep apnea patients.

Objectives: The aim of the current study was to investigate whether chronic intermittent hypoxia (CIH) activates CB stem cell niche and contributes to the pathogenesis of CB overactivation.

Methods: An animal model of CIH was applied in which adult male rats were treated with repeated episodes of hypoxia (10% ambient O₂) for 8 hours each day for 14 days. We have investigated by fluorescence activated cell sorting, immunocytochemistry, and quantitative PCR analyses the changes in CB cellular composition in a rat model of CIH.

Results: We confirmed sympathetic overactivation in this CIH model by evaluating systemic functional parameters. Using flow cytometry and immunohistochemistry, we have observed a CIH-induced neurogenesis in the CB with activation of neuroblasts, which enter a process of proliferation and differentiation into mature O₂-sensing chemoreceptor glomus cells. Isolation of individual cell classes using cell sorter has allowed us to demonstrate that maturation of CB neuroblasts is paralleled by an upregulation of genes involved in acute O₂-sensing. CIH also enhanced mitochondrial responsiveness to hypoxia in maturing neuroblasts as well as in glomus cells.



Rearrangement of cell populations in the carotid body neurogenic niche induced by chronic intermittent hypoxia.

Conclusions: These data provide novel perspectives on the pathogenesis of CB-mediated sympathetic hyperactivation that may lead to the development of new pharmacological strategies to prevent cardiovascular and metabolic disfunctions in patients with sleep apnea.

Funding: This research was supported by the Andalusian Government (FEDER Andalucía 2014-2020, 2018 Call, US-1 255 654 and Consejería de Salud, PI-0125-2016) and the Spanish Ministries of Science and Innovation and Health (Grants SAF2016-74 990-R, PID2019-106410RBI00 and PID2019-110817R funded by MCIN/AEI/10.13039/501100011033) and the Spanish Respiratory Society of Pulmonology and Thoracic Surgery (SEPAR) (grant 114/2016).

103. CLINICAL BIO AND IMMUNOMARKERS AS PREDICTORS IN COPD PATIENTS WITH SEVERE COVID-19

Joan Canseco-Ribas^{*1}, Laia Fernández-Barat^{*1,2}, Ana Motos^{1,2}, Albert Gabarrús², Ruben-López-Aladid², Jesús Bermejo-Martin^{†1,3,4},

Ferran Barbé^{§1,5}, Antoni Torres^{‡1,2} on behalf of the CIBERESUCICOVID Project Investigators

¹Centro de Investigación Biomédica en Red de Enfermedades Respiratorias (CIBERES), Madrid, Spain. ²Fundació de Recerca Clínica Barcelona-Institut d'Investigacions Biomèdiques August Pi i Sunyer (FRCB-IDIBAPS), Universitat de Barcelona, Barcelona, Departmento de pneumología, Hospital Clinic de Barcelona, Spain. ³Group for Biomedical Research in Sepsis (BioSepsis), Instituto de Investigación Biomédica de Salamanca (IBSAL), Paseo de San Vicente, Salamanca, Spain. ⁴Hospital Universitario Río Hortega de Valladolid, Valladolid, Spain. ⁵Translational Research in Respiratory Medicine, Respiratory Department, Hospital Universitari Arnau de Vilanova and Santa Maria; IRBLeida, Lleida, Spain. *Co-first authors, ‡Co-senior authors.

Introduction: COVID-19 remains a serious health concern for patients with multiple comorbidities or immunocompromised. Chronic obstructive pulmonary disease (COPD) is a chronic lung condition that has been associated with an increased risk of severe COVID-19 outcomes. Therefore, individualized clinical management for patients with both COPD having severe COVID-19 may help reduce high mortality rates in intensive care units (ICUs).

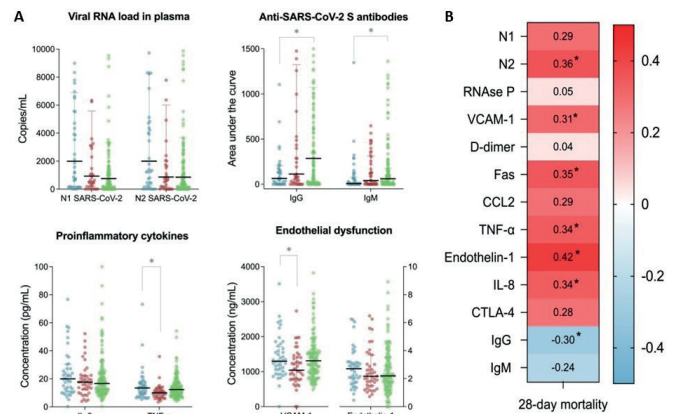
Objective: To assess the prognostic value of clinical predictors, bio and immunomarkers in patients with COPD and severe COVID-19.

Methods: Epidemiological, clinical and laboratory data was registered in REDCap for 5,999 patients hospitalized with COVID-19 across 55 Spanish ICUs and we obtained plasma samples at 24–48 h of ICU from a subset of 921 patients. We then performed statistical analysis to determine clinical, bio and immune predictors for 28-day mortality. Our study population was stratified by those with: COPD, other chronic respiratory diseases (CRD), and without respiratory comorbidities (No CRD).

Results: 328 (5%) patients had COPD; 547 (9%), CRD; and 5,124 (85%), No CRD. In the COPD group, clinical predictors were invasive mechanical ventilation (IMV) and creatinine for 28-day mortality. Additionally, high-flow nasal cannula (HFNC) was protective for 28-day mortality while non-invasive mechanical ventilation (NIMV) was not (Table). The high 28-day mortality in the COPD cohort (37%) was associated with a dysregulated immune response characterized by high plasma viral loads, low IgG titres, and significant inflammation (VCAM, TNF-Alpha, IL-8) and tissue damage (Fas, endothelin-1) (Figure).

Variables	HR (95% CI)	p-value
Age (+1 year) ^a	1.00 (0.55 to 1.80)	0.98
Female sex	1.02 (0.53 to 1.96)	0.96
Serum creatinine at ICU admission (+1 mg/dL)	1.43 (1.16 to 1.75)	0.001
Metabolic syndrome (diabetes mellitus, hypertension and obesity)	0.96 (0.51 to 1.80)	0.90
SOFA score at ICU admission (+1) ^b	1.03 (0.96 to 1.11)	0.37
Oral steroids before admission	1.20 (0.59 to 2.44)	0.61
Hypercapnia at ICU admission (PaCO ₂ ≥45 mmHg)	1.41 (0.88 to 2.24)	0.15
High-flow nasal cannula during hospitalization	0.54 (0.32 to 0.90)	0.017
Non-invasive mechanical ventilation during hospitalization	1.11 (0.63 to 1.96)	0.72
Invasive mechanical ventilation during hospitalization	1.99 (1.06 to 3.75)	0.033

Multivariable model assessing predictors of 28-day mortality of the COPD population (N = 328). Abbreviations: COPD indicates chronic obstructive pulmonary disease; HR, hazard ratio; CI, confidence interval; ICU, intensive care unit; SOFA, sequential organ failure assessment; PaCO₂, partial pressure of arterial carbon dioxide. Data are shown as estimated HRs (95%CI) of the explanatory variables in the 28-day mortality group. Cox regression model stratified on the centre variable and adjusted by COVID-19 wave. The variables included in the multivariate model were age, sex, serum creatinine at ICU admission, metabolic syndrome (diabetes mellitus, hypertension and obesity), SOFA score at ICU admission, oral steroids before admission, hypercapnia at ICU admission (≥ 45 mmHg), high-flow nasal cannula during hospitalization, non-invasive mechanical ventilation during hospitalization, and invasive mechanical ventilation during hospitalization. The P-value is based on the null hypothesis that all HRs relating to an explanatory variable equal unity (no effect). a “+1” means a one-unit increase on the scale in the predictor variable (i.e., going from 1 to 2, 2 to 3, etc.).



Bio and immunomarker differences at ICU admission and their correlations with 28-day mortality. A) Bio and immunomarkers obtained during the first 24–48h of ICU admission of patients with serum samples from the overall study population after matching (n = 225, of which 45, 45 and 135 belong to COPD, CRD and No CRD). *P < 0.05 denotes statistically significant differences between groups. B) Chart depicting correlations between bio and immunomarkers with 28-day mortality. Spearman rank correlation tests were used to assess the relationships between blood markers and mortality. Color intensity represents the strength of the correlations, with warmer colors indicating positive associations and cooler colors indicating negative associations. *P < 0.05 denotes statistically significant correlations between variables.

Conclusions: In patients with COPD and severe COVID-19, HNFC are protective for 28-day mortality but not NIMV. This population is prone to experiencing a dysregulated viral infection, reduced antibody responses, exacerbated proinflammatory profiles, and greater endothelial damage which explain their high mortality rates. Consequently, this population represents a promising target for immunotherapy interventions.

Funding: The Instituto de Salud Carlos III de Madrid (COV20/00110, ISCIII); Fondo Europeo de Desarrollo Regional (FEDER); “Una manera de hacer Europa”; CIBERES, and Donation Program “estar preparados”, UNESPA provided financial support.

108. PHASE 2B RANDOMIZED DOUBLE-BLIND, PLACEBO-CONTROLLED TRIAL TO ESTIMATE THE POTENTIAL EFFICACY AND SAFETY OF TWO REPURPOSED DRUGS, ACETYSALICYLIC ACID AND IBUPROFEN, FOR USE AS ADJUNCT THERAPY ADDED TO, AND COMPARED WITH, THE STANDARD WHO RECOMMENDED TB REGIMEN (SMA-TB)

Ziyaad Waja¹, Tumelo Moloantsoa¹, Lilibeth Arias^{2,3}, **Kaori Fonseca**^{2,3}, Nino Gogichadze², Floris Swanepoel¹, Kennedy Otwombe¹, Natasha Pillay¹, Thabiso Seiphetho¹, Kedibone Phala¹, Tamta Korinteli⁴, Kate Bajelidze⁴, Emilie Layre⁵, Mahavir Singh⁶, Judith Farrés⁷, Maria Rosa Sarrías², Tom H. M. Ottenhoff⁸, Jérôme Nigou⁵, Anne Margarita Dyrhol Riise⁹, Nestan Tukvadze⁴, Sergo Vashakidze⁴, Neil Martinson¹, Cristina Vilaplana^{2,3}

¹Perinatal HIV Research Unit, University of Witwatersrand, Johannesburg, South Africa. ²Experimental Tuberculosis Unit, Universitat Autònoma de Barcelona, Fundació Institut d'Investigació en Ciències de la Salut Germans Trias i Pujol, Badalona, Spain. ³Centro de Investigación Biomédica en Red de Enfermedades Respiratorias (CIBERES), Madrid, Spain. ⁴National Center for Tuberculosis and Lung Diseases, Tbilisi, Georgia. ⁵Institut de Pharmacologie et de Biologie Structurale, Université de Toulouse, CNRS, Université Paul Sabatier, Toulouse, France. ⁶LIONEX Diagnostics and Therapeutics GmbH, Braunschweig, Germany. ⁷Anaxomics Biotech, Barcelona, Spain. ⁸Department of Infectious Diseases, Leiden University Medical Center, Leiden, The Netherlands. ⁹Department of Infectious Diseases, Oslo University Hospital, Oslo, Norway.

Introduction: Besides many efforts and achievements, novel therapeutic approaches are still needed to improve tuberculosis (TB) disease outcomes and to shorten treatment duration. Host-Directed Therapies (HDT) propose to shorten treatment length and improve patients' outcomes while tackling drug resistance.

Objectives: A multicentre, phase IIB, double-blind, placebo-controlled, randomized trial (ClinicalTrials.gov Identifier: NCT04575519) started in March 2020 to assess the efficacy and safety of 2 repurposed drugs (acetylsalicylic acid -ASA- and ibuprofen -Ibu), for use as adjunct therapy added to, and compared with, the standard of care (SoC) WHO-recommended TB regimen in TB patients.

Methods: The trial will recruit 354 participants with pulmonary TB in 3 sites (2 in South Africa (SA) and 1 in Georgia). TB patients are being enrolled and randomly allocated to receive: 1) SoC TB treatment + placebo; 2) SoC TB treatment + ASA 600 mg/day/4 weeks, followed by ASA 300 mg/day/4 weeks; and 3) SoC TB treatment + Ibu 800 mg/day/4 weeks, followed by Ibu 400 mg/day/4 weeks. Patients are being followed-up until 6 months after treatment, and samples collected for biomarkers studies. The primary outcomes are 1) time to $\geq 67\%$ sustained reduction in the TB score during follow-up and 2) Hazard ratio for time to stable culture conversion (SCC).

Results: Since the clinical trial started, 211/354 patients have been enrolled (59.6%), with a high participant retention rate in all study sites. Preliminary analysis considering data from 144 patients, showed a median TB score at enrolment not different between countries, but a higher radiographic extent of the disease in SA patients. The 67% TB Score reduction was achieved by week 7 (week 10 in SA and week 3 in Georgia). Looking at the hazard ratio for SCC at week 16, there was no difference between countries neither when comparing DS-TB and MDR-TB groups. In general, the investigational medicinal products have been well-tolerated. Overall 27 participants experienced Serious Adverse Events. The Data Safety Management Board declared not to have any safety concerns in view of the preliminary data.

Conclusions: With this trial, we expect to provide evidence on the potential benefit of anti-inflammatories used as an adjunct to TB treatment as HDT. If proven useful, these enhanced treatment regimens have the potential to result in a better clinical practice, care management, and increased patients' wellbeing.

Funding: This project has received funding from the European Union's Horizon 2020 research and innovation programme under grant agreement No 847762.

110. IL-1R2 GENE EXPRESSION IS DOWNREGULATED IN OBESE ASTHMA

Marina Bantulà^{1,2,3}, Alberto Garcia^{1,4}, Jordi Roca-Ferrer^{1,2}, Irina Bobolea^{1,2,5}, Joaquim Mullo^{1,2,6}, César Picado^{1,2,3}, Ebymar Arismendi^{1,2,3}

¹IDIBAPS, Barcelona, Spain. ²Centro de Investigación Biomédica en Red de Enfermedades Respiratorias (CIBERES), Madrid, Spain. ³Servicio de Neumología, Hospital Clínic de Barcelona, Barcelona, Spain. ⁴CIBERES, Barcelona, Spain. ⁵Servicio de Alergología, Hospital Clínic de Barcelona, Barcelona, Spain. ⁶Servicio de Otorrinolaringología, Hospital Clínic de Barcelona, Barcelona, Spain.

Introduction: Obesity has been proven to be a major risk factor and disease modifier for asthma. Obese and asthma conditions are linked by an increased level of inflammation and oxidative stress. Accumulating evidence supports that the proinflammatory cytokine IL-1 β is involved in the pathogenesis of airway inflammation in both obesity and asthma. IL-1R2 is a decoy receptor that regulates the IL-1 β -mediated inflammatory signalling cascade. Regulation of IL-1R2 expression is a mechanism that numerous cells use to counterbalance exacerbated inflammatory responses triggered by endogenous and

exogenous stimuli. We hypothesised that obesity, via downregulation of IL-1R2, contributes to enhancing inflammatory responses and oxidative stress in patients with comorbid asthma-obesity.

Objectives: We aimed to assess the effect of obesity and asthma on IL-1R2 expression and systemic oxidative stress.

Methods: Four groups of subjects were studied: control subjects (C), non-obese asthmatics (NOA), obese asthmatic patients (OA), and non-asthmatic obese subjects (O). We analysed IL-1R2 expression by RT-qPCR in peripheral blood mononuclear cells (PBMCs), and serum levels of 8-isoprostane by ELISA.

Results: IL-1R2 was significantly reduced in both OA and O individuals compared with NOA patients and control subjects, being significantly inversely correlated ($r = -0.439$, $p < 0.0006$) with BMI. Serum levels of 8-isoprostane were significantly lower in asthma patients, both OA and NOA, compared with O individuals.

Conclusions: Obesity and asthma interact in a complex way: obesity downregulates the expression of the anti-inflammatory IL-1R2 receptor in asthmatic patients, while asthma contributes to reducing blood 8-isoprostane levels in OA subjects.

Funding: Supported by Grant of SEPAR, CIBERES and Menarini.

114. NON-TUBERCULOUS MYCOBACTERIAL INFECTIONS: BLOODSTREAM ISOLATES FROM IMMUNOCOMPROMISED PATIENTS

Luciana Urbina Luciana, Cristina Veintimilla Cristina, María Jesús Ruiz-Serrano María Jesús, Paloma Gijón Paloma, Elena Reigadas Elena, Celia Sánchez Celia, Patricia Muñoz Patricia

Hospital General Universitario Gregorio Marañón, Madrid, Spain.

Introduction: Non-tuberculous mycobacteria (NTM) are ubiquitous dwellers of the environment. NTM are generally considered less virulent, nevertheless, these organisms frequently affect patients with predisposing conditions. However, little is known about the clinical implications of different species of NTM.

Objectives: The objective was to describe the clinical involvement and microbiological characteristics of NTM recovered from bloodstream infections.

Methods: We conducted a retrospective study in a tertiary care hospital from January 2012 to October 2022. All NTM isolated from blood cultures (Myc/F lytic and aerobic BACTEC, BD) were evaluated. Clinical features were collected from electronic medical records. MALDI-TOF or hsp65 gene sequencing was used for identification and susceptibility testing was performed by E-test method on Middlebrook 7H11 (BD).

Results: During the study period 570 NTM infections were diagnosed, of which, ten (1.8%) were isolated from blood cultures. Patients had a median age of 53.5 years (IQR: 44.8-73) and 5/10 were male. Underlying immunosuppression was identified in all cases, as following: (6/10) hematologic malignancies, (3/10) HIV infection with CD4 < 200 cell/mm³ and (1/10) had chronic renal failure. According to clinical source: 5 patients had a disseminated disease and 3 had a catheter associated infection and all were treated. Of the remaining two patients, one had suspicion of infective endocarditis, and treatment was dismissed due to clinical status, finally died and one patient was considered as intravascular-catheter colonization, who did not receive treatment. Most of the isolates were identified as rapidly growing mycobacteria RGM (6/10): *M. abscessus* (n = 2), *M. brisbanense* (n = 1), *M. fortuitum* (n = 2) and *M. chelonae* (n = 1), with a mean time to positivity of 78.9h (range: 16-118.5). There were also slow-growing mycobacteria SGM (4/10): *M. avium complex* (n = 1), *M. intracellulare* (n = 1) and *M. genavense* (n = 2), with a mean time to positivity of 412.0h (range: 42-714). All NTM were susceptible to quinolones, macrolides and aminoglycosides, while all isolates showed resistance to doxycycline and trimethoprim-sulfamethoxazole.

Conclusions: NTM bloodstream infection is uncommon. Diagnosis requires a high level of suspicion, especially in immunosuppressed population. Current identification methods allow an improved and rapid detection of NTM, heading to increased detection of these microorganisms and prompt initiation of adequate treatment.

Funding: Instituto de Investigación Sanitaria Gregorio Marañón (IISGM).

116. MOLECULAR CHARACTERIZATION OF AMOXICILLIN-NON-SUSCEPTIBLE STREPTOCOCCUS PNEUMONIAE CAUSING ADULT INVASIVE PNEUMOCOCCAL PNEUMONIA (IPP) IN BARCELONA, SPAIN (1994-2020)

Aida González-Díaz¹, Fe Tubau¹, Sara Calvo¹, Inmaculada Grau¹, Román Pallarés², Carmen Ardanuy³, Jordi Càmarà¹

¹HUB-IDIBELL-CIBERES, Barcelona, Spain. ²HUB-UB-IDIBELL-CIBERES, Barcelona, Spain. ³HUB-IDIBELL-UB-CIBERES, Barcelona, Spain.

Introduction: Amoxicillin (AMX) is among the recommended first choices for pneumococcal pneumonia. Therefore, the molecular characterization of lineages and resistance mechanisms associated with AMX resistance is crucial.

Objectives: To study the epidemiology of *S. pneumoniae*, serotypes and clone of non-susceptible amoxicillin isolates causing adult invasive pneumococcal pneumonia episodes.

Methods: All adult invasive pneumococcal pneumonia episodes detected in Hospital de Bellvitge were prospectively collected (1994-2020). Isolates were tested for antibiotic susceptibility (EUCAST), serotyped (Quellung) and genotyped (PFGE). In addition, 54 isolates belonging to major clones (n > 10) were studied by whole genome sequencing.

Results: A total of 1,663 episodes were detected. Of them, 96 (5.8%) were classified as AMX-susceptible at increased exposure (0.5–1 mg/L) and 198 (11.9%) as resistant (> 1 mg/L). Among non-susceptible isolates (NSI) (> 0.5 mg/L), the most frequent serotypes were 14 (36%), 9V (24%), and 19A (12%). The CC156 clone was the most frequent (58.6%), followed by CC81 (11.2%) and CC320 (6.1%). After PCV13 introduction (2010), the percentage of AMOX-NSI dropped from 20.4% (prePCV13) to 10.7% being serotypes 19A (34%), 14 (26%) and 11A (22%) the most frequent. The PBPs analysis showed that all genomes presented changes in T371A or T371S (STMK373 motif), P432T (SRN-VP430 motif) and the 574NTGY (574TSQF) change of PBP1a and T446A (443SSNT motif) in PBP2b. The changes T338A (337STMK motif), I371T, and R384G, and the change L546V close to the 547KSG motif (PBP2x) were also present in all genomes.

Conclusions: The frequency of AMX-NSI in adults decreased after PCV13 introduction. Current isolates belong to the CC156 (11A and 14) and CC320 (19A) clones. The introduction of broader molecular surveillance of pneumococcal clones continues being necessary to monitor the impact of the PCVs vaccines.

Funding: This study was funded by Instituto de Salud Carlos III (ISCIII) through the Projects 'P118/00339', and CIBER de Enfermedades Respiratorias (CIBERES-CB06/06/0037), co-funded by the European Regional Development Fund/European Social Fund (ERDF/ESF, 'Investing in your future'), and CERCA Programme/Generalitat de Catalunya for institutional support.

117. NRF2-ACTIVATORS REVERT NUMEROUS SENESCENCE HALLMARKS IN FIBROBLASTS FROM HEALTHY DONORS AND IPF PATIENTS

Inés Roger Laparra^{1,2}, Paula Montero², Javier Milara², Julio Cortijo²

¹Centro de Investigación Biomédica en Red de Enfermedades Respiratorias (CIBERES), Madrid, Spain. ²Department of Pharmacology, Faculty of Medicine, University of Valencia, Valencia, Spain.

Introduction: Cellular senescence is recognized as a crucial mechanism that contributes to the development of Idiopathic Pulmonary Fibrosis (IPF). Senescence is a natural biological process in which cells enter a state of permanent growth arrest, but the accumulation of senescent cells over time can contribute to tissue dysfunction and disease. Oxidative stress, caused by an imbalance between the production of reactive oxygen species (ROS) and the body's ability to neutralize them, is a key contributor to cellular senescence and the development of IPF. Nrf2, a transcription factor that regulates the expression of antioxidant genes, has been shown to play a crucial role in protecting cells from oxidative stress and promoting cellular health. Understanding the mechanisms of cellular senescence may result in new treatment for IPF such as NRF2 activators.

Objectives: The aim of this project is to analyze the role of Nrf2 activators in bleomycin-induced senescent marker expression in primary fibroblasts.

Methods: Lung parenchyma tissue were obtained from control subjects (n = 33) and IPF patients (n = 18) to study the expression of senescence markers. In addition, the effect of Nrf2 activators on bleomycin-induced senescence markers was evaluated in primary fibroblasts isolated from control subjects and IPF patients.

Results: Senescence markers such as p16, p21 and telomere shortening are overexpressed in lung parenchyma tissue from IPF patients. Nrf2-activators reduce bleomycin-induced senescence markers, reducing senescence-associated secretory phenotype, reversing cell cycle arrest and DNA damage and increasing cell proliferation in fibroblast from control donors and IPF patients.

Conclusions: Nrf2 activators have shown to be effective in revert numerous senescence hallmarks induced by bleomycin *in vitro*.

Funding: This work was supported by the grants PID2020-114871RB-I00 (JC), European Regional Development Fund (FEDER), and Instituto de Salud Carlos III, PI20/01363 (JM) and by CIBERES (CB06/06/0027) from the Spanish Government. Funding entities did not contribute to the study design or data collection, analysis, and interpretation, or to the writing of the manuscript.

118. IDENTIFICATION OF COPD EXACERBATIONS BY CLINICALLY BLINDED PROTEOMIC ANALYSIS: BEYOND INFLAMMATION

César Jessé Enríquez-Rodríguez^{1,2,3,4}, Carme Casadevall^{1,2,3,4}, Sergi Pascual-Guardia^{1,2,3,4,5}, Diego Rodríguez-Chiaradia^{1,2,3,4,5}, Esther Barreiro^{1,2,3,4,5}, Joaquim Gea^{1,2,3,4,5}

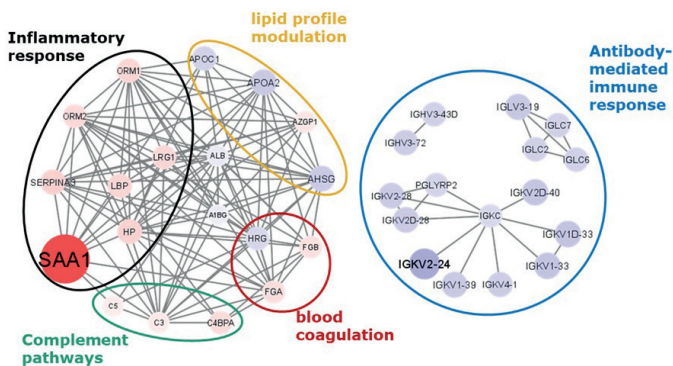
¹IMIM (Institut Hospital del Mar d'Investigacions Mèdiques), Barcelona, Spain. ²Departament de Medicina i Ciències de la Vida (MELIS), Universitat Pompeu Fabra (UPF), Barcelona, Spain. ³Barcelona Respiratory Network (BRN), Barcelona, Spain. ⁴Centro de Investigación Biomédica en Red de Enfermedades Respiratorias (CIBERES), Madrid, Spain. ⁵Servei de Pneumologia, Hospital del Mar, Barcelona, Spain.

Introduction: Although chronic obstructive pulmonary disease (COPD) is highly prevalent, its accurate diagnosis and identification of different disease circumstances can be difficult due to the heterogeneous clinical presentation. Researchers are currently exploring systems biology techniques, such as omics, to identify specific biomarkers through unbiased approaches. However, the usefulness of these techniques becomes limited due to the statistical analyses usually chosen, which are typically based on pre-defined phenotypes and complementary questions, thereby intrinsically limiting their exploratory potential.

Objectives: To assess the potential of a completely blind proteomic analysis to identify the presence of either the COPD (the disease) or exacerbations. The results were compared with those obtained through a hypothesis-driven multiplexing.

Methods: Plasma from 34 individuals recruited in our center (24 with stable COPD and 10 suffering from an exacerbation, and 10 healthy

controls) were analyzed using liquid chromatography-tandem mass spectrometry (LC-MS/MS) supplemented with an immunologic multiplex (focused mainly on inflammatory markers). The main part of the analysis was totally blind regarding clinical characteristics and based solely on an unbiased K-Means clustering. Only at the final step the blindly generated groups were confronted with clinical diagnoses. **Results:** Blind clustering did not help in COPD diagnosis, but with differentiation of acute exacerbations from stable phases ($p = 0.01$), showing a specificity of $79 \pm 25\%$ and an $80 \pm 25\%$ sensitivity (integrated accuracy, $79 \pm 25\%$). The differentially abundant proteins among this two disease circumstances were associated with inflammatory and antibody-mediated immune responses, blood coagulation, lipid profile modulation, and complement pathways. On the contrary, the clustering analysis based on multiplex (thus, driven by hypotheses) was not useful for identifying COPD or exacerbations.



PPI networks performed on DAPs between Cluster A vs Cluster B obtained in Kmeans used for identification of the exacerbation profile. Each node lists the gene name of the identified proteins. The size and shade of the nodes represent the median log₂ fold-difference of DAPs with red and blue showing over- and underrepresented proteins, respectively. Edges stand for already known and predicted protein interaction obtained from STRING database, as well as the other public databases that were selected for the study. DAPs grouped into: inflammatory markers (including cytokines, chemokines and acute-phase proteins), proteins involved in lipoprotein particle remodeling systems, the complement system, coagulation-related proteins, and antibody-mediated immunity proteins.

Conclusions: A clinically blinded LC-MS/MS strategy demonstrated that a proteomic profiling not limited to inflammation and related events could help in identification of COPD exacerbations. Funding: FIS (PI21/00785, M-BAE BA22/00009 & PFIS FI22/000003); CIBERES (CB06/06/0043), ISCIII-EU; SEPAR Grants 2019 & 2021 and the Catalan Government (2021 SGR 00100), FUCAP, MENARINI.

119. THE INFLUENCE OF SEX ON THE PROGRESSION OF PULMONARY ARTERIAL HYPERTENSION IN MICE

María Jesús Sánchez-Guisado^{1,2}, Irati Aiestaran-Zelaia^{1,3,2}, Marta Beraza^{1,2}, Ian James Holt³, Jesús Ruiz-Cabello^{1,2,4}

¹CIC biomaGUNE, San Sebastián, Spain. ²Centro de Investigación Biomédica en Red de Enfermedades Respiratorias (CIBERES), Madrid, Spain. ³Biodonostia Health Research Institute, San Sebastián, Spain. ⁴Universidad Complutense de Madrid, Madrid, Spain.

Introduction: Pulmonary arterial hypertension (PAH) is a rare disease characterized by remodeling pulmonary arteries and right ventricle failure. In PAH, the incidence is higher in women, and although men have the worst prognosis, there is no clear explanation of sex differences in the pathogenesis and progression of PAH. Though, identifying these mechanisms is crucial for developing differentiated approaches to PAH treatment in both sexes.

Objectives: The aim of this study was to study in vivo the influence of sex on the development of PAH in mice.

Methods: PAH was induced in 8-week-old female and male C57BL/6J mice by chronic exposure to normobaric hypoxia (10% O₂) for three weeks. Additionally, a VEGF receptor inhibitor, SUGEN 5416 (20 mg/kg), was injected intraperitoneally weekly. After this period, mice were functionally characterized by 18F-FDG PET/CT imaging for measuring glucose uptake and cardiac MRI for heart function characterization and mean pulmonary arterial flow measurement. 3D PET-CT scans were performed using the Molecubes β-cube (PET) and X-CUBE (CT) scanners. Scouts, short-axis, four-chambers cine, and velocity-encoding TX/RX MRI acquisitions were acquired with a 7 Tesla Bruker MRI system with a combination of a 72 mm volumetric quadrature coil for excitation and a 20 mm rat brain surface coil for the reception.

Results: Body-to-surface indexed left ventricular end-diastolic (LVED-Vi) and LV end-systolic (LVESVi) volumes were significantly decreased in female PAH mice compared with the control. In contrast, these differences were not found in male PAH mice. Right ventricular end-systolic volumes (RV ESVi) were significantly increased in male PAH mice compared with controls. This was accompanied by decreased RV ejection fraction (RV EF). No differences were found in the RV function in females PAH mice. Cardiac glycolytic phenotype evaluated by 18F-FDG PET showed that LV and RV/LV SUV-mean were statistically significant increase in PAH male mice, and interestingly differences in LV SUV-mean in the female disease group.

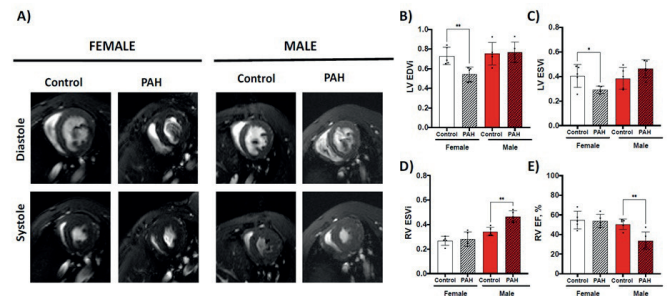


Figure 1. (a) Short-axis magnetic resonance images of the middle ventricle of control and PAH mice. In the top part the images were acquired at the end of diastole and in the bottom part at the end of systole. On the right is the female group and on the right the males, (b) LV End-Diastolic index, (c) LV End-Systolic index, (d) RV End-Systolic index and (e) RV ejection fraction.

Conclusions: We demonstrate a clear metabolic shift in LV and RV and striking differences in the disease development in both sexes. Males have a significantly worse RV function, coinciding RV MRI-derived disease biomarkers and glucose uptake increase. These differences and similar MRI-PET behavior were only observed in LV in females. We are currently evaluating additional biomarkers to fully understand these results.

Funding: MJS-G is supported by a pre-doctoral fellowship from the Spanish Ministry of Education (PRE2018-083691). JRC is funded by MCIN/AEI/10.13039/501100011033 and by "ERDF A way of making Europe" or European Union or European Union NextGenerationEU/PRTR Science, (PID2021-1232380B-I00 and PDC2021-121696-I00). JRC also received funding from La Caixa Foundation (Health Research Call 2020: HR20-00075) and from the Fundación contra la Hipertensión Pulmonar. CIC biomaGUNE is supported by the Maria de Maeztu Units of Excellence Program from the Spanish State Research Agency – Grant No. MDM-2017-0720.

122. PATHOGENETIC MECHANISMS OF PERSISTENT MUSCLE WEAKNESS IN ACUTE RESPIRATORY DISTRESS SYNDROME SURVIVORS

Israel David Duarte Herrera¹, Paula Martín Vicente¹, Cecilia Lopez Martínez¹, Sara Exojo Ramirez¹, Marcelino Gonzalez Iglesias², Raquel Rodriguez García³, Ana García de Alai², Diego Parra Ruiz³, Guillermo Muñoz Albaiceta³, Laura Amado Rodriguez³

¹Centro de Investigación Biomédica en Red de Enfermedades Respiratorias (CIBERES), Madrid, Spain. ²Uniovi, Oviedo, Spain. ³Hospital Universitario Central de Asturias, Oviedo, Spain.

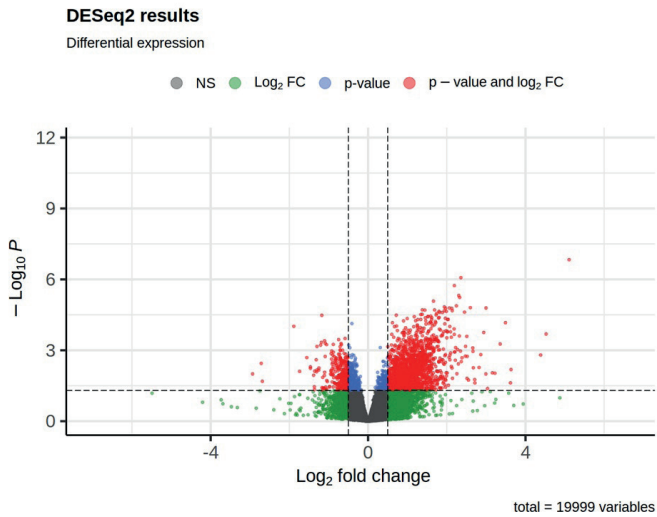
Introduction: Patients with acute respiratory distress syndrome (ARDS) frequently require mechanical ventilation and admission to the intensive care unit (ICU). Survivors may develop important sequelae including ICU-acquired muscle weakness (ICUAW). Long-term recovery ranges from complete functional restoration to persistent muscle weakness. Clinical diagnosis results inaccurate and unable to predict recovery capability.

Objectives: To identify subgroups of ICU survivors with different ICUAW pathogenesis and long-term prognosis, using transcriptomics at ICU admission.

Methods: Consecutive ARDS patients due to COVID-19 were recruited at ICU admission and followed-up at 3 and 6 months after discharge, from March 2020 to February 2022. Whole-blood transcriptomes were obtained at ICU admission. Clinical data collected included Duke Activity Status Index -DASI-, handgrip strength (HGS), sit-to-stand test (STS) and quadriceps ultrasound, as muscle-performance features. Latent class analysis was performed to identify subgroups of patients with different long-term muscle recovery capacity. Differences in gene expression and clinical data between classes were assessed. Differentially expressed genes were used for Gene Set Enrichment Analysis (GSEA). Data are expressed as median and interquartile range. Missing data were not imputed. Differences between classes were assessed using Wilcoxon or chi-square tests where appropriate. All the analyses were performed using R version 4.2.2 (2022-11-10).

Comparison of clinical variables between classes

	Strength recovery (n = 29)	Persistent weakness (n = 46)	p value
Sex			0.056
Female	4 (13.80)	17 (36.90)	
Male	25 (86.20)	29 (63.04)	
Age (years)	60 (51-64)	68 (59-71)	0.0050
BMI (Kg/m ²)	29.4 (26.9-32.7)	29.33 (25.4-33.3)	0.7464
COPD	1(3.44)	5 (10.87)	0.687
Arterial hypertension	17 (58.62)	27 (58.70)	1
Diabetes	4 (13.79)	10 (21.74)	0.578
Dyslipemia	11 (37.93)	22 (47.82)	0.547
ICU admission			
IL-6 (pg/ml)	60.5 (15-160.25)	118 (39.5-254.5)	0.2673
Ferritin (ng/ml)	1,382 (933-2,374)	967.5 (768.75-1,483.25)	0.0464
D-dimer (ng/ml)	1,086.5 (551.25-1,711.75)	1,115 (659-1,876.5)	0.6295
Leukocytes (/µl)	8,290 (5,410-10,380)	8,065 (6,187.5-11,607.5)	0.8024
Lymphocytes (/µl)	630 (480-800)	645 (562.5-1,085)	0.2208
Treatments during ICU stay			
Mechanical ventilation	24 (82.75)	44 (95.65)	0.144
Prone ventilation	14 (48.27)	31 (67.40)	0.2
Neuromuscular blockade	7 (24.14)	18 (39.13)	0.276
Vasoactive drugs			0.007
None	20 (68.96)	15 (32.60)	
One	9 (31.03)	29 (63.04)	
Two or more	0	2 (4.34)	
Steroid therapy	6 (20.68)	19 (41.30)	0.111
Hospital evolution			
IL-6 at day 7	26 (10-87)	47.5 (10.25-97.5)	0.7373
Ferritin at day 7	1,174.5 (799-1,959.75)	799 (449-1,285)	0.1257
D-dimer at day 7	1,320 (718-3,852)	1,541 (1,040-3,370)	0.5419
Leukocytes (/µl)	9,305 (6,825-10,142.5)	10,260 (7,565-12,370)	0.2384
Lymphocytes (/µl)	1,085 (555-1,545)	1,060 (715-1,405)	0.8452
Delirium	3 (11.53)	15 (32.60)	0.043
Days on ventilator	7 (4-9)	12.5 (9-16.75)	0.0005
ICU length of stay (days)	10 (6-11)	16 (9.25-26)	0.0008
Hospital length of stay (days)	19 (16-29)	35.5 (23.5-50.75)	0.0001
Clinical diagnosis of ICUAW at discharge	13 (50.00)	32 (69.56)	0.059
Muscle weakness features			
DASI at baseline	52.2 (45.83-53.7)	44.7 (33.45-47.33)	0.0001
DASI 3-month	40.2 (34.26-45.08)	21.2 (10.57-26.95)	0.0000
HGS 3 month (kg)	34.7 (29-39.7)	23 (18.7-26.6)	0.0000
STS 3 month (sec)	15 (8-23)	47.5 (36.75-56.25)	0.0000
Quadriceps cross-sectional area (cm) at 3 month ultrasound exam	3 (2.68-4.09)	1.69 (1.55-2.17)	0.0005
Delta DASI (baseline to 6 month)	4.5 (3.75-11.75)	10 (4.75-20.25)	0.0138
DASI 6-month	46.95 (37.26-54.83)	26.95 (18.51-36.89)	0.0000
HGS 6 month (kg)	35.6 (23.53-41.45)	28.7 (22.3-34)	0.0128
STS 6 month (sec)	9.8 (8.61-10.98)	15.64 (13.05-19.02)	0.0000
Quadriceps cross-sectional area (cm) at 6 month ultrasound exam	2.5 (2.11-3.06)	2.08 (1.72-2.8)	0.0373



Volcano plot result of differential expression analysis between classes.

Results: 75 survivors completed followed up and sample acquisition (AGE, % female). Patients clinically diagnosed of ICUAW at hospital discharge (n = 55, 61.8%) showed prolonged ICU stay (19 [10.5-31.5] versus 9.5 [6-13] days, $p < 0.0001$) and time on ventilator (14[9-22] versus 7 [3.25-11] days, $p < 0.0001$) than patients without ICUAW. There were significant differences in HGS (25.75 [19.75-31.32] versus 26.9 [23.45-37.7] kg, $p = 0.038$) and STS (16.06 [13.1-21.54] versus 12.86 [10.14-16.46] sec, $p = 0.041$) at 3-month timepoint. There were no differences in muscle performance at 6-month timepoint, nor in gene expression between groups. Latent class analysis based only on data related to muscular performance at 3-month, revealed two classes of patients (“persistent weakness” [n = 46] and “strength recovery” [n = 29]). Comparison of clinical variables between classes are depicted in the Table. Using an adjusted p-value cut-off point of 0,05, there were 183 differentially expressed genes. GSEA was used to identify the molecular pathways involving these differentially expressed genes. Several categories related to regulation of stem cell population maintenance and DNA replication and repair were identified.

Conclusions: Transcriptomic analysis of whole blood RNA at ICU admission may help to identify pathogenetic molecular mechanisms leading to persistent muscle weakness in ARDS survivors.

Funding: ISCIII, JR22/00066. PI21-01592. Marató TV3 854-U-2021.